SEARCH FOR MALIC ACID ACTIVATING ENZYME INVOLVED IN THE SYNTHESIS OF POLYMALIC ACID FROM PLASMODIA OF *PHYSARUM POLYCEPHALUM*

Dissertation

zur Erlangung des Doktorgrades der Naturwissenschaften (Dr. rer. nat.)

der Naturwissenschaftlichen Fakultät III

- Biologie und Vorklinische Medizin -

der Universität Regensburg

by

Till Olickal

from Kochi

INDIA

2004

Promotionsgesuch eingereicht am: 30-01-2004

Tag der mündlichen Prüfung: 30-03-2004

Die Arbeit wurde angeleitet von: Prof. Dr. Eggehard Holler

Prüfungsausschuss:

1.	Vorsitzender:	Prof. Dr. Armin Kurtz
2.	1. Gutachter: (1. Prüfer)	Prof. Dr. Eggehard Holler
3.	2. Gutachter: (2. Prüfer)	Prof. Dr. Günter Hauska
4.	3. Prüfer:	Prof. Dr. Charlotte Förster

Dedicated to my beloved parents,
and my wonderful wife Jasmine.

ACKNOWLEDGMENTS

It is my privilege to express my deep sense of gratitude to my advisor, *Prof. Dr. Eggehard Holler* for his valuable guidance, constant encouragement, insightful discussions, and work freedom, which culminated in the completion of this project.

I would like to thank *Dr. Bong-Seop Lee* for his advice, guidance, valuable technical discussions and help.

I am grateful to *Dr. Helmut Durchschlag* for his technical assistance in the usage of the scintillation counter.

I am deeply grateful to *Ms. Hermine Reisner* for her helpful suggestions and assistance during my experiments.

I would like to acknowledge *Ms. Sonja Fuchs* for introducing me to the column chromatography experiments, valuable suggestions, and especially for her patience in aiding me improve my German.

I am thankful to *Ms. Barbara Kellerer* for her technical assistance with the FPLC system.

I am extremely appreciative to all my past and present lab mates, especially *Andy* who helped me in the transition of adjusting to a new environment. I wish to thank *Anton, Christian, Elke, Nadth, Markus Haindl, Markus Richter* and all my other colleagues for creating a cheerful, pleasant, and friendly atmosphere in the lab.

I take great pleasure in thanking all my friends *Rakesh, Shobi, Simi, Sreenivasa, Stefan,* and *Suneel* for their help, suggestions, discussions, assistance, and friendship which I will cherish throughout my life.

Acknowledgments

I would like to pay tribute to my uncle *Babychen* for the encouragement and support, and to *mother and father-in-laws,* and my two *brothers-in-law* for their continuous prayers and encouragements.

I owe my existence to the love, support, sacrifice, prayers, and encouragement of my beloved *parents*. I am blessed to have an ever-loving and understanding wife *Jasmine*, without her constant support and inspiration I would not have been here. I take this opportunity to express my gratitude towards them by dedicating this thesis to them.

ABBREVIATIONS

&	And
act.	Activated
Ado	Adenosine
ADP	Adenosine 5′-diphosphate
AMP	Adenosine 5′-monophosphate
ATP	Adenosine 5′-triphosphate
AU	Arbitrary Unit
BLS	Blue Sepharose CL-6B
Bq	Becquerel
BSA	Bovine serum albumin
^{o}C	Degree Celsius
Ci	Curie
CoA	Coenzyme A
cpm	Counts per minute
Da	Dalton
DE	DEAE
DEAE	Diethylaminoethyl
DMSO	Dimethyl sulfoxide
DNA	Deoxyribonucleic acid
dpm	Decomposition per minute
DTT	Dithiothreitol
dd.	double-distilled
E_{280}	Extinction at 280 nm
E_{595}	Extinction at 595 nm
EDTA	Ethylenediaminetetraacetic acid
eg.	Example
EGTA	Ethylene glycol-bis(2-aminoethylether)-N,N,N′,N′-tetraacetic acid
eq.	Equation
Fig.	Figure
FPLC	Fast protein liquid chromatography
g	gram or relative centrifugal force
GTP	Guanosine 5′-triphosphate
hBSA	Heat-denatured bovine serum albumin
HIC	Hydrophobic interaction chromatography
HMW	Higher molecular weight
HPLC	High performance liquid chromatography
hr	Hour
hrs	Hours
IC_{50}	Concentration at 50 % inhibitory effect
kDa	Kilodalton
K_M	Michaelis-Menten constant
LMW	Lower molecular weight
M	Molar (mol/l)
mal	Malate
mg	Milligram
min	Minute
mix.	Mixture
ml	Milliliter

mM	Millimolar
M & M	Materials and methods
MOPS	3-(*N*-Morpholino)propanesulfonic acid
µCi	Microcurie
µg	Microgram
µl	Microliter
µM	Micromolar
N	Normal
NAD^+	Nicotine adenine dinucleotide (oxidized)
NADH	Nicotine adenine dinucleotide (reduced)
nm	Nanometer
No.	Number
Nos.	Numbers
PAGE	Polyacrylamide gel electrophoresis
PDK1	3-Phosphoinositide-dependent protein kinase 1
pg	Preparative grade
PGA	Poly(γ-D-Glutamate)
PHA	Poly(hydroxyalkanoate)
PHB	Poly(β-D-hydroxybutyrate)
PHK	Phosphorylase kinase
Pi	Orthophosphate
PKA	cAMP-dependent kinase
PKC	Protein kinase C
PMLA	β-Poly(L-malic acid)
PPi	Pyrophosphate
prep.	Preparative
Ref.	Reference
Rf	Retention factor
RNA	Ribonucleic acid
RP	Reversed-phase
rpm	Revolutions per minute
Ser	Serine
SDS	Sodium dodecyl sulfate
TCA	Trichloroacetic acid
Thr	Threonine
Tris	Tris(hydroxymethyl)aminomethane
Tyr	Tyrosine
tRNA	transfer RNA
U	Units
UV-VIS	Ultraviolet-visible
Vol.	Volume
vs.	Versus
w/	With
w/o	With out
w/v	Weight/volume

CONTENTS

1 INTRODUCTION

Plasmodia of *Physarum polycephalum* are reminiscent of slime, giving this group of organisms the name "slime mold". The scientific name of this group is myxomycete. These organisms exist in at least three distinct forms in a life cycle. The plasmodium is the main cell form that imprints the name of these organisms and that is unique to them.

1.1 Life cycle of *Physarum polycephalum*

As is the case with many other acellular slime molds, *Physarum polycephalum* feeds on bacteria and fungi as well as bits of decaying organic material (i.e. it is holozoic) in the most commonly observed form, the plasmodium. Plasmodia are vegetative cells, which have the purpose to accumulate large amounts of biomass. With respect to the life cycle of *Physarum polycephalum* one can differentiate a haplophase and a diplophase (**Fig. 1**).

1. The plasmodium is the main vegetative phase of the life cycle. Usually diploid, it is a large syncytium (multiple nuclei in a common cytoplasm) that can grow to very large sizes (under laboratory conditions it can be many centimeters in diameter).

2. Under certain conditions of starvation and desiccation, plasmodia assume a dormant stage called sclerotia. Properly-prepared and stored, sclerotia can be preserved for many years and then reactivated by placing small fragments on a moist food source; a favorite such food (for biologists who study plasmodia) is oatmeal flakes.

3. Sporulation, which is an example of cellular differentiation, is induced if starved plasmodia sense visible light, heat shock or other environmental stress (such as flooding, high or low pH, etc.). Cellular commitment to sporulation is followed by the sequential biosynthesis of many new proteins that are required for the formation of fruiting bodies. About eleven hours after induction, the plasmodial mass develops into cytoplasmic nodules, each of which culminates to form a fruiting body suspended by a millimeter-sized stalk. The cytoplasmic mass enclosed by the fruiting body divides up into smaller clumps, within which meiotic divisions occur,

producing haploid nuclei that become packed as spores. Sporulation is of great practical advantage for the geneticist since it allows the genetic analysis of all kinds of mutants in *Physarum*.

4. The sporulation process ends with the rupture of the sporangial mass and the release of spores into the surroundings. Mechanisms for dispersing such spores are not yet well understood.

5. Spores are induced to open in environments that have "proper" levels of moisture and nutrients, releasing haploid amoebae.

6. The amoebae that are released from the spore coat are, in most cases, haploid cells that form the gametes of the system. Amoebae can be cultured on solid substrates, with bacteria (live or formalin-killed) as a food source or in suspension culture, with a semi-defined nutrient medium. Amoebae can undergo at least four distinctive stage conversions.

7. Under unfavorable circumstances, such as limited nutrients, desiccation, too many neighboring amoebae, etc. the amoebae can form cysts, each of which is a dormant form that is resistant to adverse conditions but can reverse to its original form when conditions become more favorable. Encysted amoebae can be stored, at low temperatures, for extended periods of time.

8. When amoebae growing (in the laboratory) on "lawns" of bacteria are immersed in any of a variety of aqueous solutions, they transform into flagellate swimming cells called myxoflagellates or "swarm cells". This amoeboflagellate transformation is rapid and reversible, is believed not to require gene activation or protein synthesis, and involves extensive rearrangement of cytoskeletal elements such as actin filaments and microtubules.

9. Amoebae can also mate (fuse) with other amoebae with complementary mating alleles (6a), thus forming a diploid cell from which a new plasmodium grows up. Certain strains of amoebae have the ability to "self" without fusion and create haploid plasmodia.

10. The diploid (or haploid) cells thus formed can be considered uninucleate plasmodia that, upon being cultured, become multinucleate (syncytial) plasmodia.

11. Small plasmodia can be grown on solid substrata with a suitable food source to yield the large plasmodia discussed above (1).

12. While plasmodia growing on filter paper wet with a semi-defined liquid growth medium give rise to macroplasmodia, they can be vigorously shaken and fragmented into microplasmodia. They can be subcultured repeatedly to yield large quantities of microplasmodia grown in suspension.

13. If cultured in liquid medium that is depleted of nutrients (starvation), microplasmodia form another dormant phase, spherules, which can be dried by streaking on dry filter paper, stored indefinitely and used to start new shaker cultures of microplasmodia. Microplasmodia can also be fused to form macroplasmodia and then cultured on solid substrata.

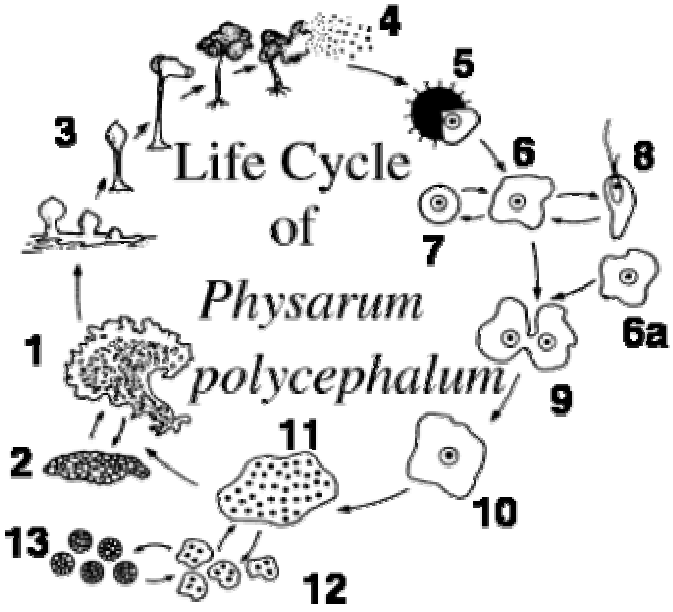

Fig. 1: Life cycle of *Physarum polycephalum*.
(Ref:http://bic.usufl.usuhms.mil/Mark/LifeCycle.html)

Myxomycetes have been traditionally classified on the basis of their sporophore characteristics alone, but in recent years, plasmodial characters and type of sporophore development have become important considerations in delimiting subclasses.

- **Phylum:** Myxomycota
- **Class:** Myxomycetes
- **Order:** Physarales
- **Family:** Physaraceae
- **Genus:** *Physarum*
- **Species:** *polycephalum*

1.2 Poly(L-malate)

1.2.1 History

β-Poly(L-malic acid) (PMLA) was first mentioned in the late 1960's, constituting an acid protease inhibitor produced by *Penicillium cyclopium* (Schimada et al., 1969). The polymer was partially characterized and purified.

The chemical synthesis of β-Poly-L-malate was first reported in 1979 (Vert and Lenz, 1979). Since then, PMLA is discussed as potential "Drug Carrier" for medical applications (Braud et al., 1985; Braud and Vert, 1993). PMLA has been identified in the myxomycete *Physarum polycephalum* (Fischer et al., 1989), in the cultures of *Aureobasidium* sp. (Nagata et al., 1993) and in other filamentous fungi (Rathberger et al., 1999). β-Poly- L-malate is synthesized by plasmodia of *Physarum polycephalum* during growth, secreted into the culture medium, and degraded there to L-malate, especially after growth has ceased. Its concentration is highest in the cell nuclei (Fischer et al., 1989; Windisch et al., 1992).

β-Poly(L-malate) is synthesized only in the plasmodial cell form of myxomycetes (Rathberger et al., 1999) whether haploid or diploid. The other, mononucleate stages of its life cycle do not produce the polymer. Microplasmodia closely resemble macroplasmodia except that they are grown under continuous shaking that physically favors disruption of the cell bodies and the formation of very small plasmodia containing few to several hundred nuclei.

The protein content of macroplasmodia (180 mg/g) is almost twice the quantity of that contained in microplasmodia (98 mg/g) (Schmidt et al., 1996).

1.2.2 Structure and chemical properties

Poly(L-malic acid) from *Physarum polycephalum* belongs to the family of poly(3-hydroxy acid)-type aliphatic polyesters (Cammas et al., 1993). β-Poly(L-malic acid) is a biopolymer of L-malic acid units, which are esterified between the hydroxyl and β-carboxylic groups (Fischer et al., 1989) (**Fig.2**). The α-carboxylic 'side chains' are ionized at neutral pH (pK_a = 4.0-4.3 at 25^{o}C) and probably extruded from the polymer backbone into aqueous solutions allowing strong electrostatic contacts to positively charged polyamines and proteins such as histones (Seki et al., 1984; Holler et al., 1992a). Due to its esteric nature it is slightly labile at neutral pH and instable at acidic or alkaline conditions. It has the maximum stability at pH 5 – 9, and is rapidly hydrolyzed under extreme conditions (Holler et al., 1992b). Highly purified samples obtained from growth media and cell extracts contained a number of average molecular mass of 50,000 and a poly-dispercity factor P = 2.0. The higher masses found were 300,000-500,000.

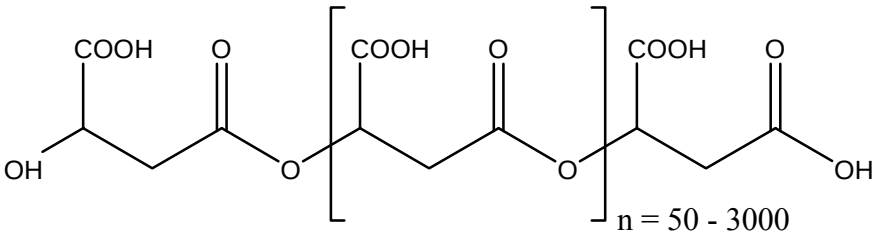

Fig. 2: Structure of Poly(β-L-malate) from *Physarum polycephalum*.

1.2.3 Biochemical properties

Poly(L-malate) strongly inhibits the activity of endogenous DNA polymerase α, but not that of β-like DNA polymerase or of any of the nucleic acid polymerases of other

organisms tested (Fischer et al., 1989). The inhibition is competitive with regard to DNA (Fischer et al., 1989) and is antagonized by free histone H1, such as from calf thymus. DNA polymerase α of *Physarum polycephalum* is constitutively expressed during the cell cycle. Poly(L-malate), histones, DNA polymerase α and newly replicated DNA may interact dynamically during the cell cycle in a competitive fashion so that the DNA polymerase α becomes active during the S phase and inactive during the G2 phase (Holler et al., 1992a). The initiation of histone synthesis marks the beginning of the S phase (Carrino et al., 1987; Laffler et al., 1986). The newly synthesized histones displace DNA polymerase α from poly(L-malate) by competition. The released polymerase becomes involves in DNA replication until histone synthesis ceases, and histones are consumed in a highly energetically favorable formation of nucleosomes by newly replicated DNA. Free poly(L-malate) reassociates with DNA polymerase α at the onset of the G2 phase and thereby terminates DNA synthesis. Thus, poly(L-malate) may function in stock piling inactive DNA polymerase during the G2 phase and M phase of the cell cycle (Holler et al., 1992a).

1.2.4 Pharmaceutical uses

Poly-β-malic acid is biodegraded with the formation of malic acid, which is an intermediate in the Krebs cycle and, therefore, is readily metabolized, and its degradation occurs within cells. Hence, this polymer and its ester derivatives should have many potential applications in the biomedical field. In particular, PMLA has pharmaceutical interest for its use in controlled drug release formulation (Braud and Vert, 1993).

The interest in simple homopolymers (consisting of a single, repeating unit) for uses in biology and medicine is rapidly increasing. Two types of compounds have been considered: macromolecules that are pharmacologically active by themselves (polymeric drugs), and drug-polymeric carrier systems, which bear drugs temporarily attached to the polymer backbone either covalently (macromolecular prodrugs) physically, or included in micro vesicles (Braud and Vert, 1983).

Water solubility is one of the prerequisites of biologically active polymers if they are to be injected into body fluids (Ringsdorf, 1975; Gebelein, 1978). Generally, the investigator's interest is focused upon characteristics like non-toxicity of the prodrug, non-

immunogenicity, when repetitively administrated, degradability and resorbability of the carrier-backbone in order to prevent accumulation in the body (Braud and Vert, 1983; Holler, 1997).

There are reasons for the interest in investigating PMLA. First of all, chains of PMLA contain L-malic acid repeating units, which is a well-known degradable metabolite. Second, carboxylic acid groups are present as side chain groups in every unit that could water-solubilize the polymeric chains at a neutral pH and provide means to attach drugs and tissue targeting molecules. Third, PMLA macromolecules have labile ester bonds in the main chain, which hydrolyze spontaneously and enzymatically (Kropachev, 1976; Braud and Vert, 1983; Korherr et al., 1995).

1.3 Polymerization of L-malate

The *in vivo* rate of PMLA synthesis was 154 µg PMLA per hr per g of plasmodium from L-malate, comparing satisfactory with 140 µg PMLA per hr per g of plasmodium from D-glucose (Schmidt et al., 1996). It was concluded from these data, that L-malate was the substrate for PMLA synthesis (Willibald et al. 1999).

As in nonribosomal peptide synthesis (Kleinkauf and von Dören, 1996), poly(γ-D-glutamate) synthesis (Gardener and Troy, 1979), and poly(hydroxyalkanoate) synthesis (Steinbüchel et al., 1998), the polymerization of malate must be endergonic, driven by chemical activation of malate at the expense of energy-rich bonds like those in ATP. This requirement was confirmed by Willibald et al., 1999, the production of PMLA was inhibited completely, when the arsenate, an uncoupler of oxidation/phosphorylation, was injected together with L-[^{14}C-malate]. According to Barners et al., 1973, oxidative phosphorylation by mitochondria is inhibited completely at 0.2 mM intracellular KCN. Because 0.4 mM KCN had no effect, when the synthesis of [^{14}C]PMLA was measured in the presence of injected KCN, PMLA polymerization did not use energy from mitochondria, but probably used ATP from the glycolytic pathway in the cytoplasm.

Two possible types of chemically activated L-malate are discussed for the polymerization of L-malate, β- L-malyl-AMP or β- L-malyl-CoA. It has been reported the

polymerization of acyl-AMP in the nonribosomal peptide synthesis (Kleinkauf and von Dören, 1996), and polymerization of acyl-CoA in the bacterial synthesis of poly(β-hydroxyalkanoates) (Steinbüchel et al., 1998; Anderson and Dawes, 1990; Steinbüchel and Schlegel, 1991). In the later case hydroxyalkanoyl-CoA is either the product of the biosynthetic pathway or is formed by particular thiokinases involving hydroxyalkanoyl-AMP as intermediates. A malyl-CoA ligase (AMP forming) has not been reported. A malyl-CoA ligase (ADP forming) is found only in the serine-isocitrate lyase pathway of certain bacteria (Hersh, 1973), but not in eukaryotes. The possibility of malyl-CoA formation in the reaction catalyzed by eukaryotic malate synthase has been discounted (Eggerer and Klette, 1967). Moreover, NMR analysis indicated the *in vivo* synthesis of ^{13}C -PMLA from D-[l-^{13}C]glucose via pyruvate carboxylation and oxalacetate reduction (Lee et al., 1999). Thus the metabolic formation of malyl-CoA in eukaryotes is highly unlikely favoring the assumption of *Physarum*-specific malyl-AMP ligase in the biosynthetic pathway of PMLA.

As because ATP had to be cleaved between the α,β phosphates to yield malyl-AMP and pyrophosphate, the noncleavable analogue α,β-methylene ATP must be inhibitory. In contrast, the analogue β,γ-methylene ATP was likely to substitute for ATP. Co-injection of these ATP analogues with L-[^{14}C-malate] was indicated by a pronounced inhibition by α,β-methylene ATP (Willibald et al., 1999). α,β-methylene ATP being a competitive inhibitor for ATP and β,γ-methylene ATP a substrate, which has less efficient than ATP. These results also supported the assumption that malyl-AMP was on the pathway of PMLA biosynthesis. To add further support, the desulfo-CoA, which is a competitor of CoA (Henkin and Abeles, 1976; Shimizu et al., 1970), and L-[^{14}C-malate] were co-injected, and had been found to have no effect on PMLA synthesis. If CoA-ester of malate was not involved, the analogue should not inhibit PMLA synthesis (Willibald et al., 1999).

1.4 The goal of the thesis

All these previous investigations suggested that PMLA was synthesized by an enzyme reminiscent of nonribosomal peptide synthetase, harboring a malyl-AMP ligase and a malyl-transferase (polymerase) activity (Kleinkauf and von Dören, 1996). The absence of the synthesizing activity in the plasmodial extract was attributed to an inactivation of malyl-transferase activity by an injury-dependent tyrosine kinase pathway (Willibald et al., 1999).

The survey of literature revealed that the enzymology of the polymerization reaction has not been elucidated, because a PMLA synthetic activity could not be identified in the plasmodial lysates. Therefore, it was felt desirable to shed light on the PMLA synthetic pathway by carrying out the optimization and the effect of the exogenous factors for the purification of enzyme malate activase, and its characterization.

Previously Bildl, 1998 and Willibald et al., 1999 have reported on an enzyme activity that catalyzed an ATP-PPi-exchange in the presence of L-malate, indicating a malate activating enzyme. Disturbingly, the exchange activity was independent on L-malate by 40-50 % of the total exchange activity. Attempts of purification did not result in higher degree of L-malate dependence. Moreover, the exchange activity was inhibited at high concentrations of L-malate.

The goal of the present investigation was to try again separation of malate-independent from malate-dependent exchange activity and from the activity that caused inhibition at high malate. If this was not possible, to understand the reasons that gave rise to these peculiarities. The ATP-PPi-exchange catalyzing protein should be purified and characterized. The involvement of L-malyl~AMP formation should then be demonstrated.

2 MATERIALS AND METHODS

2.1 MATERIALS

2.1.1 Buffers and solutions

2.1.1.1 Bradford reagent

Serva Blue G-250	250 mg
95% Ethanol	250 ml
85% H_3PO_4	500 ml
dd. H_2O to	1000 ml

2.1.1.2 Extraction buffer

50 mM Tris-HCl, pH 7.5
10 mM KCl
10 mM $MgCl_2$
5 mM $NaHSO_3$
5 mM EGTA
1 mM EDTA
5 mM β-Mercaptoethanol
1 mM DTT
0.5 % Triton X-100
1 µM Pepstatin A
10 µM Leupeptin
2 µg/ml Aprotinin
2 µg/ml E64
0.1 mM Pefabloc SC

2.1.1.3 Dialysis Buffer

50 mM Tris-HCl, pH 7.5
10 mM $MgCl_2$
5 mM $NaHSO_3$
5 mM β-Mercaptoethanol
1 mM DTT
1 µM Pepstatin A
10 µM Leupeptin
2 µg/ml Aprotinin
2 µg/ml E64
0.1 mM Pefabloc SC

2.1.1.4 Chromatography buffer (Hydrophobic interaction chromatography)

$\underline{CB_0}$:

50 mM Tris-HCl, pH 7.5
5 mM $MgCl_2$
5 mM $NaHSO_3$
5 mM β-Mercaptoethanol
1 mM DTT
0.1 mM Pefabloc SC
10 % Glycerol

CB_0 : Chromatography buffer
$\underline{CB_{AS}}$: CB_0 + 1.5 M Ammonium Sulfate

2.1.1.5 Chromatography buffer (Blue Sepharose CL-6B)

CB A:

10 mM MOPS, pH 7.5
5 mM $MgCl_2$
0.2 mM EDTA, pH 7.5
1 mM DTT
10 % Glycerol

CB B:

CB A + 1 M KCl

2.1.1.6 Chromatography buffer (HPLC)

CB_1:

10 mM Phosphoric acid, pH 2.1

CB_1:

100 % Acetonitrile

2.1.1.7 Concentrating gel buffer

0.5 M Tris-HCl, pH 6.8

2.1.1.8 Separating gel buffer

1.5 M Tris-HCl, pH 8.8

2.1.1.9 Hemin solution

Hemin	50 mg
1 N NaOH	25 ml

2.1.1.10 Ligase buffer

60 mM Tris-HCl, pH 8.0
10 mM $MgCl_2$
0.5 mM DTT
50 µg/ml BSA
30 mM NaCl

2.1.1.11 MMZ-solution ($MgSO_4$, $MnCl_2$ and $ZnSO_4$)

$MgSO_4 \cdot 7\ H_2O$	6 g
$MnCl_2 \cdot 2\ H_2O$	0.84 g
$ZnSO_4 \cdot 7\ H_2O$	0.34 g
dd. H_2O to	100 ml

2.1.1.12 Running buffer

0.25 M Tris	3 g
Glycine	14.4 g
10 % SDS solution	10 ml
dd. H_2O to	1 L

2.1.1.13 Sample buffer (5X)

1 M Tris-HCl, pH 6.8	15.5 ml

1 % solution of bromophenol blue	2.5 ml
Glycerol	25 ml
dd. H_2O to	50 ml

2.1.1.14 SDS buffer (2X)

Concentrating gel buffer	5 ml
10 % SDS	8 ml
Glycerol	4 ml
β-Mercaptoethanol	2 ml
Bromophenol blue	0.02 g
dd. H_2O to	20 ml

2.1.2 Cell extracts

For the entire cell extracts, microplasmodia from *Physarum polycephalum* [strain M_3CVII (Fischer et al., 1989)] were used.

2.1.3 Chemicals

Acetic acid (glacial) 100 % GR	Roth
Acetone GR	Merck
Acetonitrile 100 %	Merck
Acrylamide 40 % (rotiphorese Gel 29:1)	Roth
Adenosine	Sigma
Adenosine 5′-diphosphate	Sigma
Adenosine 5′-monophosphate	Sigma
P^1,P^4-Di(adenosine 5′)tetraphosphate ammonium salt	Sigma
Adenosine 5′-triphosphate	Roche
Aprotinin	Serva
1-amino-2-naphthol-4-sulfonic acid p.A. (Eiconogen)	Serva
Ammonia solution 25 % GR	Merck
Ammonium molybdate GR	Merck
Ammonium sulfate GR	Merck
5′-AMP-Sepharose 4B	Pharmacia Fine Chemicals
[α-^{32}P]ATP	Amersham Biosciences

[γ-^{32}P]ATP	Amersham Biosciences
Blue Sepharose CL-6B	Pharmacia Fine Chemicals
Bovine serum albumin	Roche
Calcium chloride dihydrate GR	Merck
Calf Thymus DNA activated	Sigma
Citric acid monohydrate GR	Merck
Coomassie Brilliant Blue G-250	Serva
Diethylaminoethyl (DEAE) DE 52	Whatman
Dimethyl sulfoxide (DMSO)	Merck
1,4-Dioxan GR	Merck
1,4-Dithiothreitol (DTT)	Biomol
Dowex 1X2 (100-200 mesh, Cl-form)	Serva
E64 (Protease inhibitor)	Roche
EDTA (Titriplex III) GR	Merck
EGTA	Sigma
Ethanol absolute	J. T. Baker
Ferritin	Sigma
Formaldehyde solution 37 % GR	Merck
Fumaric acid minimum 99 %	Merck
Iron (II) sulfate heptahydrate GR	Merck
D(+)-Glucose monohydrate for microbiology	Merck
Glutardialdehyde 25 % aqueous solution	Merck
Glycine GR	Merck
Glycerol	J. T. Baker
Hemin	Fluka
Heparin-Sepharose CL-6B	Pharmacia Fine Chemicals
HiTrap Blue	Amersham Pharmacia Biotech
Hydrochloric acid fuming 37 %	Merck
Hydroxylapatite	Bio-Rad
Catalase	Boehringer Mannheim
KT 5720 minimum 98 %	Sigma
Leupeptin	Serva
Magnesium chloride hexahydrate GR	Merck
L(-) malic acid, mono sodium salt	Sigma
L-[1,4(2,3)-^{14}C]malic acid	Amersham Pharmacia Biotech
Manganese chloride tetrahydrate GR	Merck
β-Mercaptoethanol	Merck
Mercuric thiocyanate	Sigma
α,β-methylene-adenosine 5′-triphosphate	Sigma
β,γ-methylene-adenosine 5′-triphosphate	Sigma
MOPS GR	Biomol
Nitric acid 65 % GR	Merck
Norit A pract.	Serva
Oxalic acid GR	Merck
Pefabloc SC	Serva
Pepstatin A	Calbiochem
ortho-phosphoric acid 85 % GR	Merck
[^{32}P]Phosphoric acid	Hartmann
Potassium chloride GR	Merck
Potassium dihydrogen phosphate GR	Merck

Potassium fluoride GR	Merck
Tetra potassium pyrophosphate	Sigma
Rotiszint 2200	Roth
Rottlerin	Sigma
Silver nitrate	Roth
Sodium acetate trihydrate GR	Merck
Sodium carbonate anhydrous GR	Merck
Sodium chloride GR	Merck
Sodium dodecyl sulfate (SDS)	Serva
di-sodium hydrogen phosphate dihydrate GR	Merck
Sodium hydrogen sulfite solution 38-40 % pure	Riedel-de Haën
Sodium hydroxide GR	Merck
Tetra sodium pyrophosphate	Sigma
Sodium sulfite GR	Merck
Sodium thiosulfate pentahydrate GR	Merck
Spermine tetrahydrochloride	Sigma
Succinic acid minimum 99 %	Sigma
Sucrose for microbiology	Merck
Sulfuric acid 95-97 % GR	Merck
T4 DNA Ligase	MBI Fermentas
TLC aluminium sheets Silica gel 60 F_{254}	Merck
Butyl-Toyopearl 650-M	Tosoh
Butyl-Toyopearl 650-S	Tosoh
Trichloroacetic acid (TCA)	Roth
Tris ultra pure	USB
Triton X-100 GR	Merck
Bacto-Tryptone	Difco
Tyrphostin A 23	Santa Cruz Biotechnology
Tyrphostin 23	Sigma
Bacto-Yeast Extract	Difco
Zinc sulfate heptahydrate GR	Merck

2.1.4 Growth medium

Bacto-Tryptone	10 g
Bacto-Yeast Extract	1.50 g
Glucose	11 g
Citric acid monohydrate	3.54 g
$FeSO_4 \cdot 7\ H_2O$	84 mg
KH_2PO_4	2 g
$CaCl_2 \cdot 2\ H_2O$	0.60 g
MMZ-Solution (see below)	10 ml
dd. H_2O to	1000 ml

2.1.5 Instruments

Analytical weighing machine L-610D/ P-1200	Mettler
Biofuge B/17RS	Heraeus Sepatech
Blockthermostat BT 100/BT 200	Kleinfeld
Centrifuge 5415/5415C	Eppendorf
Centrifuge RC 2-B/RC 5C Plus	Sorvall
DC power supply PS 500X	Hoefer Scientific Instruments
Electrophoresis gradient former	Hoefer Scientific Instruments
Electrophoresis power supply EPS 200	Pharmacia
Fastblot B 34	Biometra
FLPC system	Pharmacia
Fraction collector RediFrac	Pharmacia
HPLC system	Merck-Hitachi
Magnetic stirrer MR 2002	Heidolph
Oven Modell 200 (max. 300^{o}C)	Memmert
pH-Meter 761 Calimatic	Knick
Peristaltic pump Miniplus 2	Gilson
Peristaltic pump P-1	Pharmacia
Power pack P 25	Biometra
Recorder REC 102	Pharmacia
Scintillation counter LS 6000TA	Beckman
Shaker Gio-Gyrotory/G-33-B	New Brunswick Scientific
Ultra Turrax T 25	Ika
UV/Visible Spectrophotometer Ultrospec III	Pharmacia
Vertical electrophoresis systems Minigel-Twin	Biometra
Vortex Reax 2000	Heidolph
Water-bath HOR	Daglef Patz KG

2.1.6 Miscellaneous accessories

Centrifugal concentrators for 50-500 µl (300 K)	Nanosep
Dialysis tubing (12-14 kDa)	Serva
Filter paper 3	Whatman
FPLC columns	Pharmacia
Glass microfibre filter GF/C	Whatman
Glass vessels	Brand/Schott
Glass wool superfine	Assistant
Immobilon-P	Millipore
Lumi-Film Chemiluminescent Detection Film	Boehringer Mannheim
Pipettes	Eppendorf
pH Indicator paper (Universalindikator, pH 1-10)	Merck
Reversed phase C_{18} column	Macherey-Nagel

2.1.7 Computer softwares

Adobe Photoshop 7.0	Adobe Systems
ChemOffice 2002	CambridgeSoft Corporation
Corel Graphics Suite 11	Corel Corporation
OptiQuant 3.0 Image Analysis Software	Packard Instrument Corporation
Microcal Origin 6.0	Microcal Software, Inc.
Microsoft Excel 2002	Microsoft Corporation

2.2 METHODS

2.2.1 Growth medium

Micro plasmodium of *Physarum polycephalum* were grown in half synthetic medium (see **chapter 2.1.4**). (Daniel and Baldwin, 1964).

The pH of the growth medium was adjusted to 4.6 (± 0.05) with 1 N NaOH and the medium was autoclaved. While inoculating the cells into the growth medium, the Hemin solution (see **chapter 2.1.1.8**) was also added.

2.2.2 Growth condition

100 ml of sterile growth medium and 0.5 ml of sterile Hemin were poured into a 500 ml Erlenmeyer flask. From a two days old culture of *Physarum polycephalum* [strain M_3CVII (Fischer et al., 1989)], 2.5 ml of the settled cells were inoculated into the flask. The microplasmodia were shaken at 150 rpm at 23^{o}C. They were then subcultured for two to three days. Four days old cells were not suitable as a result of the commitment for spherule formation.

2.2.3 Preparation of cell extracts (Willibald et al., 1999)

After the microplasmodia were shaken for two to three days, they were harvested by straining the culture through a fine mesh for medium removal. The entire mesh containing the cells was immediately freed from excess liquid by transferring it onto paper towels. The so prepared cells were weighed out in a ratio of 1:2 with ice-cold extraction buffer (see **chapter 2.1.1.2**) and the cells and nuclei were ruptured using the Ultra Turrax T 25 at high speed (instrument setting No. 6: 24,000).

The cell rupture was carried out at a temperature of 4°C in an ice bath. The cell debris was separated by centrifugation at 18,000 × g (12,000 rpm) for 20 min at 4°C (Sorvall RC 5C Plus). The cell extract was dialyzed unless mentioned otherwise.

2.2.4 Dialysis

The samples were dialyzed against a 10-fold volume of the dialysis buffer (see **chapter 2.1.1.3**) for 5 to 8 hours or over night.

2.2.5 Preparation of [^{32}P] pyrophosphate from [^{32}P] phosphoric acid

2.2.5.1 Pyrolysis

[^{32}P] Pyrophosphate was synthesized from [^{32}P] Na_2HPO_4 (Kornberg and Pricer, 1951)

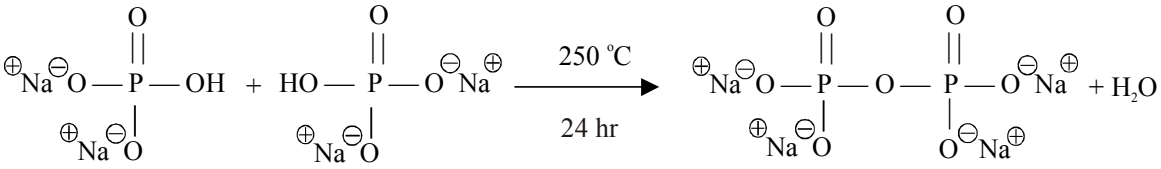

$H_3{}^{32}PO_4$ (2 mCi, carrier-free, 8,000 Ci/mmol, Hartmann) was dissolved in a very small volume of 0.02 N HCl in a bulkhead test tube, to which 0.4 ml of 0.1 M $Na_2HPO_4 \cdot 2H_2O$ (pH 8) was added. The whole process was carried out behind a protection glass. The phosphate solution was kept in an oven for 2 hrs at 110°C until it became a white powder. Then, pyrolysis was carried out by keeping it for 24 hrs at a temperature of 250°C. The product was dissolved in 0.4 ml of double-distilled water.

2.2.5.2 Separation of orthophosphate from pyrophosphate

Since the phosphoric acid does not completely convert into pyrophosphate, the remaining orthophosphate has to be separated from the desired pyrophosphate by column chromatography on Dowex 1X2 (100-200 mesh, Cl-form).

For the separation, a 2 ml syringe (without a piston) was sealed with glass wool and glass filter, and the mouth of the syringe was attached to a Teflon tube, which had a simple clamp to control the flow rate of elution. The column material was dissolved in 10 ml of 3 N HCl. The settled material was about 2 to 2.5 ml. For the preparation of the column, the slurry was poured into the column and washed with 40 to 50 ml of 3 N HCl until most of the absorbing materials were eluted at 260 nm. Following this, the material was washed with about 100 ml of water until the chloride test was negative.

The dissolved pyrolyzed product was passed through the column and washed with 0.4 ml of water. The orthophosphate fractions were eluted out with 25 ml of 0.05 M NaCl in 0.01 N HCl. Ten fractions of 2.5 ml each were collected. Then the pyrophosphate fractions were eluted out with 10 ml of buffer containing 0.5 M NaCl. Ten fractions of 1ml each were collected. The whole elution process was carried out only under gravitational forces.

At the end, the column could be regenerated by washing it with 3 N HCl and water so that it would be ready for another separation.

From each of the fractions 10 µl were diluted at a ratio of 1:100 with water and from this diluted solution 10 µl were added to a scintillation tube containing 10 ml of Rotiszint 2200. Finally, the cpm was measured by a scintillation counter (Beckman LS 6000TA). The total radioactivity of the individual fractions was accessed. The pyrophosphate fractions, which had adequate radioactivity (> 300 cpm), were taken for enzyme tests.

2.2.5.3 Measurement of chloride by the mercuric thiocyanate method

The measurement of chloride ions is based on the capability of Cl^- to displace thiocyanate ions from mercuric thiocyanate in the presence of ferric ion. An intensely colored

ferric thiocyanate complex is formed, and the intensity of the color (460 nm wavelength) is proportional to the chloride-ion concentration (Vogel, 1961).

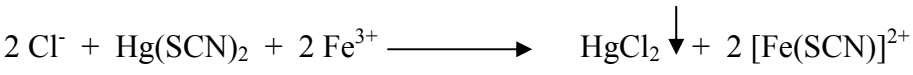

$$2\ Cl^- + Hg(SCN)_2 + 2\ Fe^{3+} \longrightarrow HgCl_2 \downarrow + 2\ [Fe(SCN)]^{2+}$$

2.2.5.3.1 Solution A

0.25 M $NH_4Fe(SO_4)_2 \cdot 12\ H_2O$ in 9 N HNO_3

2.2.5.3.2 Solution B

Saturated amount of $Hg(SCN)_2$ in ethanol.

The test solution contained 100 µl of solution A, 100 µl of solution B and 800 µl of the sample. A calibration curve was constructed using a standard solution, 1 mg/ml NaCl that covered the range of 0 to 100 µg (0 to 100 µl from the stock solution, made upto 800 µl with double-distilled water). The absorbance was measured after 10 min in a spectrophotometer at 460 nm and water was used as the reference.

2.2.5.4 Quantification of orthophosphate

Phosphate reacts with ammonium molybdate to form molybdophosphate.

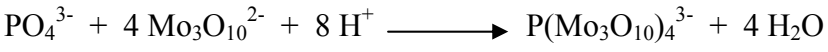

$$PO_4^{3-} + 4\ Mo_3O_{10}^{2-} + 8\ H^+ \longrightarrow P(Mo_3O_{10})_4^{3-} + 4\ H_2O$$

The reaction is specific for orthophosphate. By reacting with sulfite and eiconogen, a part of the molybdenum is reduced from Mo(VI) to Mo(IV). The emerging charge transfer causes a blue coloring (Vogel, 1961).

2.2.5.4.1 Solution A

2.5% Ammonium molybdate in 5 N H_2SO_4

2.2.5.4.2 Solution B

Solution from 40mg Eiconogen (1-amino-2-naphthol-4-sulfonic acid) and 0.1g Na_2SO_3 in 1ml H_2O was added to a solution of 2 g $NaHSO_3$ in 19 ml H_2O.

The precipitate was separated by filtration, and the clear solution was stored in a dark bottle on an ice bath. The test solution contained 100 µl of solution A, 40 µl of solution of B, the sample and double-distilled water to add up to 1 ml. The absorbance was measured at 720 nm (Pharmacia Ultrospec III) after incubation of 20 or 30 min at room temperature. Water was used as the reference. Samples and standard solutions were equally incubated for 20 or 30 min. A calibration curve was for KH_2PO_4 in the range of 0 to 200 µM.

2.2.5.5 Quantification of pyrophosphate

The measurement of pyrophosphate was carried out indirectly by hydrolyzing pyrophosphate into orthophosphate, which was then analyzed. The test sample which contained 100 µl of sample and 20 µl of H_2SO_4 was heated at 100^{o}C for 20 min. Then, 100 µl of solution A and 40 µl of solution B were added and the volume was adjusted to 1 ml with double-distilled water, and orthophosphate measured by the method above.

2.2.6 Quantification of ATP concentration

Low ATP concentrations are proportional to the absorbance at 260 nm, provided that other nucleotides can be neglected. The molar extinction coefficient is 1.54×10^{-2} $cm^{-1}.M^{-1}$ (Segel, 1976). For the absorbance measurement the test samples were routinely diluted 20-fold with double-distilled water. Water was used as the reference.

2.2.7 Quantification of protein

2.2.7.1 Measuring the absorbance at 280 nm

The relative protein content in the test sample was estimated by absorbance measurement at 280 nm. As a rule of thumb, it is convenient to assume a mean extinction of 1.0 for a 1 mg/ml solution (Janson et al., 1989).

2.2.7.2 The Bradford method

This method is based on the observation that Coomassie Brilliant Blue G-250 exists in two different color forms, red and blue. The red form is converted to the blue form upon binding of the dye to protein. The protein-dye complex has a high extinction coefficient thus providing excellent sensitivity in the measurement of the protein. The binding of the dye to protein is a very rapid process (approximately 2 min), and the protein –dye complex remains dispersed in solution for a relatively long time (approximately 1 hr), thus making the procedure very rapid and yet not involving a critical timing for the assay readings (Bradford, 1976).

A calibration curve was established using by diluting a standard solution of 5 mg/ml BSA to cover the range of 0 to 1.2 mg/ml. The sample was diluted in 1:100 with Bradford reagent (see **chapter 2.1.1.1**) and the absorbance of the protein-dye complex was measured at 595 nm.

2.2.8 Optimized assay for the measurement of L-malate dependent ATP-PPi-exchange activity

2.2.8.1 Principle

The search in this work for a malate activating enzyme based on the assumption that polymalate synthesis requires activation of malate at its β-carboxyl group, and that the activation involves carboxyl adenylation (Willibald et al., 1999). A test system was established that involved ATP-PPi-exchange according to the following reaction:

$$\text{L-malate} + \text{ATP} \underset{}{\overset{Mg^{2+}}{\rightleftharpoons}} \text{L-malyladenylate} + \text{PPi}$$

The malyladenylate is formed by transfer of the AMP group of ATP and the release of PPi. In the reverse reaction, PPi labeled with ^{32}P will form [^{32}P]ATP, which is measured by its radioactivity. Charcoal, which has affinity towards ATP, was used to adsorb [^{32}P]ATP and separate it from the eluate [^{32}P]PPi (Crane and Lipmann, 1953; Berg, 1956).

The specificity of the assay reaction is inferred by L-malate, being one of the substrates. An independent exchange activity could be due to other activases, such as aminoacyl-tRNA synthetases, which find corresponding amino acids as impurities in the proteins sample. Because of this it was unavoidable to dialyze the sample before activity measurement of cell extracts. If adenylation occurs with an enzyme-intrinsic side chain, such as a particular carboxylate at the active site, the ATP-PPi-exchange reaction could be independent of extrinsic carboxylic groups such as malic acid or amino acids. In this case, an enzyme adenylate intermediate is formed in the absence of L-malate or any other acid. The enzyme-adenylate can then react with the acid substrate (i.e. L-malate) to yield acyl~AMP. The other possibility is to react with PPi to yield again ATP and the free intrinsic group at the enzyme active site.

2.2.9 [^{32}P]ATP-PPi-exchange assay

2.2.9.1 Composition of the reaction solution

50 mM Tris /HCl, pH 7.5
5 mM $MgCl_2$
50 mM KF
5 mM β-Mercaptoethanol
1 mM L-malate
2 mM $Na_4P_2O_7$
2 mM ATP (pH 6-8)
1 mM Spermine tetrahydrochloride
0.5 mg/ml BSA (heat-denatured hBSA)

Potassium Fluoride impedes inorganic pyrophosphatase to hydrolyze pyrophosphate. Pyrophospholysis would interfere with the assay. Spermine favours L-malate dependant PPi-ATP-exchange similarly as has been observed with aminoacyl-tRNA synthetases (Holler, 1973). BSA acts as a protector against proteases.

A cocktail buffer involved the above components. The volume of each fraction was adjusted to 1 ml with double-distilled water and contained a sufficient amount of [^{32}P] pyrophosphate to show radioactivity of 10^6 cpm. L-Malate and the sample were added separately. One mM of L-malate was added to the cocktail where indicated, and finally the reaction was started by the addition of protein sample. The test mixture was mixed properly with a vortex and incubated for 40 min at 30^{o}C. The reaction was terminated by the addition of 0.5 ml of ice-cold 10 % trichloroacetic acid (TCA). The precipitate was collected by centrifuging for 1 min using an Eppendorf Centrifuge 5415.

To determine the ATP exchange, 100 µl was taken from the supernatant fraction and diluted in 1:10 with double distilled water. To this, 0.2 ml of ice-cold 15 % Norit A was added and kept aside for 5 min for adsorption. The charcoal was centrifuged and washed 3 times with 1.5 ml of 0.1 M sodium tetra pyrophosphate, each time being mixed by vortexing

followed by centrifugation in order to remove non-specifically bound [^{32}P] pyrophosphate. [^{32}P]ATP was desorbed from the charcoal by washing with 50 % ethanol solution containing 1 M ammonia, followed by pelleting the charcoal. One ml of the supernatant fraction was added to 10 ml Rotiszint 2200 and was then shaken until the suspension was clear. The radioactivity in cpm (≅ dpm, decomposition per minute, because of the high counting efficiency in the case of ^{32}P) was measured for 1 ml in a scintillation counter (Beckman LS 6000TA).

The malate-specific exchange rate was obtained by subtracting the counts in the absence of malate.

2.2.10 Methods for the purification of L-malate activating enzyme

2.2.10.1 Ammonium sulfate precipitation

A saturated ammonium sulfate solution that had been titrated with 25 % of ammonia solution, to a pH of 7, was used to precipitate the protein (Segel, 1976).

The cell extract (see **chapter 2.2.3**) was adjusted with 100 % saturated ammonium sulfate to give a saturation degree of 40 % saturated ammonium sulfate. The solution was stirred gently for 10 min and left standing for 30 min to allow for protein precipitation. The solution was then centrifuged at 40,000 × g (18,000 rpm) for 30 min at 4^{o}C (Sorvall RC 5C Plus) and the pellet formed was discarded.

The resulting supernatant solution was adjusted with 100 % saturated ammonium sulfate to give a saturation degree of 65 % saturated ammonium sulfate, stirred for 10 min and allowed to stand for 30 min for further protein precipitation. The suspension was centrifuged this time at 31,000 × g (16,000 rpm) for 30 min at 4^{o}C. The formed pellet was dissolved in minimum amount of dialysis buffer and dialyzed against 10 volumes of the dialysis buffer.

The malate-specific ATP-PPi-exchange was tested in the crude extract, supernatant, and the dissolved pellet from the 65 % ammonium precipitate before and after dialysis.

2.2.10.2 Hydrophobic Interaction Chromatography (HIC)

Protein binding to HIC adsorbents is promoted by moderately high concentrations of anti-chaotropic salts, which also have a stabilizing influence on protein structure. Elution is achieved by a linear or stepwise decrease in the concentration of salt in the adsorption buffer.

Close to the surface of the hydrophobic column and solute, the water molecules are more highly ordered (less entropically favorable) than in the bulk water. To minimize the extent of ordered water structure, hydrophobic residues come together as to form a minimum contact surface with water ("hydrophobic binding"). Added salt interacts strongly with the water molecules around the interfaces leaving less structured water available and thus eliminating hydrophobic binding (Melander and Horvath, 1977).

The protein precipitated in the presence of 65 % saturated ammonium sulfate was suspended in a minimum amount of dialysis buffer. After adjusting the conductivity to close to that of the initial buffer, the sample was loaded onto 50 ml butyl-Toyopearl 650-M (TosoHaas, Japan) hydrophobic interaction column (0.8 × 25 cm) equilibrated with 1.5 M ammonium sulfate in chromatography buffer (see **chapter 2.1.1.4**). The elution was carried out in a descending gradient of 130 ml from 1.5 to 0 M ammonium sulfate with 50 mM Tris/HCl buffer, pH 7.5, at 1ml/min.

2.2.10.2.1 Details are as follows:

A Pharmacia fast-performance liquid chromatography (FPLC) system was used. Buffers were degassed. Pump A and B of the FPLC instrument were washed with CB_0 and CB_{AS} respectively. The hydrophobic interaction column (50 ml butyl-Toyopearl 650-M) was equilibrated with CB_{AS}. The protein sample was loaded onto the equilibrated column and eluted with CB_{AS} (Pump B; 1 ml/min) till the breakthrough appears (UV absorbance), and the unbound protein was washed out completely. The elution was then carried out in a descending ammonium sulfate gradient. It started with 100 % CB_{AS} with Pump B and ended with 100 % CB_0 with Pump A at a rate of 1ml/min for 130 min. Two ml fractions were collected. The ATP-PPi-exchange assay was carried out with the fractions showing high E_{280}. Active

fractions were concentrated against solid sucrose and stored at –80°C. The amount of sucrose was calculated to give a 10 M solution if completely dissolved in the sample solution.

2.2.10.3 Chromatography on Blue Sepharose CL-6B

The dye (cibacron blue F3G-A, which is covalently attached to the highly cross-linked agarose gel via the triazine part of the dye molecule) is supported to mimic nucleotides such as AMP and NAD (Bohme et al., 1972). Thus Blue Sepharose CL-6B could be called as affinity column. Affinity chromatography is a powerful and generally applicable means of purifying the proteins on the basis of the substrate binding specificities. The proteins retained on the column are those that bind specifically to a ligand cross-linked to the beads. After non-specific proteins are removed by washing the column, the bound protein of interest is eluted by a solution containing free ligands, or in many cases, high salt concentrations.

A column (0.8 × 10 cm) filled with Blue Sepharose CL-6B was suspended in 10 mM MOPS buffer at a pH of 7.5 and then equilibrated by washing with two volumes of *CB A* (see **chapter 2.1.1.5**).

Sucrose concentrated pooled fractions from hydrophobic interaction chromatography were loaded onto the equilibrated column and washed with buffer *CB A* (Pump B; 0.2 ml/min) until measured E_{280} had returned to the baseline. In this breakthrough, the unbound protein is washed out completely. Then a step-elution was carried out with buffer *CB B*, collecting 1 ml fractions. Active fractions of the step-elution were concentrated against solid sucrose and stored at –80°C.

2.2.11 Protein-adenylate formation studies with [α-^{32}P]ATP

Enzyme-adenylate formation reaction was studied by carrying out the assay with the reaction mixture (100 µl) contained ligase buffer (see **chapter 2.1.1.9**), 5 µCi of [α-^{32}P]ATP (3,000 Ci/mmol, Amersham Corp.), and 66 µg of the concentrated Toyopearl 650-M fraction. Effects of different concentrations of following reagents were carried out:

non-labeled ATP (stock solutions: 40 µM, µl ranging from 4-25 and 5 mM, µl ranging from 1-20),

α,β-methylene ATP (stock solutions: 40 µM, µl ranging from 4-25 and 5 mM, µl ranging from 1-20),

β,γ-methylene ATP (stock solutions: 40 µM, µl ranging from 4-25 and 5 mM, µl ranging from 1-20),

L-malate (stock solutions: 10 mM, µl ranging from 1-10 and 100 mM, 10 µl),

pyrophosphate (stock solutions: 200 µM, µl ranging from 5-25, 2 mM, µl ranging from 5-10, and 20 mM µl ranging from 3-15),

oxalic acid and succinic acid (stock solutions: 100 mM, µl ranging from 1-10 and 1 M, µl ranging from 5-10). Kinetics of protein-adenylate formation was carried out. Effects of various kinase inhibitors like Tyrphostin A 23 (stock solutions: 1 mM, 4 µl and 50 mM, µl ranging from 1-20, ethanol as solvent), Rottlerin (stock solutions: 1 mM, µl ranging from 1-5 and 40 mM, µl ranging from 2,5-25), and KT 5720 (stock solutions: 1 mM, µl ranging from 1-5 and 50 mM, µl ranging from 2-20, DMSO as solvent) on protein-adenylate formation were studied. Reaction mixtures were incubated at 25^{o}C for 15 min (all experiments except in kinetics study, where different incubation time ranges were selected). Aliquots of 20 µl sample from each of the reaction mixtures were mixed with 20 µl of SDS buffer (see **chapter 2.1.1.13**) and heated at 85^{o}C for 5 min. The proteins were separated by electrophoresis on a 10 % SDS-PAGE and the protein-adenylate formation was detected by autoradiography (Lumi-Film Chemiluminescent Detection Film, Boehringer Mannheim) transferred onto the nitrocellulose filter at -80^{o}C for respective time periods.

2.2.12 Phosphorylation studies with [γ-^{32}P]ATP

Phosphorylation studies were studied by carrying out the assay with the reaction mixture (100 µl) contained ligase buffer (see **chapter 2.1.1.9**), 5 µCi of [γ-^{32}P]ATP (5,000 Ci/mmol, Amersham Corp.), and 66 µg of the concentrated Toyopearl 650-M fraction. Effect of different concentrations of α,β-methylene ATP, β,γ-methylene ATP, L-malate, oxalic acid, and succinic acid, and kinetics of phosphorylation were carried out. Effects of various kinase inhibitors like Tyrphostin A 23, Rottlerin, and KT 5720 on phosphorylation studies were conducted. Reaction mixtures were incubated at 25^{o}C for 15 min (all experiments except in kinetics study, where different incubation time ranges were selected). Aliquots of 20 µl

sample from each of the reaction mixtures were mixed with 20 µl of SDS buffer (see **chapter 2.1.1.13**) and heated at 85°C for 5 min. The proteins were separated by electrophoresis on a 10 % SDS-PAGE and the phosphorylation was detected by autoradiography (Lumi-Film Chemiluminescent Detection Film, Boehringer Mannheim) transferred onto the nitrocellulose filter at -80°C for respective time periods.

2.2.13 Non-denaturing PAGE

Adenylation and phosphorylation were carried out in reaction mixtures of 100 µl containing ligase buffer (see **chapter 2.1.1.9**) and 5 µCi of either [α-^{32}P]ATP (3,000 Ci/mmol, Amersham Corp.) or [γ-^{32}P]ATP (5,000 Ci/mmol, Amersham Corp.), 66 µg of the concentrated Toyopearl 650-M fraction. After incubation of the reaction mixtures at 25°C for 15 min, 20 µl samples were combined with 20 µl of sample buffer (see **chapter 2.1.1.12**). The proteins were separated by electrophoresis and then transferred onto nitrocellulose filters. The nitrocellulose filters were stained with Ponceau S and the proteins were visualized (Walker, 2002). The bands formed were detected by autoradiography (Lumi-Film Chemiluminescent Detection Film, Boehringer Mannheim) at -80°C for 14 days.

2.2.14 Thin Layer Chromatography (TLC)

The chromatography tank was filled with the solvent system (dioxane:ammonia:water in a ratio of 6:1:4 by volume) (Guranowski et al., 2000) to a level of approximately 0.5 cm and kept closed with a lid for 1 hr to saturate the chamber.

The sample of approximately 1 µl was loaded on to the TLC plate 1.5 to 2 cm from the bottom by means of a micropipette. Right afterwards, the sample spots were dried gently using a hair dryer. While immersing the TLC plate into the solvent system, care was taken to maintain the sample spots above the solvent level. The TLC plate was developed for approximately 90 min and dried with a hair dryer. The nucleotides on the chromatogram were visualized by an ultraviolet light (254 nm). The TLC plates were incubated with a film (Lumi-Film Chemiluminescent Detection Film, Boehringer Mannheim) at -80°C for 4 days.

The Rf values of standards ATP, ADP and AMP were obtained with stock solutions of 5 mM and 10 mM nucleotides to be 3.7, 5.7 and 7 respectively.

2.2.15 L-[^{14}C]malic acid studies

The reaction mixture cocktail of 100 µl contained ligase buffer (see **chapter 2.1.1.9**), 1 µCi of L-[1,4(2,3)-^{14}C]malic acid (55 mCi/mmol, Amersham Corp.), 2 mM ATP, and 66 µg of the concentrated Toyopearl 650-M fraction and incubated at 25^{o}C for 40 min. Then, the reaction was stopped by mixing 10 µl of sample with 10 µl of 50 mM of ATP, and spotted onto a TLC plate (see **chapter 2.2.14**) (TLC aluminium sheets Silica gel 60 F_{254}, Merck). The plate was then developed on autoradiography (Lumi-Film Chemiluminescent Detection Film, Boehringer Mannheim) -80^{o}C for 14 days. The experiment was also conducted with a higher concentration of radioactivity of 5 µCi instead of 1 µCi.

2.2.16 Product analysis by reversed-phase HPLC

The detector of the high performance liquid chromatography (HPLC) system translates the changes in the chemical composition of the column effluent during the chromatographic run into an electrical signal. This signal can then be recorded or digitized and processed to give the required information about the sample composition (Kok, 1998). Reversed-phase (RP) mode of HPLC uses a non-polar stationary phase and a polar mobile phase. RP is ideally suited for separations of non-polar and moderately polar compounds. Thus solutes that are not separated by liquid-liquid chromatography (LLC) or liquid-solid chromatography (LSC) can be easily resolved using this technique (Krustulović et al., 1982).

The analysis of the reaction products mentioned in **chapter 3.12.3** were carried out on a C_{18} reversed-phase column (Macherey-Nagel) and a Merck-Hitachi HPLC system, which consisted of LaChrom L-7100 pump, LaChrom L-7400 UV-Monitor, LaChrom D-7500 Integrator, and a 7725i inject valve. Pump A and B of the HPLC instrument were washed with buffers, *CB$_1$* and *CB$_2$*, respectively. Buffers were degassed. The reversed-phase column (C_{18}) was washed with *CB$_1$*. The sample (20 µl from the 100 µl of reaction product, pH adjusted to 2.1 with phosphoric acid) was loaded onto the column and eluted with a gradient. The elution

program (CB_1, as aqueous component, 1 ml/min) was as follows: 0-5 min 10 % CB_2, 5-15 min 20 % CB_2, 15-25 min 90 % CB_2, 25-27 min 90 % CB_2, and 27-35 min 0 % CB_2. Eluted peaks (220 nm scanning wavelength) of interest were integrated for quantitation (Gasslmaier et al., 2000). At the end, the column was washed with CB_1 at 0.5 ml/min for 1 hr, so that it would be ready for another analysis.

3 RESULTS AND DISCUSSION

3.1 Preparation of [^{32}P]-pyrophosphate by pyrolysis of orthophosphate and ion exchange chromatography

In pilot tests, non radioactive samples were used to optimize separation conditions. Both Pi and PPi were separated by chromatography on a Dowex 1X2 (100-200 mesh, Cl-form) column and the elution profiles were determined with the colorimetric phosphate test (**chapters 2.2.5.4 & 2.2.5.5**). The optimized conditions under **chapter 2.2.5.2** were applied to completely separate Pi and PPi in the radioactive sample after pyrolysis. In **Fig. 1**, the results of the separation of two batches are represented.

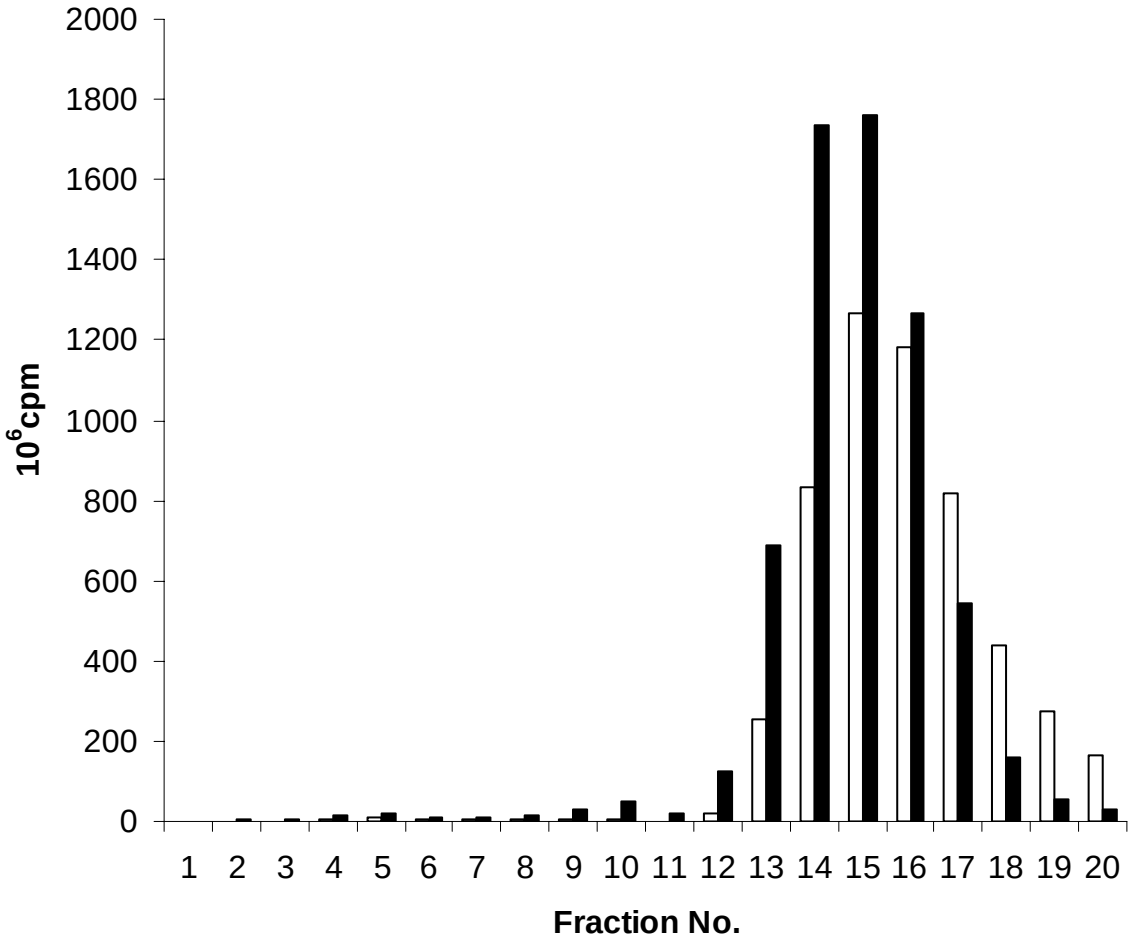

Fig. 1: Elution profiles of the separation of [^{32}P] orthophosphate and [^{32}P] pyrophosphate of two different batches by chromatography on Dowex 1X2 (0.6 × 3 cm) column: The total radioactivity of the pyrolyzed product, which to be separated into Pi and PPi, was 2 mCi (= 4.44 × 10^9 dpm). The orthophosphate fractions were eluted within the first 25 ml of 0.05 M NaCl in 0.01 N HCl. Ten fractions of 2.5ml each (1 to 10) were collected. This fraction was immediately followed by the elution of pyrophosphate fractions with 10 ml of 0.5 M NaCl. Ten fractions of 1ml each (11 to 20) were collected. The yields of 6.55 × 10^9 cpm (black columns) and 5.3 × 10^9 cpm (white columns) were determined by counting the radioactivity of all the fractions. The black and white columns were two batches of experiments. In both cases approximately 99 % of separation was achieved.

3.2 Purification of an L-malate-dependent ATP-[^{32}P]PPi-exchange activity from microplasmodia and concomitant optimization of an enzyme assay

3.2.1 Preface

The optimization of the ATP-[^{32}P]PPi-exchange assay was based on the original assay reported by Bildl, 1998. The assay was, however, qualitatively not reproducible depending on the kind of preparation and degree of protein purification. After each purification step, the activity of the protein sample was investigated for various assay conditions, especially for the dependence on the concentration of L-malate.

The various attempts were aimed at the establishment of an overall assay, that gave qualitatively reproducible results for all enzyme samples investigated.

3.2.2 Ammonium sulfate precipitation of plasmodium extract

Microplasmodia were cultured and harvested according to the standard conditions given in materials and methods. Microplasmodia, which had been harvested from two to three days old shaken cultures, were weighed in a ratio of 1:2 with ice-cold extraction buffer (**chapter 2.1.1.2**) and ruptured using the Ultra Turrax T 25 at high speed (instrument setting

No. 6: 24,000). The cell debris was separated by centrifugation at 18,000 × g (12,000 rpm) for 20 min at 4°C. The supernatant protein sample was divided into two fractions.

A 100 % saturated ammonium sulfate solution that had been titrated with 25 % of ammonia solution, to a pH of 7, was used to precipitate the protein in the first fraction (Segel, 1976) by adjusting the concentration of ammonium sulfate to 40 % saturation in the sample. The solution was stirred gently for 10 min and left standing for 30 min to allow for protein precipitation. The solution was then centrifuged at 40,000 × g (18,000 rpm) for 30 min at 4°C, and the pellet formed was discarded.

The resulting supernatant was adjusted to 65 % saturation by the 100 % ammonium sulfate solution, stirred for 10 min, and allowed to stand again for 30 min for further protein precipitation. The solution was centrifuged at 31,000 × g (16,000 rpm) for 30 min at 4°C. The formed pellet was dissolved in a minimum amount of dialysis buffer (**chapter 2.1.1.3**). The protein solution was dialyzed against 10 volumes of dialysis buffer.

The second fraction of the supernatant after cell ruptue was dialyzed without the addition of ammonium sulfate. The L-malate-specific ATP-PPi-exchange was tested with both fractions of ammonium sulfate-precipitated and non-precipitated protein solutions.

The reaction mixture (1 ml) contained 50 mM Tris /HCl at a pH of 7.5, 5 mM magnesium chloride, 50 mM potassium fluoride, 5 mM β-mercaptoethanol, 1 mM L-malate, 2 mM tetra sodium pyrophosphate, 2 mM ATP (pH 6-8), 1 mM spermine tetrahydrochloride, 0.5 mg/ml BSA (heat-denatured, hBSA) and a sufficient amount of [^{32}P] pyrophosphate was added to adjust it to 10^6 cpm, and finally, the sample was added.

In **Fig. 2**, the results of the L-malate-dependent exchange reactions of both the ammonium sulfate-precipitated and non-precipitated fractions are displayed as a function of L-malate concentration.

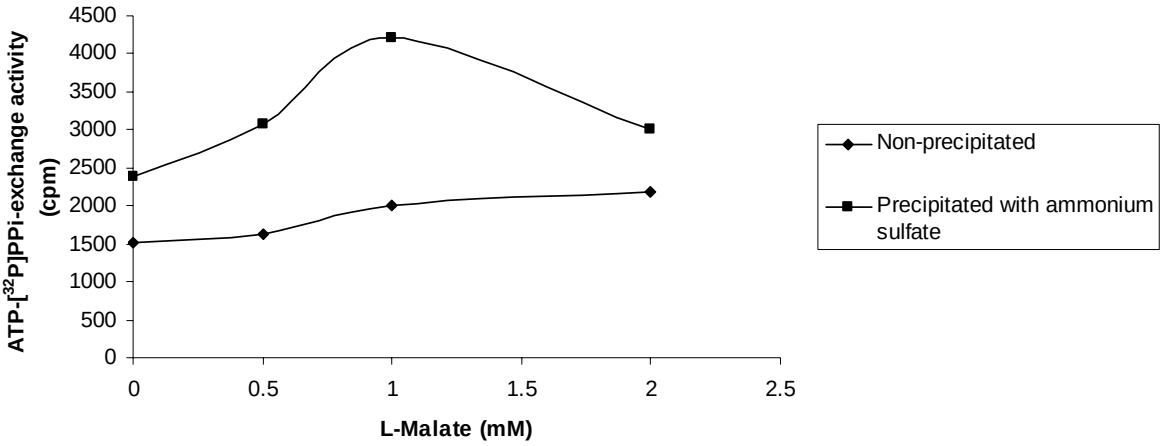

Fig. 2: Effect of ammonium sulfate precipitation on the L-malate-dependent ATP-[^{32}P]PPi-exchange reaction.

The dependence shown in the **Fig. 2** exhibited exchange activity in the absence of added L-malate. Addition of L-malate caused an increase in exchange activity that proceeds through a maximum. Then the activity declined. Thus, at least 3 phases in the concentration dependency are summarized: (1) spontaneous exchange activity, (2) L-malate-dependent activity, (3) inhibition of exchange activity by high concentration of L-malate. The goal of the many attempts during protein purification was to eliminate (1) and (3) by varying conditions in the assay and during sample purification. Ideally, a dependence of the exchange activity was desired, which followed the hyperbolic dependence of L-malate concentration according to Michaelis-Menten.

3.2.2.1 *The effect of the ammonium sulfate percentage used for precipitation*

The supernatant after removal of cell debris was divided into four fractions. An adequate amount of saturated ammonium sulfate was added to the first fraction until it was 35 % saturated, similarly, each of the remaining three fractions achieved 45 %, 55% and 65 % saturation respectively. Each fraction was treated as in the chapter before, and activity measured after dialysis. The results of the radioactive exchange assay are shown in Table 1. From the results of this experiment, an improved ammonium sulfate precipitation method was designed in such a way that an adequate amount of saturated ammonium sulfate was added at first until 50 % saturation. Then, the solution was stirred gently for 10 min and left standing

for 30 min for protein precipitation. The suspension was centrifuged at 40,000 × g (18,000 rpm) for 30 min at 4°C and the pellet formed was discarded. To the supernatant again a sufficient amount of saturated ammonium sulfate solution was added until it was 65 % saturated. It was stirred for 10 min and left standing for 30 min for the precipitation of protein. The solution was centrifuged at 31,000 × g (16,000 rpm) for 30 min at 4°C.

Ammonium Sulfate Saturation (%)	**1mM L-Malate (cpm)**	
	-	+
35	133	150
45	130	186
55	449	397
65	1102	1741

Table 1: The fractions, which were saturated with 55 and 65 % of ammonium sulfate, were found to have the highest activity.

The radioactive assays of the 65 % saturated samples, of two independent experiments, of which the 40 % and 50 % precipitation had been previously removed, were compared. The comparison of activities, however, proved that the sample after the 50 % pre-fractionation showed a very low activity cpm count compared to that of the 40 % pre-fractionation (data not shown). In future experiments, 40 % pre-fractionation was carried out and then followed by 65 % fractionation.

3.2.2.2 *The effect of dialysis on the enzyme activity after ammonium sulfate precipitation*

The pellet of protein, which had been precipitated with saturated ammonium sulfate to a correspondence of 65 % saturation, was suspended in a minimum amount of dialysis buffer. One portion was dialyzed against 10 times of its volume for 5 to 8 hours or kept over night. Another portion was not dialyzed. Both solutions were tested for enzyme activity of the L-malate-dependent/independent exchange. In **Fig. 3**, the results of the exchange assay of both dialyzed and non-dialyzed fractions are shown.

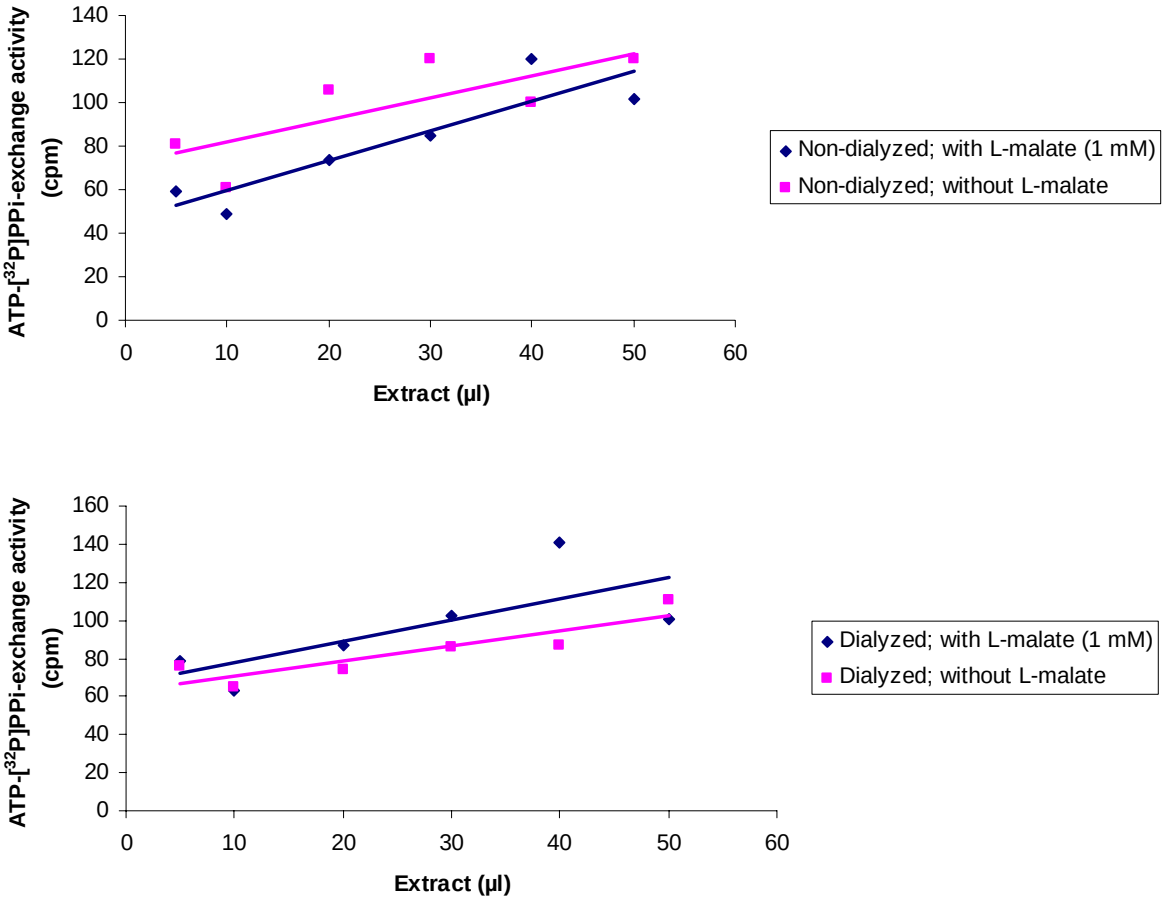

Fig. 3: The effect of dialysis in the L-malate-dependent exchange reactions.

The results show a clear concentration dependence of the sample. However effects of dialysis or L-malate were marginal. This was intriguing, because most previous results had shown a higher activity in the presence of L-malate than in its absence.

3.2.3 Effects of the presence of tetra sodium pyrophosphate and tetra potassium pyrophosphate in the assay mixture

To search for the reason of the L-malate-insensitivity, several experiments were conducted.

The previous ATP-PPi-exchange was carried out in the presence of potassium ions. It was tested whether the exchange of these cations against sodium ions had an effect.

The 65 % ammonium sulfate saturated protein precipitate was suspended in a minimum amount of dialysis buffer and dialyzed against 10 times its volume with dialysis buffer for 5 to 8 hours or kept over night. The effect of the addition of 1 mM of either tetra sodium pyrophosphate or tetra potassium pyrophosphate to the assay mixture was tested, and the results are represented in **Fig. 4**.

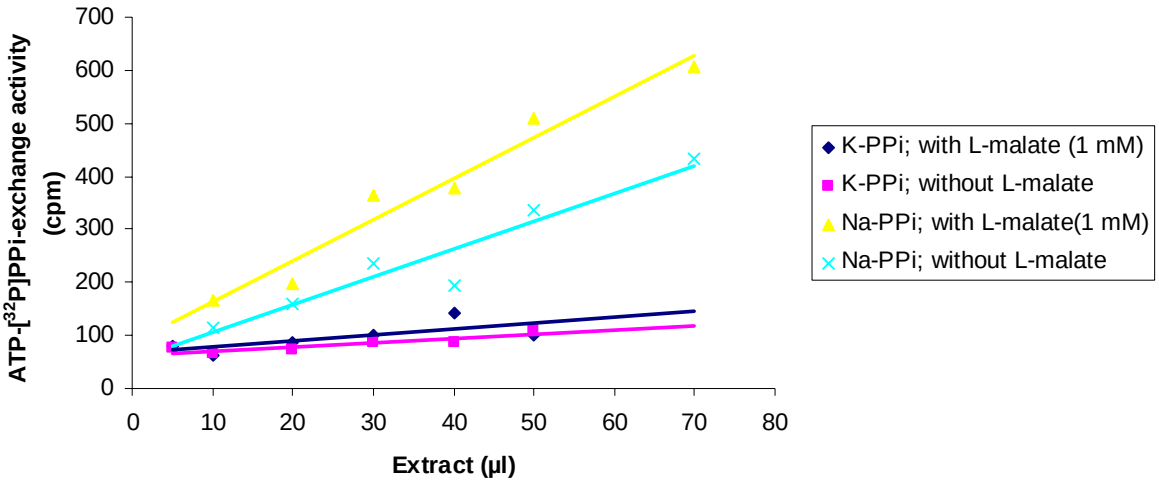

Fig. 4: Effects of tetra sodium pyrophosphate and tetra potassium pyrophosphate in the ATP-PPi assay mixture.

The experiment showed that tetra sodium pyrophosphate resulted in an increased activity compared to that tetra potassium pyrophosphate. Also, in the presence of Na^+, a pronounced activation by L-malate was seen. Future assay mixtures contained from now on Na^+ instead of K^+.

3.2.4 Effects of the assay incubation time on enzyme activity

The volume of each reaction mixture was made up to one ml with water and a sufficient amount of [^{32}P] pyrophosphate was added to adjust it to 10^6 cpm, excluding the L-malate and the sample. L-malate (1 mM) was added to the cocktail buffer (**chapter 2.2.9**) and finally the exchange activity containing sample (usually 40 µl) was added. The test mixture was incubated for various time periods ranging from 20 to 120 min at 30°C. The activity was found to be proportional to the incubation period, which is shown in **Fig. 5**. In future

experiments, the reaction mixture was incubated for 40 min at 30°C, since with this time period no deviation from the linear time dependence occurred.

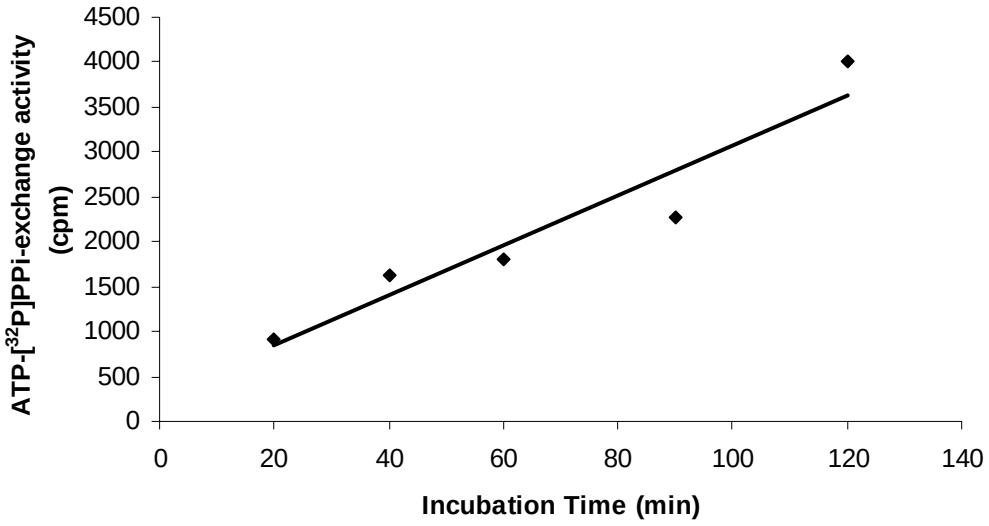

Fig. 5: ATP-PPi-exchange as a fraction of time. The assay contained 40 µl of the 65 % ammonium sulfate precipitate fraction after dialysis (**see chapter 2.2.4**). The assay contained 1 mM of L-malate.

3.2.5 Dependence of ATP-PPi-exchange counts on the amount of supernatant/TCA present during adsorption on charcoal of the standard assay

To examine, whether the amount of reaction solution in the assay after TCA-precipitation has an effect on the yield of [^{32}P]ATP adsorption on the charcoal, the supernatant after the precipitation with TCA in the assay was varied and diluted with water before charcoal adsorption.

The ATP-PPi-exchange reaction was carried out with the 65 % ammonium sulfate precipitated fraction according to standard condition given in materials and methods. To determine the degree of the ATP-PPi-exchange, the reaction was carried out as before and terminated by the addition of 0.5 ml of ice-cold 10 % trichloroacetic acid (TCA). Then immediately various amounts of 50, 100, 300 and 500 µl were removed from the supernatant after centrifugation of the reaction mixture, diluted in 1:20, 1:10, 1:3.3 and 1:2 respectively with double distilled water, and processed for charcoal adsorption as described in materials and methods. The results are shown in **Fig. 6**.

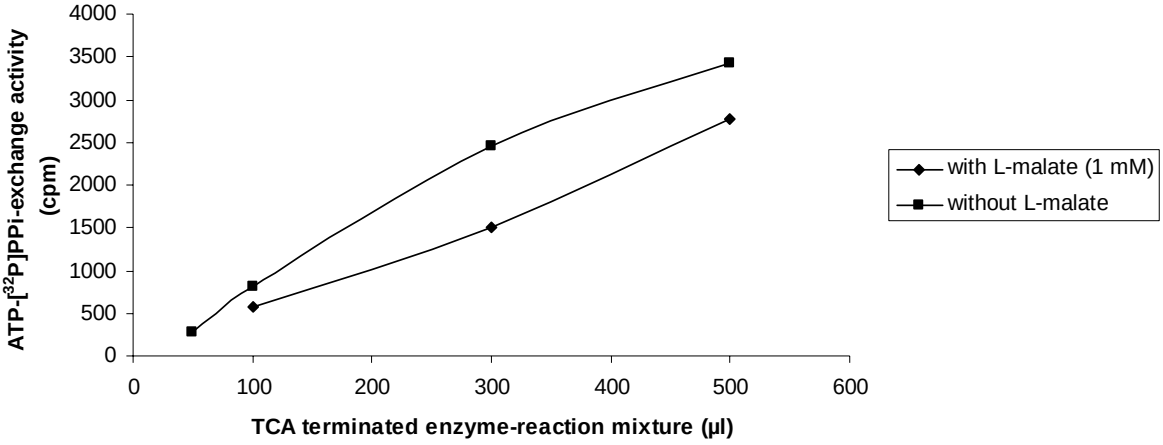

Fig. 6: Dependence on the amount of supernatant after TCA-precipitation. For details see text.

The results show, that the measured counts of [^{32}P]ATP adsorbed to the charcoal is proportional to the amount of reaction product exposed to charcoal adsorption. There is no obvious effect on the malate-dependency.

3.2.6 Dependence of the role of ATP-PPi-exchange on the concentration of tetra sodium pyrophosphate

The ATP-PPi-exchange reaction was carried out with the 65 % ammonium sulfate precipitated fraction and the reaction mixture (**chapter 2.2.9**). The concentration of added unlabelled tetra sodium pyrophosphate varied from 0 to 2 mM. The results are represented in **Fig. 7**.

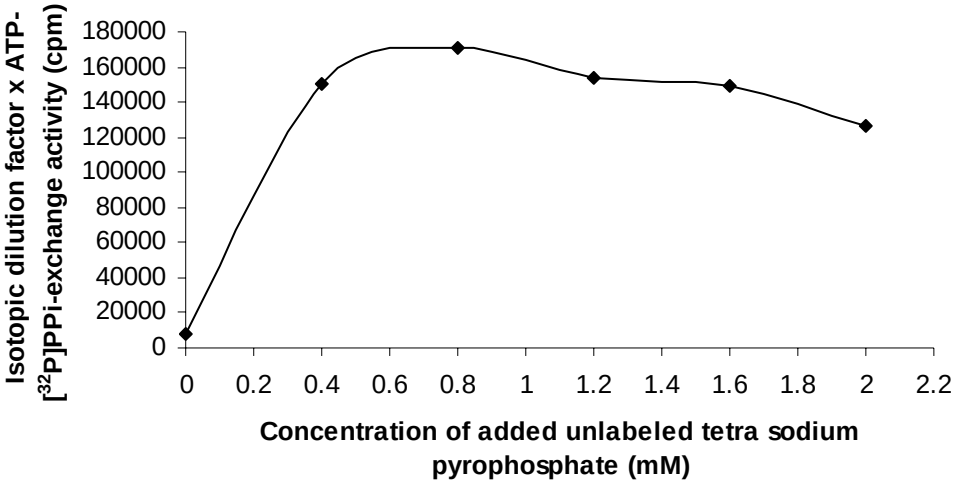

Fig. 7: Concentration dependency of tetra sodium pyrophosphate. The assay contained 1 mM of L-malate.

The decline in cpm corresponds to isotopic dilution of [^{32}P]PPi, opposed to an expected saturation dependence for the substrate. The routine ATP-PPi-exchange assays were carried out in the presence of 2 mM tetra sodium pyrophosphate. When the L-malate concentration dependency was measured, 0.4 mM tetra sodium pyrophosphate was used.

3.3 Purification of the fraction containing ATP-PPi-exchange activity by FPLC Chromatography

3.3.1 Gel Filtrations

3.3.1.1 *Superdex S-200*

The sample after 65 % ammonium sulfate precipitation was suspended in a minimum amount of dialysis buffer. The solution was adjusted to the conductivity of almost close to that of the starting buffer (10 mM MOPS buffer, pH 7.5, containing 0.2 M KCl). The sample was then loaded onto a gel permeation chromatography column, which was a Pharmacia HiLoad 16/60 Superdex S-200 pg column equilibrated with 10 mM MOPS buffer pH of 7.5, containing 0.2 M KCl. The elution was carried out in 1ml fractions of totally 140 ml of 10

mM MOPS buffer pH of 7.5, containing 0.2 M KCl, at a rate of 1ml/min. Extinction at 280 nm was recorded, and the fractions (96 to 106) of the highest protein peak were selected and assayed for ATP-PPi-exchange activity in the presence/absence of L-malate. Protein was measured according to Bradford (1976) and specific activities calculated. The results are shown in **Fig. 8**.

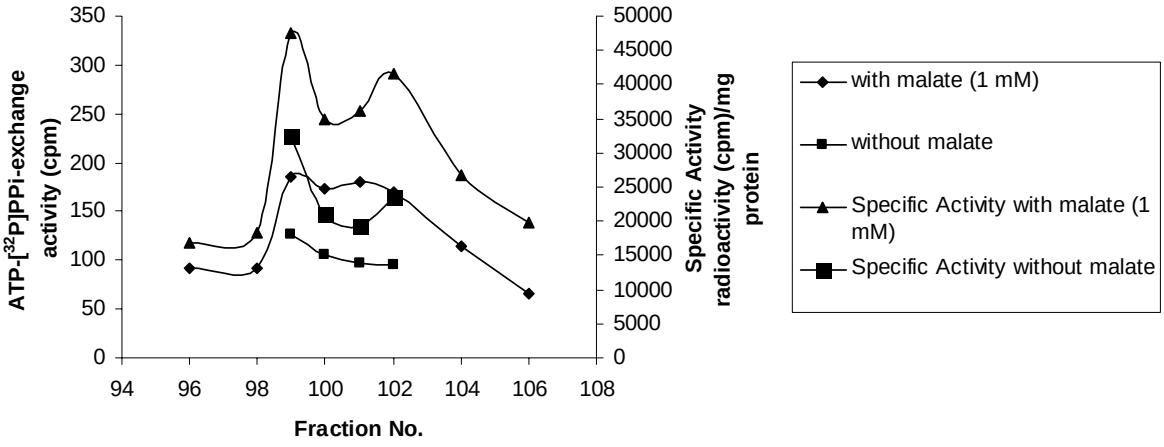

Fig. 8: The ATP-PPi-exchange reactions of the fractions obtained from the gel permeation chromatography.

The activities show a clear dependence in the presence of L-malate and the activity peaks.

3.3.1.1.1 Dependency of the ATP-PPi-exchange activity as a function of eluate concentration after chromatography on 16/60 Superdex S-200 prep. grade

Protein was chromatographed as above. According to E_{280} the eluate was fractionated into pools containing vials of No., 50 – 62 (F1), 63 – 73 (F2) and 74 – 95 (F3). (see **Fig. 9**). ATP-PPi-exchange activity was assayed for F1 and F3 as a function of sample concentration (**Fig. 10**).

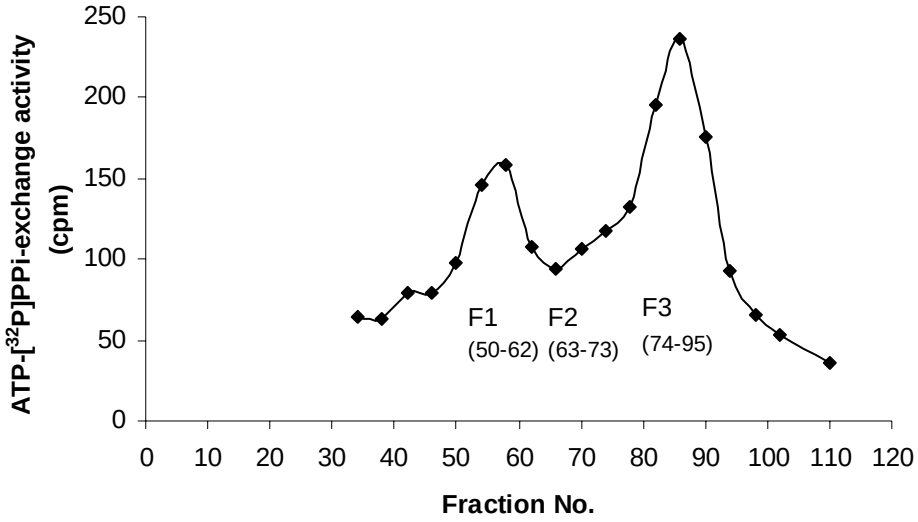

Fig. 9: The ATP-PPi-exchange reactions with the Superdex S-200 fractions. The protein peak fractions from Superdex S-200. The pooled fractions 50 - 62, 63 - 73 and 74 - 95 were called F1, F2 and F3 respectively.

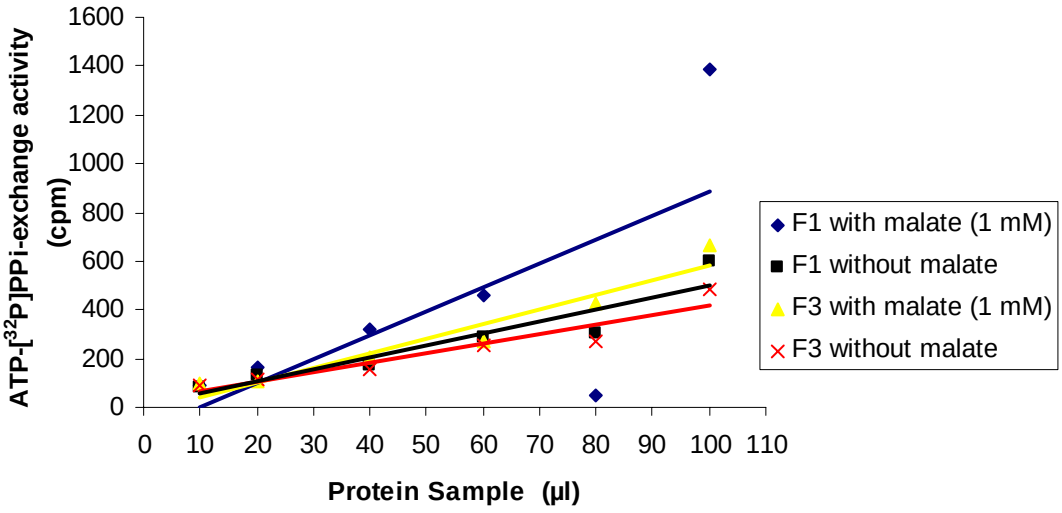

Fig. 10: The ATP-PPi-exchange activity of eluate fractions F1 and F3 as a function of sample concentration. The pooled fractions F1 and F3 from Superdex S-200 pg were tested for their malate-specific ATP-PPi-exchange activity.

The exchange activity shows clearly a concentration dependence. The pool F1 with the higher molecular mass indicates a higher degree of L-malate dependence than pool F3 (lower molecular mass).

3.3.1.2 *Sephacryl S-200*

The 65 % ammonium sulfate precipitate was dissolved in a minimum amount of dialysis buffer. The solution was then adjusted to the conductivity close to that of the starting buffer. The sample was loaded onto a 16/60 Sephacryl S-200 gel permeation column. The elution was carried out in 1 ml fractions with 10 mM MOPS buffer at a pH of 7.5, containing 0.2 M KCl, at a rate of 0.5 ml/min. From the extinction (E_{280}) profile, the fractions (34 - 50) in the absorbance peak, which was in breakthrough, and fractions 62 - 78 were selected, pooled and the ATP-PPi-exchange assay was performed. No activity was found. It was assumed that this type of chromatographic material destroyed the exchange activity.

3.3.2 FPLC Affinity Chromatography

3.3.2.1 *Blue Sepharose CL-6B (HiTrap)*

The 65 % ammonium sulfate precipitated fraction was diluted (2:1) with 10 mM MOPS buffer at a pH of 7.5 and the conductivity was adjusted to close to that of the starting buffer. Then, 3 ml of sample (2 ml of 65% precipitated protein and 1 ml of buffer) was loaded onto a HiTrap Blue (Blue Sepharose CL-6B) pre-made one ml column, which was equilibrated with 10 mM MOPS buffer at a pH of 7.5. The elution was carried out in 1 ml fractions with 10 mM MOPS buffer at a pH of 7.5 and followed by an elution with the same buffer containing 1.5 M KCl (0.5 ml/min). The E_{280}-elution profile shows a high protein peak in the breakthrough and a minor one during under high ionic strength. The ATP-PPi-exchange assay was carried out for fractions under the E_{280}-peaks.

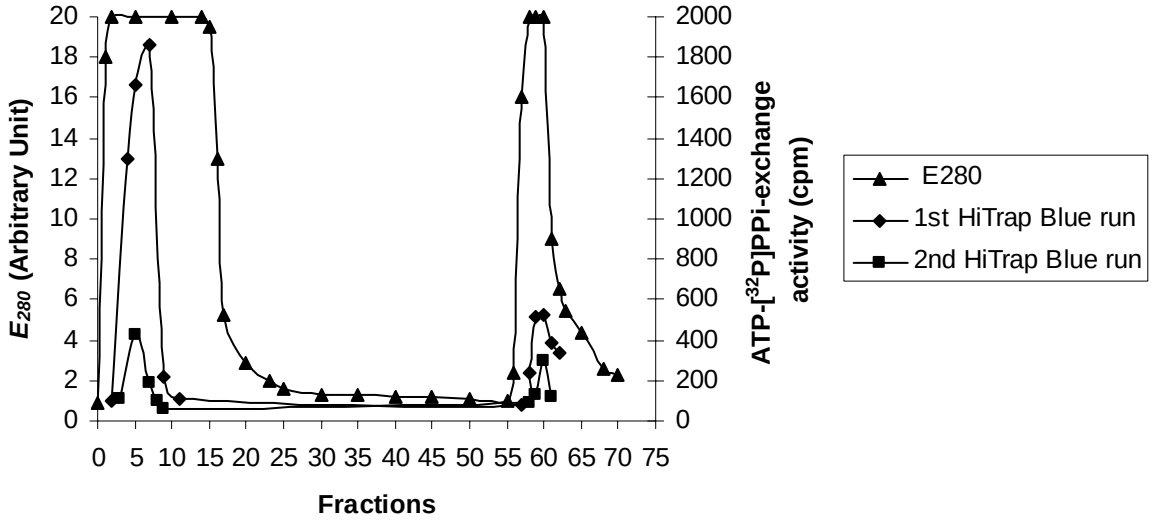

Fig. 11: Chromatography on Blue-Sepharose (HiTrap). The E_{280}-profile is indicated. The ATP-PPi-exchange was carried out for breakthrough fractions 3 to 9 of the 1st run (—◆—) and the re-loaded second run (—■—). The ATP-PPi-exchange was measured in the presence of 1 mM L-malate.

Breakthrough fractions 3 to 9 were pooled and re-loaded onto a second 1ml HiTrap Blue column and eluted as before. The results showed very similar profiles with less cpm counts in the second run. This result indicated that in the first run, the HiTrap Blue column was over loaded (**Fig. 11**).

From the above experiments, a decision was made to increase the column capacity and observe a systematic variation in KCl concentration instead of a step-elution.

The 65 % ammonium sulfate precipitated protein was diluted (2:1) with the 10 mM MOPS buffer at a pH of 7.5 and was then loaded onto a HiTrap Blue (Blue Sepharose CL-6B) pre-made 5 ml column, which was equilibrated with 10 mM MOPS buffer at a pH of 7.5.

A gradient of 30 ml from 0.5 to 1.5 M KCl with 10 mM MOPS buffer (pH 7.5) at a rate of 0.5 ml/min and 0.5 ml fractions was used for elution. From the E_{280}-profile, the fractions with the highest protein content appeared to be at the breakthrough and two other peaks, one at 1 M and another at 1.5 M KCl. These, and other regions of the eluate were tested by the ATP-PPi-exchange assay (**Fig. 12**). The fractions which had the highest cpm counts were pooled as P1 (4 - 20), P2 (70 - 100) and P3 (116 - 125). Pool P1 (4 - 20) was in the breakthrough probably again the result of overload. The malate-dependent ATP-PPi-

exchange was carried out with fractions P2 (70 - 100) and P3 (116 - 125) (**Fig. 13**). From the data, it appears that P2 (70 - 100) was not dependent of L-malate. In the case of P3 (116 - 125), as the L-malic acid concentration was increased from 0 to 1.8 mM the activity achieved a maximum (increased by 30 %) and dropped to low levels after further addition of L-malate.

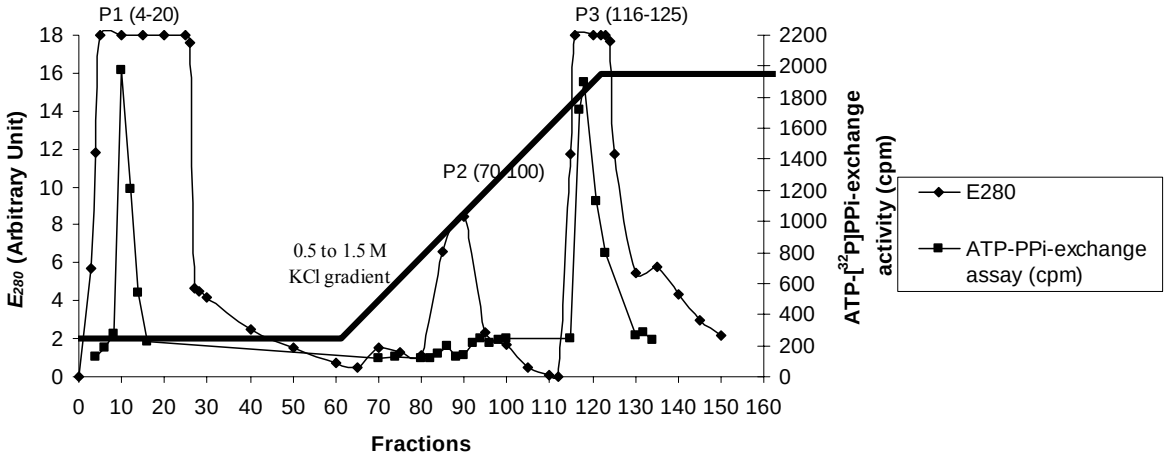

Fig. 12: The ATP-PPi-exchange activity after HiTrap Blue gradient elution. A gradient of 30 ml from 0.5 to 1.5 M KCl with 10 mM MOPS buffer, pH 7.5 at 0.5 ml/min was carried out in a 5 ml HiTrap Blue column. The breakthrough fractions and two other fractions of the eluate were tested by the ATP-PPi-exchange assay. The assay contained 1 mM of L-malate.

The results show that the malic acid-sensitive ATP-PPi-exchange activity can be purified by chromatography on Blue Sepharose HiTrap. It is interesting to note that the activity-malic acid dependence is again biphasic showing an activating and an inhibitory branch.

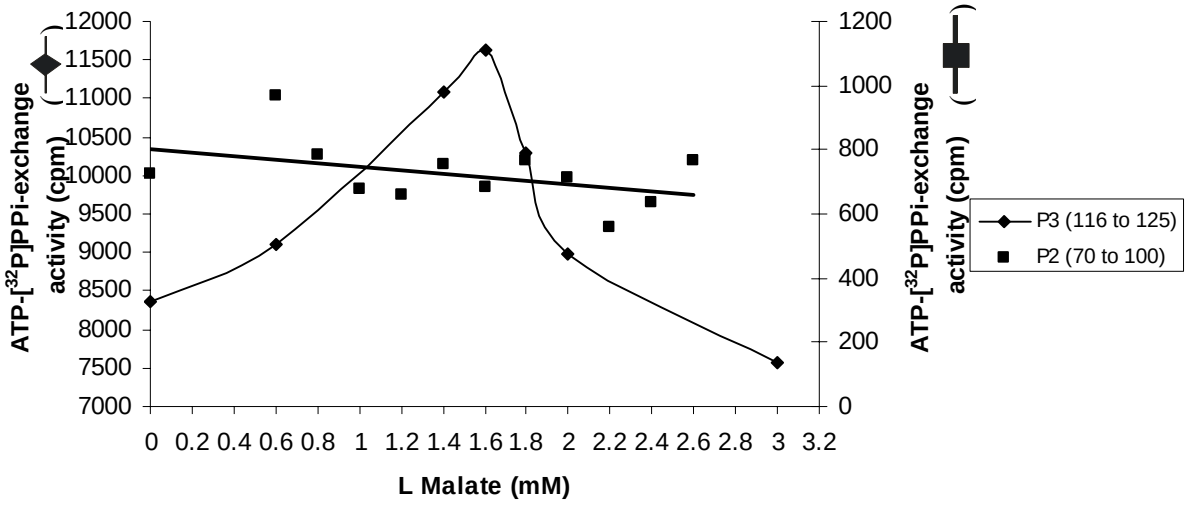

Fig. 13: The malate-dependence of the ATP-PPi-exchange assay for pools P2 and P3. An increase of L-malic acid concentration from 0 to 1.8 mM in the assay resulted in a 30 % increase in activity. However, a decrease of 35 % was obtained for an increase in concentration of L-malate from 1.8 to 3 mM.

Chromatography on Blue Sepharose HiTrap was repeated under various conditions of elution rate and gradient forms such as single salt steps before salt gradients, applying low and high salt concentrations with upper limits of 2 M KCl.

From all these experiments it was understood that the protein of interest which gave the ATP-PPi-exchange activity counts appeared approximately at 0.8 M salt. If the experiment is carried out in shallow gradient such as 0.5 to 1.5 M or 0.5 to 2 M, the eluate splits into two activity peaks. **Fig. 14** depicts the result of the gradient from 0.5 to 2 M KCl. The splitting into different elution peaks suggested that different protein complex might be involved.

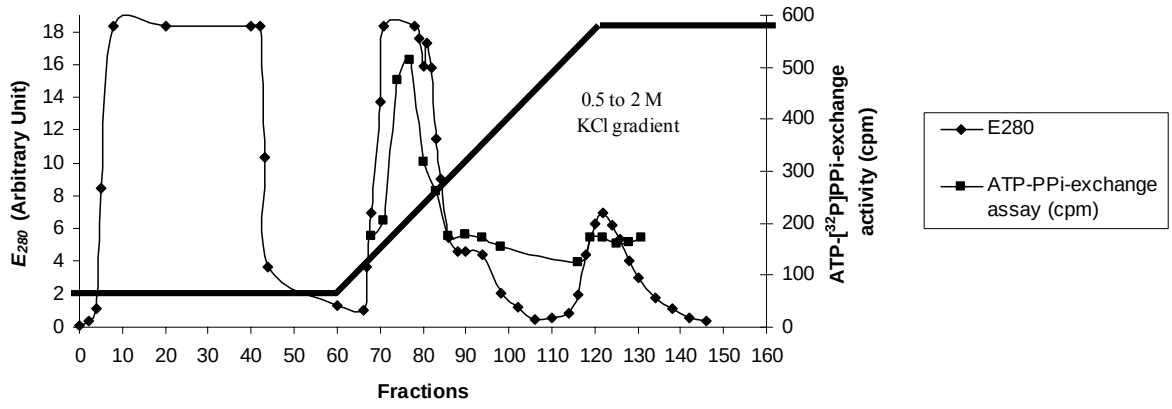

Fig. 14: The ATP-PPi-exchange assay with Blue Sepharose CL-6B shallow gradient fractions. A gradient of 30 ml from 0.5 to 2 M KCl with 10 mM MOPS buffer, pH 7.5, at 0.2 ml/min were carried out in a 6 ml Blue Sepharose CL-6B. Breakthrough fractions 1 to 62 were eluted with 10 mM MOPS buffer, pH 7.5, and fractions 66 to 126 appeared in the gradient profile of 0.5 to 2 M KCl with 10 mM MOPS buffer, pH 7.5. Two protein peaks could be seen in the FPLC UV absorbance profile, as well as by the ATP-PPi-exchange assay. The assay contained 1 mM of L-malate.

In future experiments it was found advantageous using a step-elution with 1 M KCl, in which all the protein of interest that were bound to Blue Sepharose CL-6B column was eluted. The results are shown in **Fig. 15**, in which no activity was found when a step elution of 2 M KCl was followed the elution at 1 M KCl.

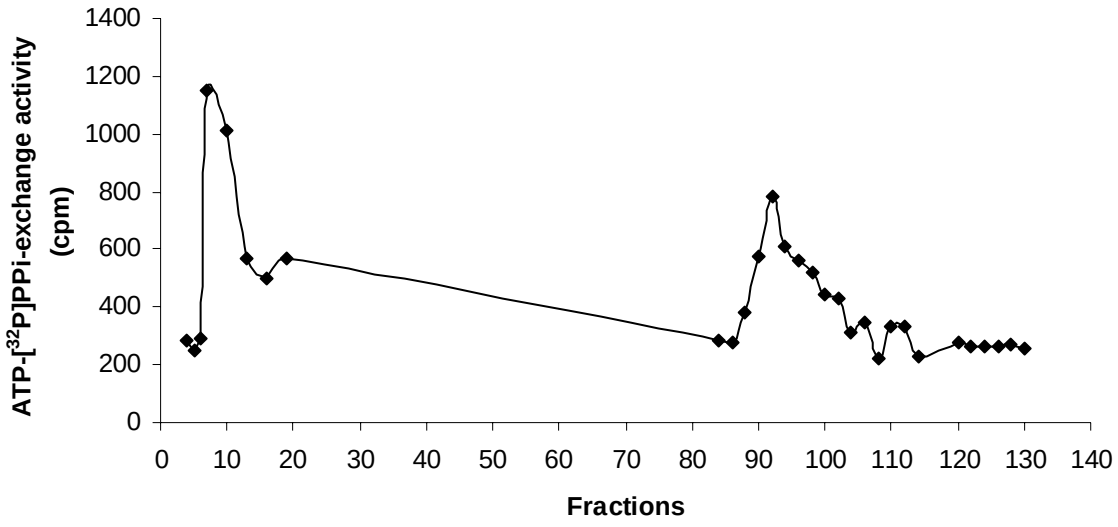

Fig. 15: The ATP-PPi-exchange assay with Blue Sepharose CL-6B step-elution fractions. Step-elutions of 1 M and 2 M KCl with 10 mM MOPS buffer, pH 7.5, at 0.2 ml/min were carried out in a 6 ml Blue Sepharose CL-6B. Fractions from 67 to 116 and 117 to 156 were eluted by the step-elutions 1 M and 2 M KCl respectively. The activity in fractions, 8-15 belongs to the breakthrough. The assay contained 1 mM of L-malate.

3.3.3 FPLC Ion Exchange Chromatography

3.3.3.1 *DE 52 anion exchange column*

3.3.3.1.1 Optimization of chromatography on DE 52 column:

A column was packed with 20 ml of DE 52 and equilibrated with 10 mM MOPS buffer, pH 7.5, at 0.2 ml/min. The column was tested for breakthrough elution by adding different quantities of crude extract. One ml of crude extract which was precipitated with ammonium sulfate corresponding to 65 % saturation, and subsequently dialyzed as described in materials and methods, was loaded onto the column and eluted with 10 mM MOPS buffer, pH 7.5, at 0.2 ml/min. After washing with approximately 20 ml of buffer, the extinction (E_{280}) returned to the base line. Another 2 ml of the crude extract was then injected into the column making the total amount of crude extract 3 ml. Again, the column was washed with the same buffer to bring the absorbance back to the base line. The procedure was repeated by adding to the column further increments of 2 ml of crude extract to a total of 5 ml, 7 ml, and finally 9 ml. All these fractions were assayed by the ATP-PPi-exchange reactions. It was concluded from both the activity and E_{280}-measurments (not shown) that 5 ml volume was optimal for loading.

After loading a fresh column with 5 ml of the ammonium sulfate precipitation and subsequently dialyzed fraction, the column was washed with 10 mM MOPS buffer, pH 7.5, at 0.2 ml/min, until the extinction (E_{280}) was returned to the base line. A two step-elution was carried out with 0.3 M KCl and 0.5 M KCl in 10 mM MOPS buffer, pH 7.5, at 0.2 ml/min. The breakthrough and step-elution fractions were tested for ATP-PPi-exchange (± L-malate) (results are not shown). The ATP-PPi-exchange activity was found only in the breakthrough fractions.

To account for the elution at higher than 0.5 M KCl in the above experiment, the column after clearing from the breakthrough was eluted in the presence of 0.8 M KCl in 10 mM MOPS buffer, pH 7.5, at 0.2 ml/min. The ATP-PPi-exchange activity in the eluate was low and scattered. The results suggested that the purification method was not useful.

3.3.3.2 *Mono Q anion exchange column*

A column was packed with 1 ml of Mono Q and equilibrated with 10 mM MOPS buffer, pH 7.5 at 0.2 ml/min. 1 ml of crude extract, after precipitation with saturated ammonium sulfate (to give the final concentration of 65 % saturation), and dialyzed, was loaded onto the column and eluted with 10 mM MOPS buffer, pH 7.5, at 0.2 ml/min, until the extinction (E_{280}) came down to the base line. This was followed by 2 separate step-elutions of 0.3 M KCl and then to 1.5 M KCl in a solution of 10 mM MOPS buffer, pH 7.5, at 0.2 ml/min (results are not shown). Again, only the breakthrough fraction contained ATP-PPi-exchange activity.

3.3.3.2.1 Chromatography of the DE 52 breakthrough over Hydroxylapetite

A column was packed with 10 ml of Hydroxylapetite and equilibrated with 10 mM MOPS buffer, pH 7.5 at 0.2 ml/min. 4 ml of crude extract, which had been precipitated with saturated ammonium sulfate (corresponding to 65 % saturation) and then dialyzed, was loaded into a 20 ml DE 52 anion exchange column. The column was washed with 10 mM MOPS buffer, pH 7.5, at 0.2 ml/min, until the extinction (E_{280}) was brought back to the base line. Then the fractions showing high E_{280} (> AU 4, see **Fig. 14**) in the breakthrough were tested for ATP-PPi-exchange.

The active fractions were pooled, and 8 ml of the pool was loaded onto the equilibrated Hydroxylapetite column and eluted with the 10 mM MOPS buffer, pH 7.5, at 0.2 ml/min, until the extinction (E_{280}) came down to the base line. Next, step-elutions with 0.5 M KCl and 1.5 M KCl in 10 mM MOPS buffer, pH 7.5, at 0.2 ml/min were carried out (results are not shown). Only the breakthrough was found to contain ATP-PPi-exchange activity.

3.3.3.2.2 Purification of the DE 52 breakthrough over 5-AMP-Sepharose

A column was packed with 3 ml of 5-AMP-Sepharose and equilibrated with 10 mM MOPS buffer, pH 7.5, at 0.2 ml/min, and 2 ml of active fractions of the DE-column breakthrough that had been prepared as before were loaded. The column was eluted with the 10 mM MOPS buffer, pH 7.5, at 0.2 ml/min, until the extinction (E_{280}) was brought down to the base line, followed by two step-elutions of 0.5 M KCl and 1.5 M KCl in 10 mM MOPS buffer, pH 7.5, at 0.2 ml/min (results are not shown). Again, only the breakthrough contained the ATP-PPi-exchange activity.

3.3.3.3 *Heparin Sepharose CL-6B*

Three ml of crude extract, which had been precipitated with saturated ammonium sulfate (65 % saturation) and then dialyzed, was loaded onto the column of Heparin Sepharose CL-6B (20 ml), which had been equilibrated with 10 mM MOPS buffer, pH 7.5, at 0.2 ml/min. After loading the sample to the column, it was washed with 10 mM MOPS buffer, pH 7.5, at 0.2 ml/min, until the extinction (E_{280}) fell back to the base line. Similarly as with Blue Sepharose HiTrap , various experiments were performed, employing different gradients such as 0 to 1.5 M KCl and 0 to 0.6 M KCl with 10 mM MOPS as buffer, pH 7.5, at 0.2 ml/min (results are not shown).

The E_{280}-elution peaks were tested for the ATP-PPi-exchange. It was found that the E_{280}-peaks were shifting to different positions across the gradient depending on the various parameters in analogy as has been previously noted in the case of the Blue Sepharose CL-6B columns. If the elution was carried out in a shallow gradient, the elution profile contained two activity peaks. When the experiment was carried out with a steeper gradient such as 1 to 2 M KCl or 0 to 0.6 M KCl, a single peak appeared at the beginning and at the end of the gradient, respectively; it seemed advantageous to conduct an experiment in a step-elution rather than a gradient elution.

3.3.3.3.1 Chromatography of the DE 52 breakthrough over Heparin Sepharose CL-6B

A column was packed with 2 ml of Heparin Sepharose CL-6B and equilibrated with 10 mM MOPS buffer, pH 7.5, at 0.2 ml/min. Four ml of crude extract, which had been precipitated with saturated ammonium sulfate (65 % saturation) and dialyzed, were loaded onto a 20 ml DE 52 anion exchange column. The breakthrough during elution with 10 mM MOPS buffer, pH 7.5, at 0.2 ml/min, was assayed by the ATP-PPi-exchange reaction, and the fractions with highest activity were pooled. Two ml of the pool were loaded onto Heparin Sepharose CL-6B column. The column was eluted with the 10 mM MOPS buffer, pH 7.5, at 0.2 ml/min, until the extinction (E_{280}) returned to the base line. Step-elutions of 0.5 M KCl and 1.5 M KCl in buffer, pH 7.5, at 0.2 ml/min were performed (**Fig. 16**). The ATP-PPi-exchange assay was carried out for the fractions with high E_{280} (> AU 4, see **Fig. 16**). Both the breakthrough and the 0.5 M KCl step-elution showed ATP-PPi-exchange activity.

From all these experiments, it was concluded that the protein with ATP-PPi-exchange activity was bound to the Heparin Sepharose CL-6B column and could be eluted with solution at ionic strength of 0.5 M KCl.

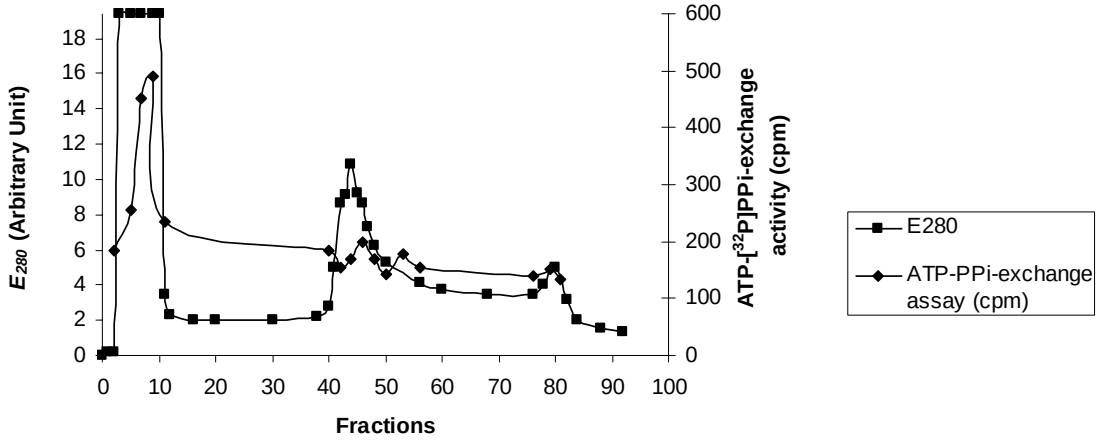

Fig. 16: The ATP-PPi-exchange assay of the eluate after chromatography on Heparin Sepharose CL-6B. A 2 ml Heparin Sepharose CL-6B column was used. Two steps of 20 ml each of 0.5 M and 1.5 M KCl in 10 mM MOPS buffer, pH 7.5, at 0.2 ml/min were applied for elution. Fractions 0 to 20 were breakthrough and fractions 20 to 60 were the elution during the first step in the presence of 0.5 M KCl. Fractions 60 to 92 were eluted in the presence of 1.5 M KCl with 10 mM MOPS buffer, pH 7.5, at 0.2 ml/min. The highest E_{280}-peaks were tested by the ATP-PPi-exchange assay in the presence of 1 mM malate.

3.3.3.3.2 Chromatography of the DE 52 breakthrough over Blue Sepharose CL-6B

The purification of the DE 52 breakthrough over Heparin Sepharose CL-6B was compared with that over Blue Sepharose CL-6B: Five ml of crude extract, which had been precipitated with ammonium sulfate (65 % saturation) and dialyzed, was loaded into a 20 ml DE 52 anion exchange column. The breakthrough was prepared as described (**chapter 3.3.3.3.1**). Also, a step-elution by 0.8 M KCl in 10 mM MOPS buffer, pH 7.5, at 0.2 ml/min was carried out. The fractions with the high E_{280} (> AU 4, see **Fig. 16**) were tested for ATP-PPi-exchange activity in the presence of 1mM malate, and a slight activity was noted in 0.8M KCl fraction.

The breakthrough fractions P1 (13 - 22) and of the 0.8 M KCl eluate P2 (59 - 61) were pooled separately and loaded separately onto different 6 ml Blue Sepharose CL-6B columns, which were equilibrated with 10 mM MOPS buffer, pH 7.5, at 0.2 ml/min. The breakthrough was collected. Then, a gradient of 42 ml from 0 to 0.8 M KCl in 10 mM MOPS buffer, pH 7.5, at 0.2 ml/min followed with both columns, and the ATP-PPi-exchange activity in the eluates were measured. The results (not shown) indicated that the DE 52 breakthrough as well as the 0.8 M eluate of the DE 52 eluted mainly in the breakthrough of the Blue Sepharose CL-6B column, similarly as for the DE 52 breakthrough during chromatography on Heparin Sepharose CL-6B. In addition a small amount of activity appeared at the end of the gradient, however lesser amounts than in the case of Heparin Sepharose CL-6B. It was concluded that the enzyme activity resided in different molecular forms, which were detected similarly on Blue Sepharose and Heparin columns, and which were supposed to reflect different protein complexes.

3.3.4 FPLC Hydrophobic Interaction Chromatography

The protein was precipitated from the cell extract with saturated ammonium sulfate (proportionate to 65 % saturation) and was suspended in a minimum amount of dialysis buffer. The conductivity was adjusted to close to that of the initial buffer. The content of ammonium sulfate was raised to 1.5 M before loading onto an equilibrated (1.5 M ammonium

sulfate in 50 mM Tris/HCl buffer, pH 7.5) 30 ml butyl-Toyopearl 650-S (TosoHaas, Japan) hydrophobic interaction column (0.8 × 15 cm). The elution was conducted in 80 ml of 1.5 M to 0 M ammonium sulfate gradient in 50 mM Tris/HCl buffer, pH 7.5, at 1ml/min. All fractions showing high E_{280} (> AU 4, see **Fig. 16**) were tested for ATP-PPi-exchange activity. The largest fraction of the ATP-PPi-exchange activity appeared towards the end of the gradient, and a slight activity was noted in the breakthrough.

Chromatography was also performed on Toyopearl 650-M, which has a particle size of 65 µm compared to 35 µm particle size of Toyopearl 650-S. A 19 ml quantity of the ammonium sulfate precipitated crude extract was loaded onto 30 ml butyl-Toyopearl 650-M (TosoHaas, Japan) hydrophobic interaction column (0.8 × 15 cm) equilibrated with 1.5 M ammonium sulfate in 50 mM Tris/HCl buffer, pH 7.5. Protein eluted with a descending gradient of 1.5 M ammonium sulfate to 50 mM Tris/HCl buffer, pH 7.5, at a flow rate of 1ml/min. Fractions 162 to 180 with ATP-PPi-exchange activity were pooled and concentrated with sucrose and stored at –80^{o}C. After 24 hrs, an aliquot of 4 ml was loaded again onto a 30 ml column of butyl-Toyopearl 650-S (TosoHaas, Japan) hydrophobic interaction column (0.8 × 15 cm) (equilibrated with 1.5 M ammonium sulfate in 50 mM Tris/HCl buffer, pH 7.5). The column was eluted following the same procedure as in the case of Toyopearl 650-M. The fractions corresponding to the activity peak (fractions 111 to 125) were combined and concentrated with sucrose and stored at – 80^{o}C. The fraction chromatographed on a single Toyopearl 650-M column had an almost 5 times higher activity compared to the fraction additionally chromatographed on Toyopearl 650-S. It was not clear, whether this decrease in activity was due to loss of protein or inactivation by proteolysis.

The fractions purified single or in sequence over the two different Toyopearl hydrophobic interaction columns were analyzed by SDS-PAGE and silver staining (shown in **Fig. 17**). The protein bands distribution and staining intensities were similar. In future purification work, only a single HIC was carried out.

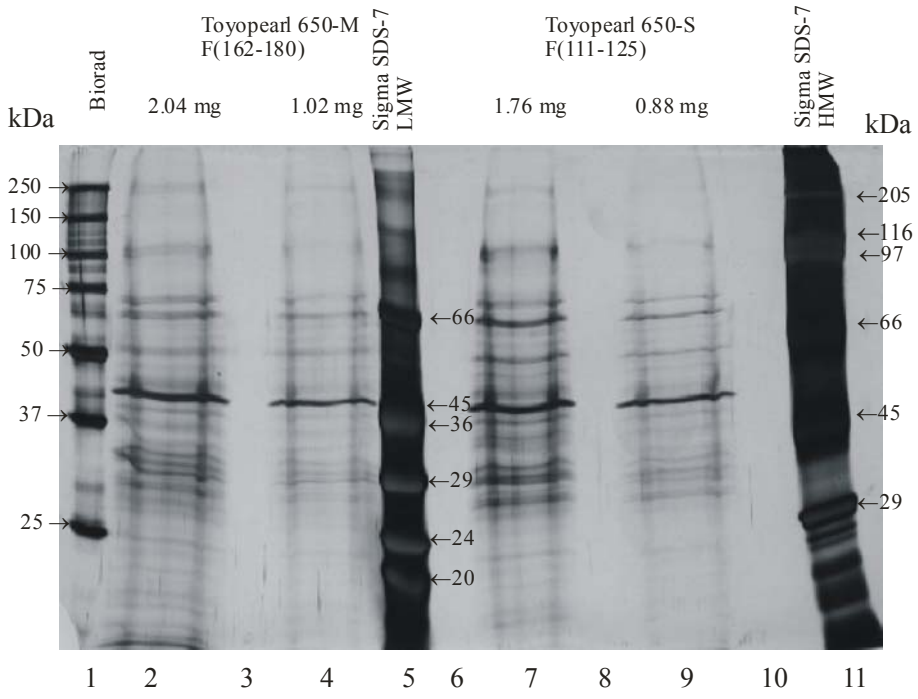

Fig. 17: SDS-PAGE analysis of fractions after chromatography on Toyopearl 650-M or 650-S. 5 % concentration gel and 10 % separating gel. The amounts of loaded proteins are indicated. The markers from Sigma were partially degraded and overstained. Lanes 2 and 4 and lanes 7 and 9 contain pooled fractions of Toyopearl 650-M and 650-S, respectively. Marker proteins were from Biorad (25 to 250 kDa) (lane 1), Sigma HMW SDS-6H (29 to 205 kDa) (lane 5) and Sigma LMW SDS-7 (14 to 66 kDa) (lane 11).

3.3.4.1 *Investigation of the ATP-PPi-exchange activity as a function of protein concentration with sucrose*

In previous chromatography experiments it had been noted (**chapters 3.3.2.1 & 3.3.3.3.2**) that the ATP-PPi-exchange activity appeared to migrate with protein complexes. To examine such a possibility, the following experiment was conducted. The fractions corresponding to the activity peak during elution of the Toyopearl 650-M column were pooled and concentrated with sucrose and stored at – 80^{o}C. The ATP-PPi-exchange activity was measured for this sample as a function of concentration, as shown in **Fig. 18**.

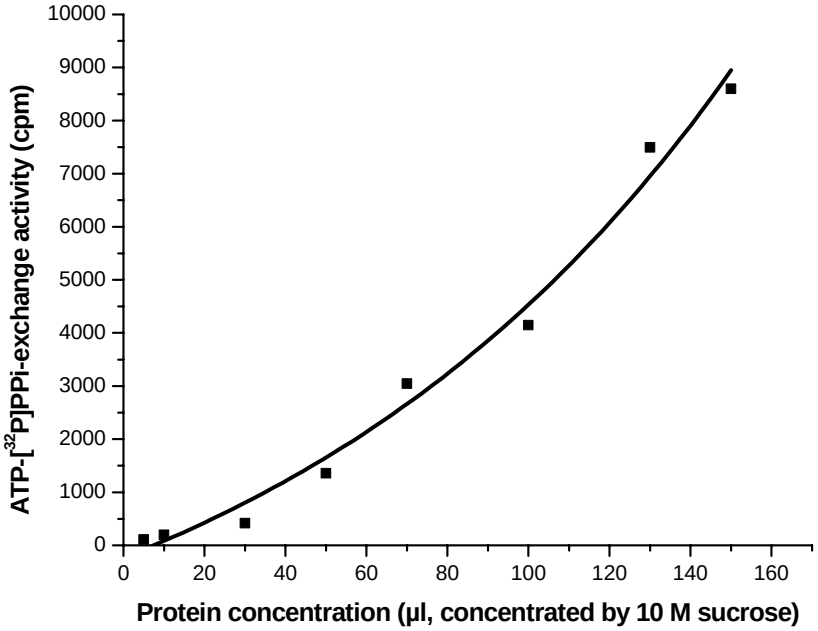

Fig. 18

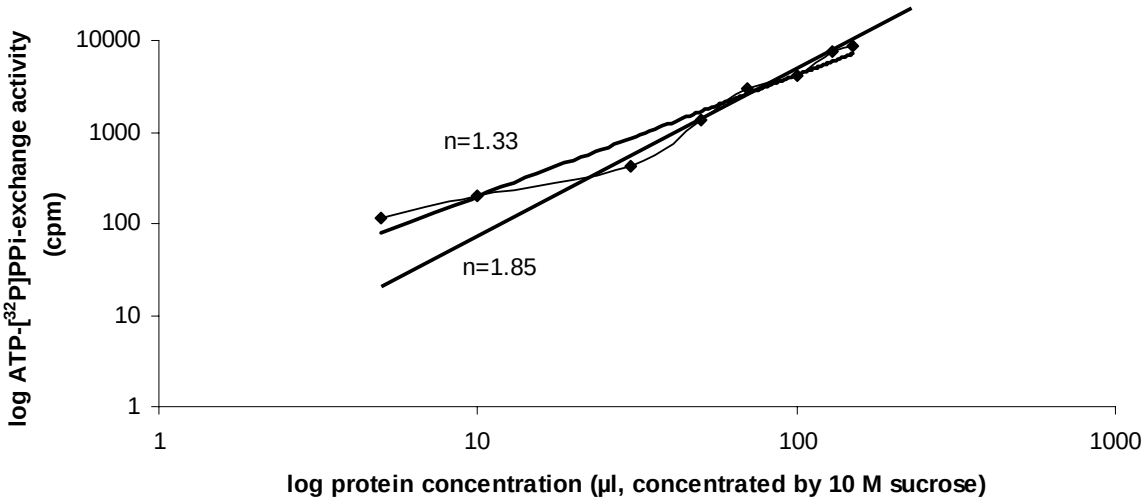

Fig. 19: Concentration dependency of the ATP-PPi-exchange activity of the sucrose-concentrated protein sample after Toyopearl 650-M chromatography. The reaction mixture (1 ml) contained 50 mM Tris /HCl at a pH of 7.5, 5 mM magnesium chloride, 50 mM potassium fluoride, 5 mM β-mercaptoethanol, 1 mM L-malate, 2 mM tetra sodium pyrophosphate, 2 mM ATP (pH 6-8), 1 mM spermine tetrahydrochloride, 0.5 mg/ml BSA (heat-denatured, hBSA) and a sufficient amount of [^{32}P] pyrophosphate was added to adjust it to 10^6 cpm, and finally, the sucrose-concentrated protein sample was added varying the amount from 5 to 150 µl. **Fig. 18**, plot of activity versus relative concentration of sample protein. **Fig. 19**, plot of log activity vs. log relative concentration. The data points were fit by two possibilities, yielding slopes of 1.33 and 1.85, respectively.

Fig. 18 indicates that the dependence of exchange activity on relative protein concentration is not linear. A double-log-plot in **Fig. 19** reveals that the data points can be fit by linear dependencies. Two possibilities are indicated for the fit, one with a slope of 1.33 and another one with a slope of 1.85. The approximately linear fit indicates that the concentration dependence is parabolic, in agreement with the assumption that the exchanging enzyme requires the association of at least 2 subunits for displaying optimal catalysis. This conclusion rests on the following considerations.

If the enzyme complex consisted, for instance, of equal subunits, each carrying a single active site, and the active sites are not active in the dissociated complex, then the concentration of active sites is

(1) $n \cdot SU \rightleftharpoons (SU)_n$

SU is dissociated subunits, $(SU)_n$ is the complex, consisting of n subunits.

(2) $n[(SU)_n] = K[SU]^n$

(3) Total protein forming subunits and complex

$[P] = [SU] + n[(SU)_n]$ = relative concentration

(4) In the beginning, when $[SU] >> [(SU)_n]$ is $[P] \sim [SU]$

Comparing equations (2) and (4),

$n[(SU)_n] = K[P]^n$

(5) For enzyme kinetics, the Michaelis-Menten equation describes the exchange rate (v)

$$v = n \cdot k_{cat}[(SU)_n] \frac{[S]_o}{K_M + [S]_o}$$

Under assay conditions $[S]_o$, which is substrate concentration is constant, and

(6) $v \sim [P]^n$

This calculation may be extended to hetero protein complexes. The result is principally similar, exhibiting the exchange rate to be a parabolic function of the (relative) protein concentration.

Logarithmation of (6) leads to

(7) $\log v = n \cdot \log[P] + C$

A plot of log v versus log [P] is linear with a slope equal to *n*.

The number *n* could be equal to the number of associating subunits. Because the deduction eq. (1) to (4) was arbitrarily simplified, the realistic size of *n* probably is less than the number of associating subunits.

Similar calculations can be carried out if the complex consisted of hetero subunits, some catalytic, some not catalytic, but essential for optimal exchange activity, and number *m* in analog to *n* could be defined that indicated the number of associating subunits. The number *m* would again appear in the exponent, and the dependence of activity of protein concentration would be parabolic, similarly as in eq. (6).

An experiment was conducted to prove that the simultaneously increased concentration of sucrose did not give rise to the observed increase in the ATP-PPi-exchange activity. The activity of non-concentrated Toyopearl 650-M pool was measured in **Fig. 20** as a function of sucrose ranging from 0 to 0.15 M. From the graph (**Fig. 20**) it is apparent that sucrose has rather an inhibiting effect, not explaining the parabolic dependency in **Fig. 18**. IC_{50}-value for inhibition (concentration at 50 % inhibitory effect) was approximately 0.02 M sucrose. High concentrations of sucrose did not show a further inhibition.

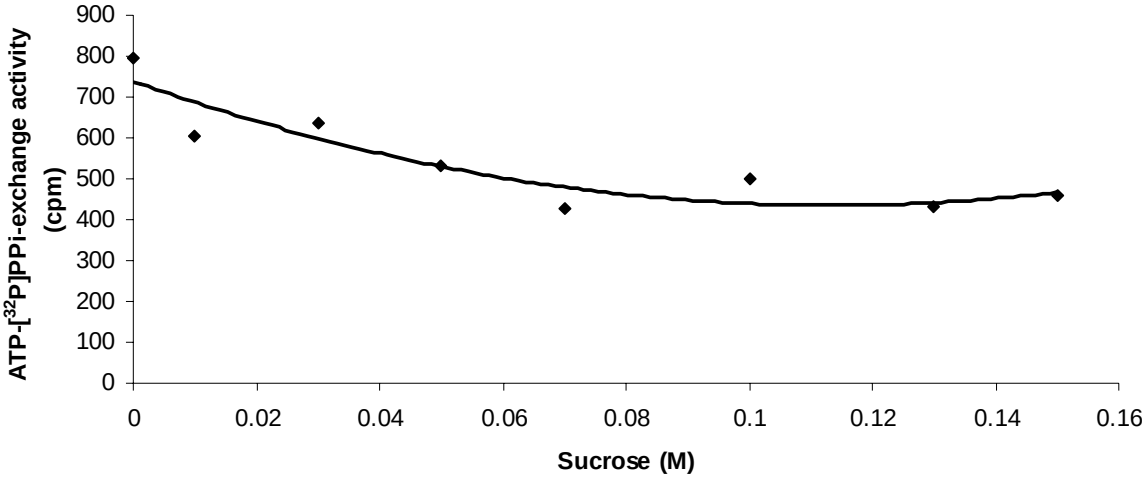

Fig. 20: Effect of sucrose concentration on the ATP-PPi-exchange activity. The standard ATP-PPi-exchange was carried out in the presence of various concentration of added sucrose. Active protein samples (100 µl) were taken from the non-concentrated active fraction after chromatography on Toyopearl 650-M (see **chapter 3.3.4**).

3.3.5 Purification of the Toyopearl 650-M active fractions by chromatography on Blue Sepharose CL-6B

The sucrose-concentrated fraction from the hydrophobic interaction column (Toyopearl 650-M) was loaded onto the equilibrated 20 ml Blue Sepharose CL-6B column (0.8 × 10). It was eluted with 10 mM MOPS buffer, pH 7.5, at 0.2 ml/min, until the extinction (E_{280}) returned to the base line. The unbound protein was expected to be washed out completely. A step-elution of 1 M KCl solution in 10 mM MOPS buffer, pH 7.5, at 0.2 ml/min was then carried out, and 1 ml fractions were collected and tested by the ATP-PPi-exchange assay. The data values are plotted in **Fig. 21**. Active fractions, P1 (20 - 30) and P2 (80 - 87), from the breakthrough and step-elution profiles, respectively, were concentrated with sucrose and stored at –80°C separately. Activity measurement indicated that a concentration by 10-fold was paralleled by an activity of 10-12-folds.

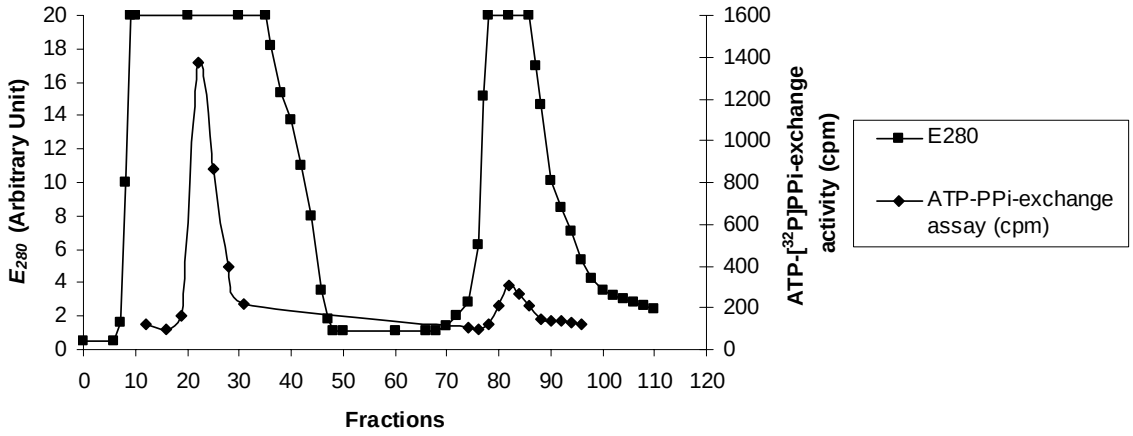

Fig. 21: Purification of Toyopearl 650-M fractions over a Blue Sepharose CL-6B Column. The sucrose-concentrated fraction from the Toyopearl 650-M column was loaded onto an equilibrated Blue Sepharose CL-6B column. The column was washed with 10 mM MOPS buffer, pH 7.5, and step-eluted with a 1 M KCl solution in 10 mM MOPS buffer, pH 7.5, at 0.2 ml/min. The eluate was tested for ATP-PPi-exchange activity in the presence of 1 mM L-malate.

The fractions from Toyopearl 650-M and from Blue Sepharose CL-6B columns were analyzed by 10 % SDS-PAGE and silver staining (shown in **Fig. 22**).

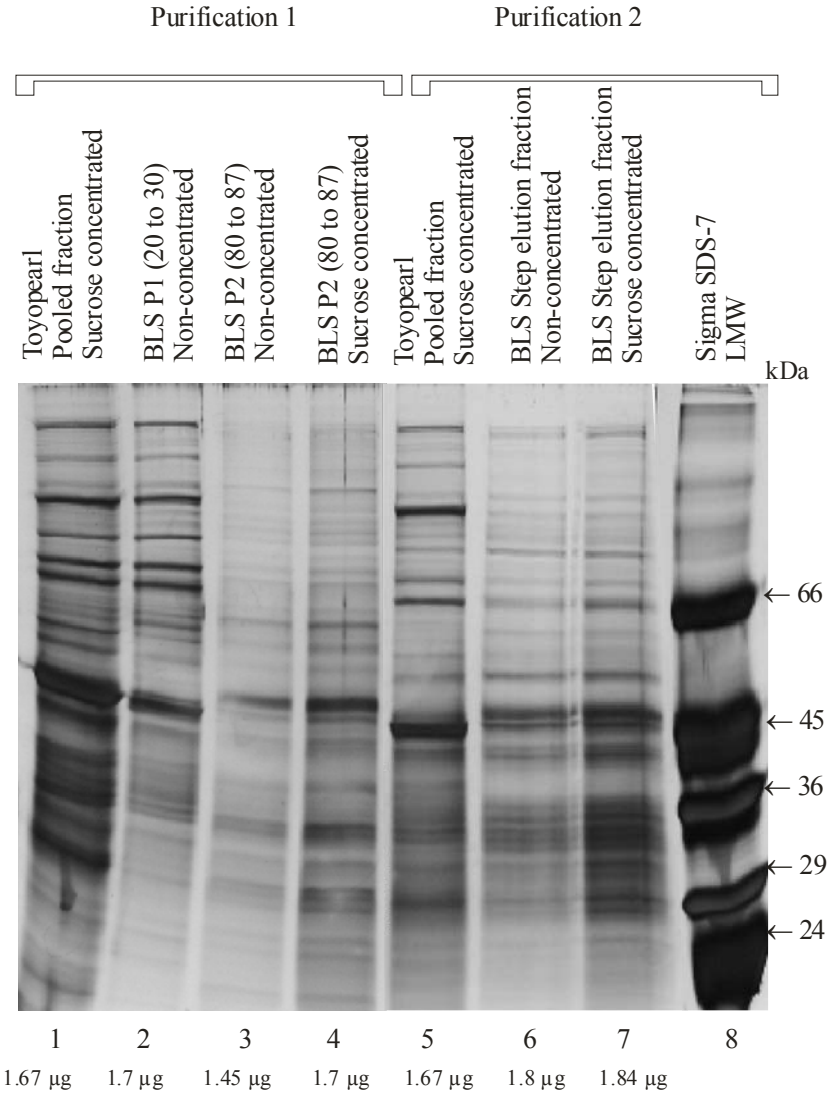

Fig. 22: SDS-PAGE analysis of Toyopearl 650-M and Blue Sepharose CL-6B pooled active fraction. 5 % concentration gel and 10 % separating gel. The amounts of loaded proteins are indicated. The results of two different purifications are shown. Lanes 1 to 4 and 5 to 7 are two batches of experiments, which were reproduced. Lane 8 contained the standard test mixture Sigma LMW SDS-7 (14 to 66 kDa). Lanes 1 and 5 were the sucrose-concentrated pooled fractions from the gradient of the hydrophobic interaction column (Toyopearl 650-M). Lane 2 was the non-concentrated Blue Sepharose CL-6B (BLS) breakthrough fraction. Lanes 3 and 6 were non-concentrated Blue Sepharose CL-6B step-elution fractions. Lanes 4 and 7 were sucrose-concentrated Blue Sepharose CL-6B step-elution fractions. See also **Fig. 41** for other purification.

The gel (**Fig. 22**) displays number of bands, typical of silver staining that yields non-proportional intensities, which are considerably higher for low amounts of applied samples. The purity is better envisaged when comparing with **Fig. 41**. A careful inspection shows that

the most intensive band is located at 45 kDa, suggesting a purity of higher than 50 % based on total staining in **Fig. 41**, lane 8. This high degree of purification could not be exceeded by subsequent chromatography as shown in **Fig. 22** (lanes 3, 4 and 6, 7). In contrast, this chromatography produced a new band located at a position of slightly higher molecular mass than 45 kDa. This band corresponds to the rather low activity eluted by the step-elution in **Fig. 21**, and is at variance with the band of 45 kDa (lane 2) and comparably high activity in the breakthrough of Blue Sepharose chromatography. The concentration by applying high sucrose did not effect the appearance of this band of slightly high molecular mass.

The purification is summarized in **Table 2**. It is seen by comparison that the purification of the protein is not paralleled by an increase in specific ATP-PPi-exchange activity, but rather by a considerable decrease as much as a factor of 6 with regard to the ammonium sulfate fraction. The purification could be later on increased as much as 180,000 cpm/mg specific activity (see **Fig. 41**, lane 8), but still reflecting absence of an increase in specific activity after chromatography Toyopearl and Blue Sepharose. The decrease was also accompanied by a large loss of activity, indicating that, while protein was purified (i.e. the 45 kDa in Toyopearl and the protein migrating in a position somewhat above 45 kDa) it must have lost intrinsic properties as an enzyme.

Step	**Protein** **mg/ml**	**Specific activity** **radioactivity (cpm)/mg protein**	**Purification** **(fold)**	**Yield** **%**
Extract	6.4	198242	1	100
Ammonium sulfate	5.6	255669	1.2	15
Toyopearl 650-M	6.65	85000	0.42	5
Blue Sepharose CL-6B	7.85	46656	0.23	0.4

Table 2: Summary of purification of protein fraction from the crude extract of *P. polycephalum.* 100 % yield corresponds to 12,687500 cpm.

3.4 Discussion of the attempts of enzyme purification

The purification list in **Table 2** indicated that specific exchange activity was lost as a result of purification. The appearance of a band with molecular mass of 45-50 kDa during

chromatography on Blue Sepharose suggests that the more active species of 45 kDa gives rise to this new species by an unknown reaction causing this change in molecular mass and chromatographic mobility. The argument that the difference in the band position is caused by different solvent composition in the samples loaded to the SDS-PAGE seemed unlikely in face of absence of effects of dialysis and of concentrating by sucrose. According to this observation and other results, namely the indication of dissociation into subunits and concomitant loss of activity (**Fig. 18**) and splitting of activity during purification on DEAE-Cellulose (**chapter 3.3.3.1.1**) and in all trials of chromatography on Blue Sepharose (**chapters 3.3.2.1 & 3.3.3.3.2**), we thus strongly favor the interpretation of the 45 kDa species (from now on p45) as the catalytically active protein (subunit). The origin of the band shifting during chromatography on Blue Sepharose remained unknown. It could be due to a structural rearrangement accompanying covalent reactions, partially resisting the effect of SDS, which normally underlies the technique of molecular mass measurements by SDS-PAGE. Such particular abnormalities are known, for instance, for histone H1 (*Physarum polycephalum*) that migrates in the position of > 55 kDa, although of molecular mass 28 kDa (Albert et al., 1993).

3.5 The malate-specific ATP-PPi-exchange studies

To further characterize the enzyme purified by hydrophobic interaction chromatography, we measured the dependence of exchange activity on L-malate concentration (**Fig. 23**). At 1 mM added L-malate, 50 % of the activity was generated in a malate-dependant fashion. This is comparable to 40-60 % observed in previous assays (this work and Bildl, 1998).

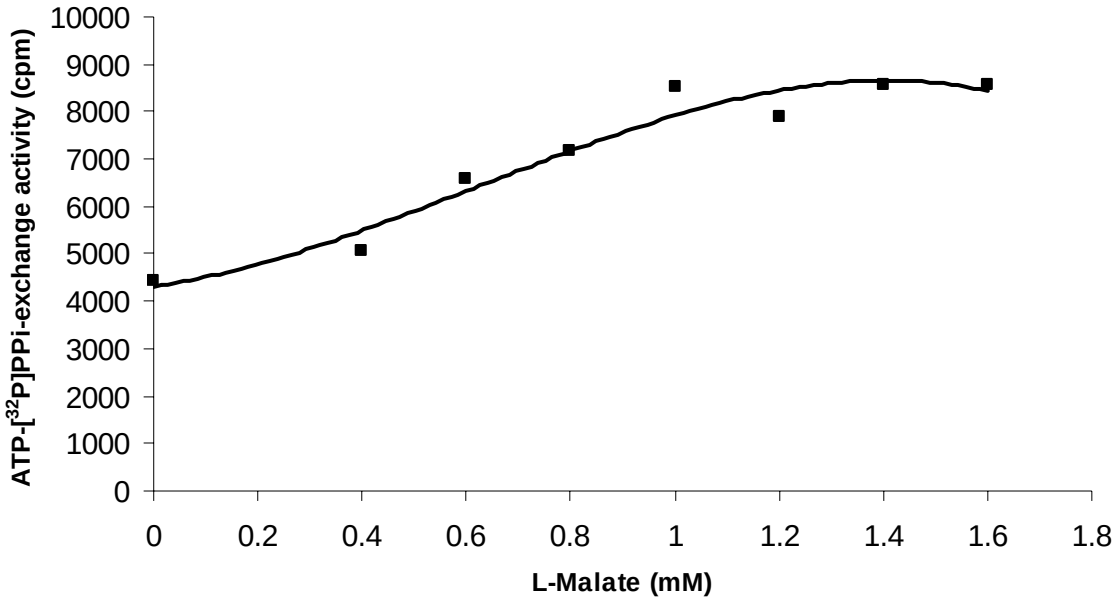

Fig. 23: The malate-specific ATP-PPi-exchange assay with the sucrose-concentrated fractions from the Toyopearl 650-M column. The malate-specific ATP-PPi-exchange assay was carried out in the presence of 1320 µg protein of the sucrose-concentrated fraction purified by hydrophobic interaction chromatography (Toyopearl 650-M) in a range from 0 to 1.8 mM of L-malate.

3.5.1 Effect of Triton X-100 on preparation of probes to be examined by the malate-specific ATP-PPi-exchange assay

The low reproducibility of the L-malate concentration dependence in the ATP-PPi-exchange activity in the various preparations together with the observed parabolic dependence in **Fig. 18** and change in molecular mass from hydrophobic interaction chromatography of Toyopearl to affinity chromatography of Blue Sepharose purification of probes was puzzling. One possible explanation was that the question whether the activity resided in membrane fractions or adhered to the surface of membranes. To shed light on this possibility, we prepared samples after cell lysis in the presence of Triton X-100, in order to extract membrane proteins. Microplasmodia grown for two to three days were harvested by straining the culture through a fine mesh for medium removal. The entire mesh with the cells was immediately dried by transfer onto paper towels. The cells stripped from adhered solute was weighed out in a ratio of 1:2 with ice-cold extraction buffer, which contained different percentages of Triton X-100 ranging from 0.1 to 3 %. The cells together with nuclei were

ruptured using the Ultra Turrax T 25 at high speed (instrument setting No. 6: 24,000). The ruptured cells were kept at 4°C on ice and then centrifuged at 18,000 × g for 20 min at 4°C. Then, 40 µl of the supernatant sample was added to the assay reaction mixture making a total volume of 1 ml. The ATP-PPi-exchange activity is shown in **Fig. 24**. The results indicated that Triton X-100 at concentrations 0.1 – 3 % (w/v) had no effect and also did not support a measurable dependence on the presence of L-malate.

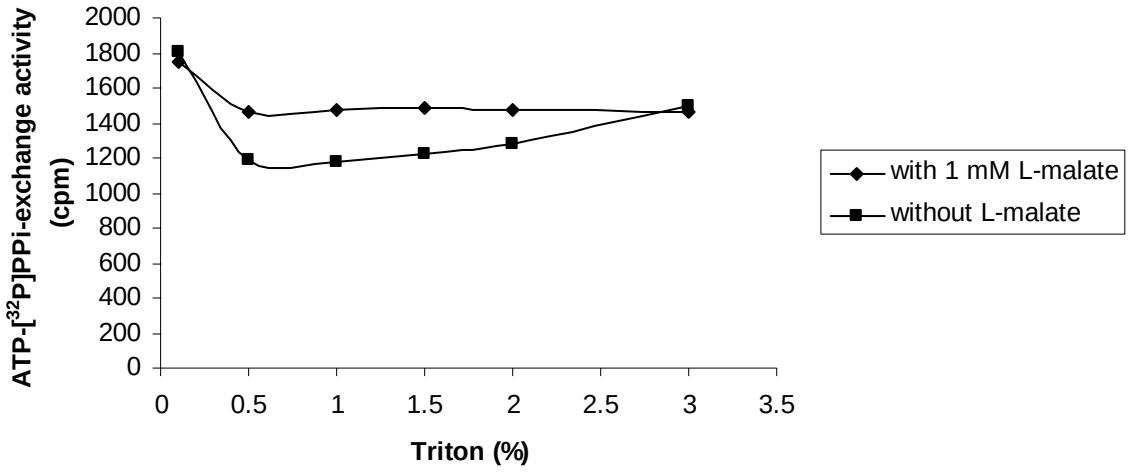

Fig. 24: Effect of Triton concentration on ATP-PPi-exchange assay. Different percentages of Triton X-100 ranging from 0.1 to 3 % were present during preparation of plasmodial cell extracts. Cells were ruptured in an Ultra Turrax T 25. Immediately, without precipitation or dialysis, the ATP-PPi assay was carried out in the presence and absence of L-malate.

The extract containing arbitrarily 1 % Triton X-100 was incubated and exposed to room temperature to see whether the activity changed with time (**Fig. 25**).

In a parallel experiment, an aliquot of the same 1 % Triton X-100 extract was dialyzed against 10 volumes buffer for 5 hrs and then tested for ATP-PPi-exchange activity (**Fig. 25**).

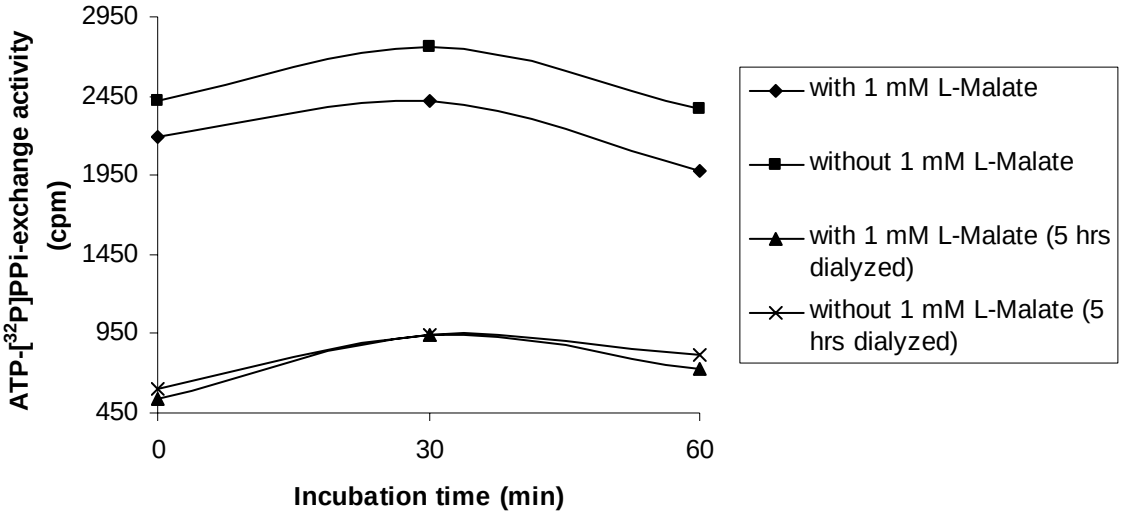

Fig. 25: Effect of time of exposure to room temperature on the ATP-PPi-exchange activity of dialyzed and non-dialyzed extracts obtained in the presence of 1 % Triton X-100.

The result shows that a malate dependency was not inferred by the presence of Triton X-100 during cell disruption. The activity decreased substantially after dialysis.

Morita and Nishi (1993) reported an increase of glycosidase activities, when plasmodia were ruptured in the presence of Triton X-100 and incubated at room temperature for 72 hrs. We repeated their conditions in our sample preparation and measured the ATP-PPi-exchange activity. As before, an aliquot of the extract were dialyzed against 10 volumes of buffer for 5 hrs. The exchange activities and the effect of the presence of L-malate were measured as shown in **Fig. 26**.

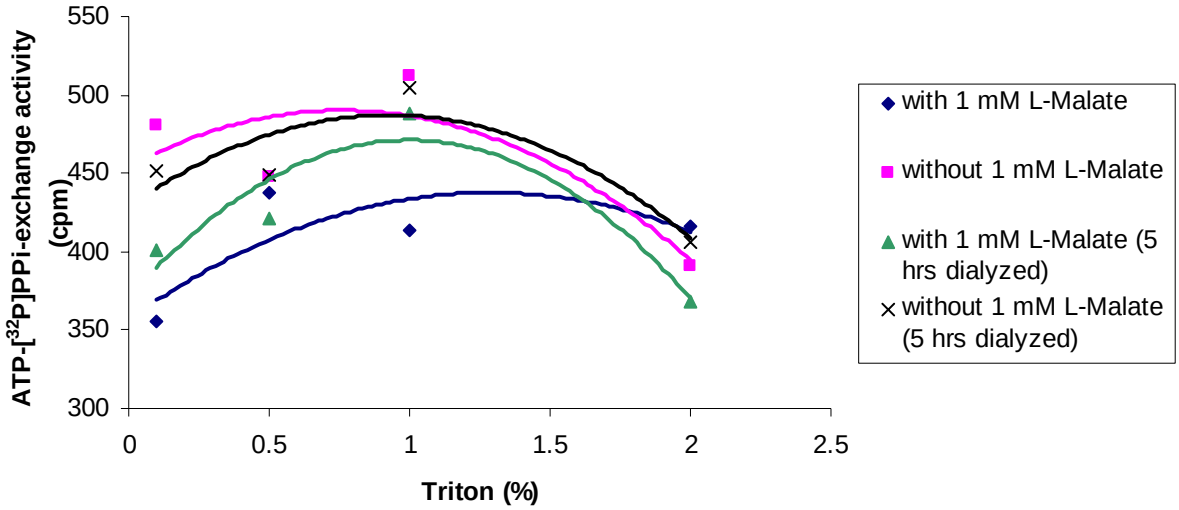

Fig. 26: The effects of Triton during plasmodia extraction and 72 hrs incubation of the extract according to the method by Morita and Nishi (1993) on ATP-PPi-exchange activity. The cells were ruptured in the presence of various concentrations of Triton X-100. After incubation for 72 hrs at room temperature, the ATP-PPi assay was carried out. An aliquot was dialyzed for 5 hrs before performing the ATP-PPi assay.

An increase in activity when L-malate was present could not be detected. The overall activity was low and of the order seen in **Fig. 25** after dialysis, i.e. after prolonged standing. The results suggest that the activity declined sharply with time in the presence of Triton X-100. The presence of detergent during plasmodia extraction did not effect an increase in the L-malate dependence of the ATP-PPi-exchange activity. It is concluded, that the enzyme activity was not increased by the treatment of membranes with Triton X-100.

3.5.2 Dependency of the ATP-PPi-exchange activity on the amount of protein in the untreated cell extract

To examine the effect of protein concentration in non-fractionated cell extracts an ATP-PPi-exchange was carried out as given below. It was of interest to see, whether the concentration dependence reflected complex dissociation as previously observed after purification (**Fig. 18**).

After plasmodia ruptured by Ultra Turrax T 25 at 4°C and centrifugation at 18,000 × g (12,000 rpm) for 20 min at 4°C, aliquots of crude extract ranging from 20 to 250 µl were tested for ATP-PPi-exchange activity (**Fig. 27**).

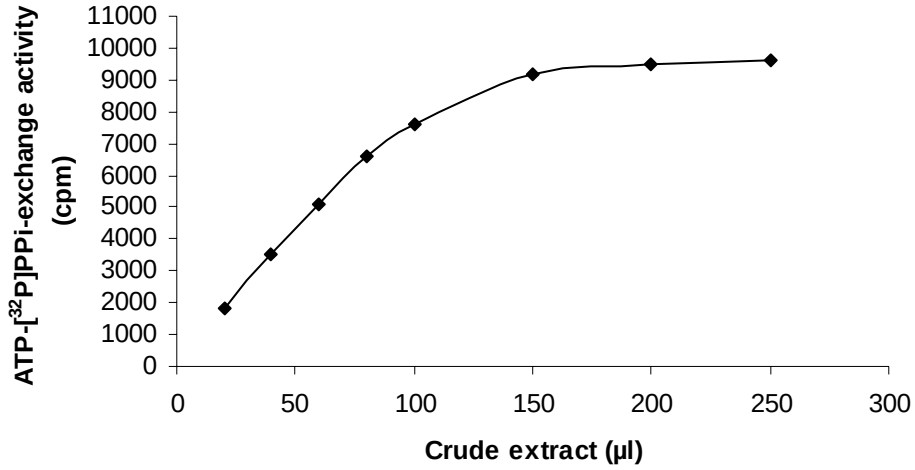

Fig. 27: Concentration dependency of the crude extract for ATP-PPi-exchange assay.

From the graph (**Fig. 27**), it is seen that the exchange activity was proportional to the amount of sample in the range 20 – 100 µl. At very high amounts, the activity became independent of the amount of extract.

3.5.3 Effects of acetic, malic, oxalic, and succinic acids in the ATP-PPi-exchange assay

The effects of acetate, malate, oxalate, and succinate on the ATP-PPi-exchange activity were measured at various concentrations of the sample in order to see whether any effects seen by L-malate were specific for these dibasic acids. The results are shown in **Fig. 28**.

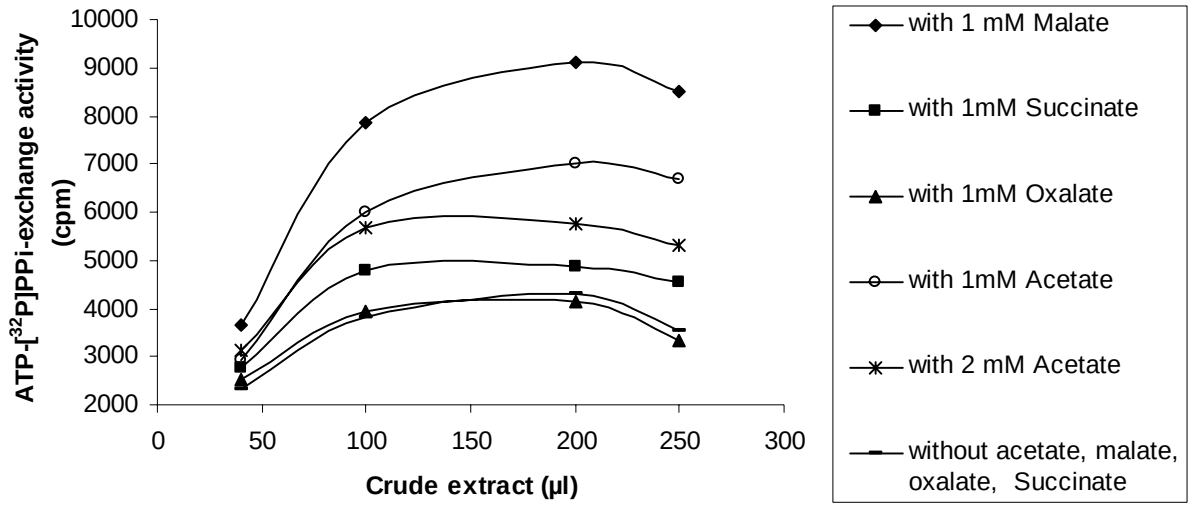

Fig. 28: Effects of acetic, malic, oxalic, and succinic acids in the ATP-PPi-exchange assay. The extract was obtained from microplasmodia after rupture with the Ultra Turrax T 25 (see M & M). ATP-PPi-exchange was measured in the presence of various amount of extract and the chemicals at the concentrations indicated.

The figure reveals that the highest activity was obtained in the presence of 1 mM L-malate. Acetate and succinate had a minor and oxalate had no effect.

3.6 Conclusions

In the foregoing chapter, the protein(s) with ATP-PPi-exchange activity had been partially purified and tentatively attributed to a protein of molecular mass 45 kDa (p45). Previous (Willibald et al., 1999) and present results have shown that:

(a) 40-60 % of the total activity was L-malate-dependent at optimal concentrations (1 mM) of L-malate, and the remainder was independent of added L-malate.

(b) at higher than optimal concentrations of L-malate, the exchange activity decreased.

(c) the fraction of L-malate-dependent over L-malate-independent activity did not change systematically during purification, otherwise showed unpredictable fluctuations like a decrease in activity at increasing L-malate concentrations.

(d) the dependence of ATP-PPi-exchange activity of crude plasmodial extracts was linear at low and tended to become independent at high concentrations of the protein sample.

(e) after partial purification over Toyopearl 650-M, the concentration dependence of the protein sample was parabolic, indicating that the exchange activity resided in a protein complex (activase), which dissociated as a function of sample dilution, rendering the dissociated proteins less active than the complex.

From observations (a) – (c), it may be suggested that the activase followed a mechanism, which involved an enzyme-adenylate. The adenylate was formed in the absence of L-malate, and reacted with [^{32}P]PPi to give [^{32}P]ATP.

(1) $$E + ATP \xrightleftharpoons{Mg^{2+}} E\sim AMP + PPi$$

Alternatively, the enzyme could catalyzed the formation of malyl-adenylate according to

(2) $$E + ATP + malate \xrightleftharpoons{Mg^{2+}} E\cdot malyl\sim AMP + PPi$$

It is not excluded that E~AMP has also formed via malyladenylate:

(3) $$E\cdot malyl\sim AMP \rightleftharpoons E\sim AMP + malate$$

The inhibitory effect of high concentrations of L-malate could be tentatively explained by assuming that activase was a constituent of PMLA-polymerase, and that malyl~AMP or E~AMP reacted with an incoming malate residue according to

(4) $$E\cdot malyl\sim AMP + malate \rightarrow E + malyl\text{-}malate + AMP$$

$$E\sim AMP + malate \rightleftharpoons E\cdot malyl\sim AMP$$

Observations (d) and (e) suggested that activase-polymerase constituted a protein complex, which dissociated at high dilutions. p45, like other components of the complex could have modulate activities or partial activities that were now uncoupled from each other.

The following experiments were performed towards validation and additional insight into reactions (1) – (4).

3.7 Validation of reactions involving ATP, PPi, L-malate, and AMP

3.7.1 Strategy

Several reactions were conducted in order to validate reactions (1) – (4). These include the reactions of proteins with [α-^{32}P]ATP and the identification of p45~AMP, the effect of L-malate and other dicarboxylic acids on this reaction, the reaction of [γ-^{32}P]ATP to intensify effects of protein phosphorylation, the identification of the radioactively labeled protein products and the effects of dibasic acids as inhibitors of the ATP-PPi-exchange activity, and of kinase inhibitors on this labeling. We showed that p45~AMP was not an intermediate involved in DNA-ligation. The sucrose-concentrated Toyopearl 650-M protein fraction was used.

3.7.2 Reaction of [α-^{32}P]ATP, the effect of added L-malate

To investigate reactions (1) and (2), [α-^{32}P]ATP was employed in the presence and absence of L-malate. To show that the formed p45~[^{32}P]AMP was not an intermediate, activated DNA was included in the experiments, which should avoid formation of p45~AMP if this were used for ligation.

Experiment was performed by adding different concentrations of L-malate (0, 1, 10 and 100 mM) to 100 µl of reaction mixture, which contained DNA ligase buffer (60 mM Tris-HCl at a pH of 8.0, 10 mM $MgCl_2$, 0.5 mM DTT, 50 µg/ml BSA and 30 mM NaCl) , 5 µCi of [α-^{32}P]ATP (3,000 Ci/mmol, Amersham Corp.) and 66 µg of the concentrated Toyopearl 650-M fraction. In the DNA ligase experiment, activated calf thymus DNA was present instead of L-malate (see **chapter 3.7.3**).

Reaction mixtures were incubated at 25^{o}C for 15 min. Then, 20 µl of sample of the reaction mixture was mixed with 20 µl of SDS buffer and heated at 85^{o}C for 5 min. The proteins were separated by electrophoresis by 10 % SDS-PAGE and then electroblotted onto a nitrocellulose filter. The nitrocellulose filter was stained with Ponceau S and the marker

proteins were localized. Protein p45~[^{32}P]AMP was detected by autoradiography on the nitrocellulose filter at -80^{o}C for 64 hrs (**Fig. 29**).

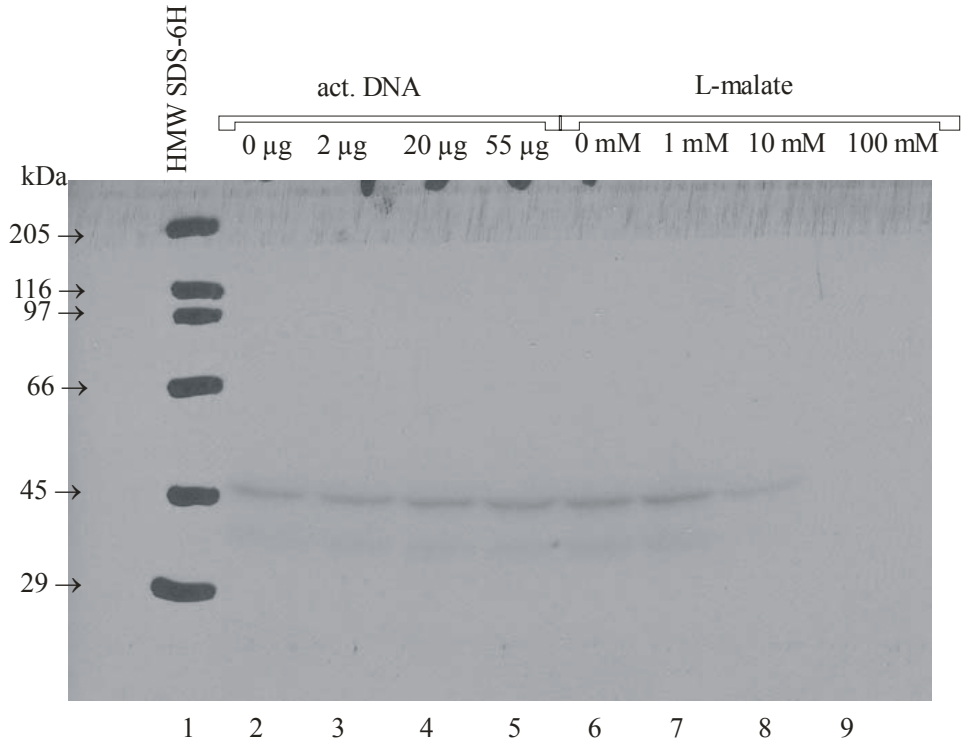

Fig. 29: Effects of added L-malate and activated calf thymus DNA. 5 % concentration gel and 10 % separating gel. Lane 1 contained the standard protein test mixture Sigma HMW SDS-6H (29 to 205 kDa). Lanes 2 to 5 contained activated calf thymus DNA at various concentrations indicated and lanes 6 to 9 contained L-malate at the concentration indicated. Reaction conditions are indicated in the text. Amount of protein (sucrose-concentrated Toyopearl fraction) was 13 µg per lane.

Fig. 29 indicates the labeling of a protein band of molecular mass 45,000. The band is in the same position as p45, shown to be enriched during protein purification (**Fig. 21**). Lane 6 of the **Fig. 29** indicates that labeling occurred in the absence of L-malate in the reaction mixture. Tentatively, the labeling is referred to [^{32}P]AMP~protein in reaction (1). Comparing the reactions of lane 6 which had an absence of L-malate to that of lane 7 which contained 1 mM of L-malate, the differences were narrow. On the other hand, the band intensity had been reduced by almost half when comparing concentrations of 1 mM and 10 mM (lanes 7 and 8, respectively). In lane 9 where the reaction mixture contained 100 mM of L-malate, the band had vanished completely. The dependence on malate concentration parallels the concentration

dependent decrease in ATP-PPi-exchange activity (**Fig. 23**) (Bildl, 1998 and Willibald et.al., 1999), and is tentatively referred to reaction (4).

3.7.3 p45 was not a DNA ligase

To examine whether p45 was a DNA ligase, different concentrations of activated calf thymus DNA (0, 2, 20 and 55 µg) were added to 100 µl of reaction mixture containing ligase buffer, 5 µCi of [α-^{32}P]ATP (3,000 Ci/mmol, Amersham Corp.) and 66 µg of the concentrated Toyopearl 650-M fraction. In this experiment L-malate was not present.

In contrast to L-malate, activated calf thymus DNA had no effect on the intensity of the radioactive staining (lanes 2 – 5 of **Fig. 29**), ruling out the possibility that the enzyme activity, i.e. formation of p45~[^{32}P]AMP, was due to the reaction of DNA Ligase.

In a positive control reaction, T4 DNA ligase was studied (**Fig. 30**) to validate the technique carried out with activated calf thymus DNA. The 100 µl reaction mixtures contained 28.6 µl of ligase buffer (60 mM Tris-HCl at a pH of 8.0, 10 mM $MgCl_2$, 0.5 mM DTT, 50 µg/ml BSA and 30 mM NaCl) (Tomkinson et al., 1991), 20 µg/ml activated calf thymus DNA, 1 µCi of [α-^{32}P]ATP (3,000 Ci/mmol, Amersham Corp.), and different concentrations of T4 ligase ranging from 0.01 U to 0.3 U. The reaction mixtures were incubated at 25^{o}C for 15 min. Aliquots of 20 µl of each of the reaction mixtures were mixed with 20 µl of SDS buffer and heated at 85^{o}C for 5 min.

Proteins were separated by 10 % SDS-PAGE. Standard protein test mixture Sigma HMW SDS-6H (29 to 205 kDa) was used. The proteins were electro transferred to nitrocellulose filters and stained with Ponceau S. The ligation activity was detected by autoradiography at -80^{o}C for 15 hrs.

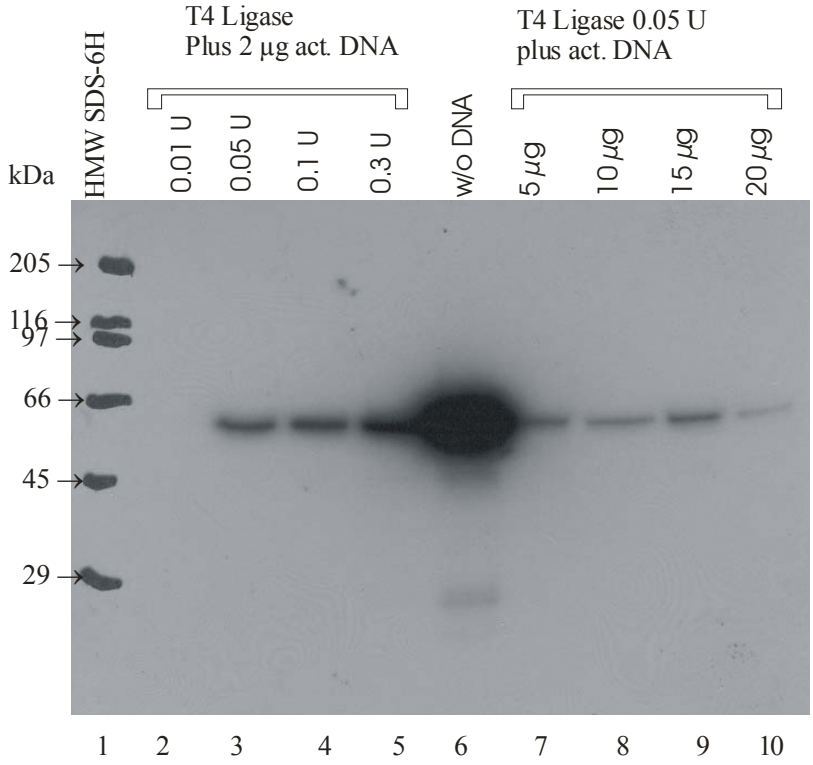

Fig. 30: T4 DNA ligase reaction with [α-^{32}P]ATP in the presence of activated calf thymus DNA. 5 % concentration gel and 10 % separating gel. Lane 1 contained the standard protein test mixture Sigma HMW SDS-6H (29 to 205 kDa). Lanes 2 to 5 contained different T4 Ligase concentrations ranging from 0.01 U to 0.3 U and 2 µg of activated DNA. Lanes 6 to 10 contained various concentrations of activated DNA from 0 to 20 µg and 0.05 U of T4 Ligase. w/o DNA: Ligase (0.05 U) in the absence of DNA.

The intensity of ligase-[^{32}P]AMP was highest in the absence of activated DNA. In the presence of 2 µg activated DNA, the intensity was less, but still considerable, and increased with the concentration of ligase (lanes 2 – 5). Presence of increasing amounts of activated calf thymus DNA provoked a concentration dependent decrease of the radioactive labeling (lanes 7 – 10), showing only faint labeling at 20 µg activated DNA (lane 10). This decrease of labeling was later on taken as a criterion to decide that p45 was not a DNA ligase.

Another experiment was performed, including variable concentration of [α-^{32}P]ATP, to enforce the validation that p45 was not a DNA ligase. Various concentrations of [α-^{32}P]ATP (3,000 Ci/mmol, Amersham Corp.) from 1 to 10 µCi were added to the reaction mixture which contained 66 µg of the sucrose-concentrated Toyopearl 650-M fraction and ligase buffer. The ligase assay was performed for each radioactive concentration in the presence and absence of activated calf thymus DNA. The reaction mixtures were incubated at

25°C for 15 min. 20 µl of each of the reaction mixtures were mixed with 20 µl of SDS buffer and heated at 85°C for 5 min. The proteins were separated by electrophoresis on a 10 % SDS-PAGE and then transferred onto nitrocellulose filters in 25 mM Tris-HCl, 192 mM glycine, and 20 % methanol at a pH of 8.3. The nitrocellulose filters were stained with Ponceau S and the marker proteins were visualized. The ligation activity was detected by autoradiography at -80°C for 56 hrs.

The results in **Fig. 31** show that the band intensities in the position of p45 of pairs absence/presence of activated calf thymus DNA are identical at all concentration of [α-^{32}P]ATP tested, validating the conclusion that p45 is not a DNA ligase.

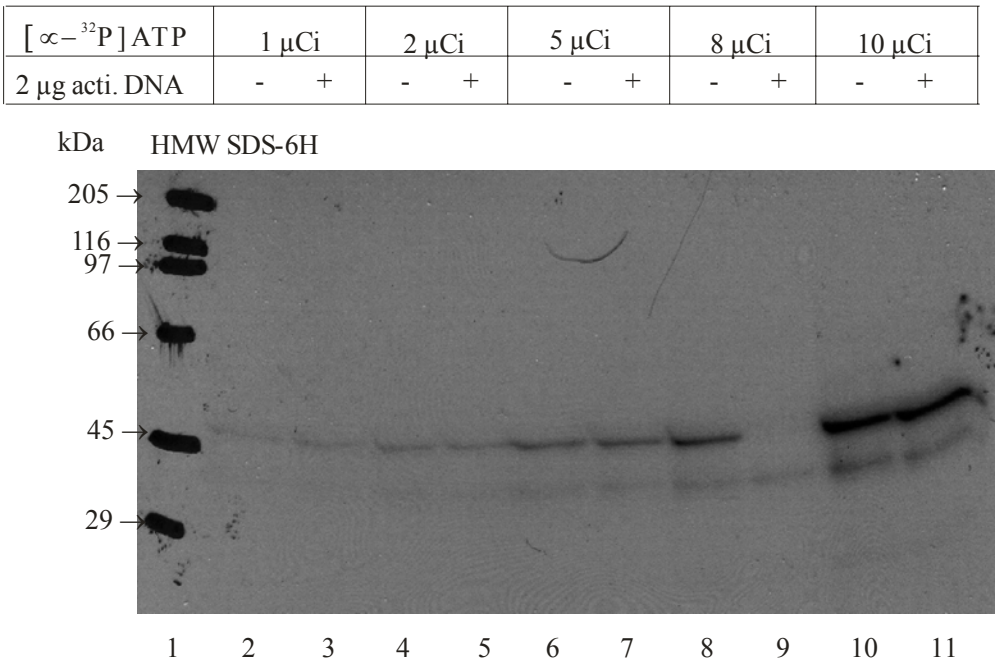

Fig. 31: DNA ligase assay at various concentrations of [α-^{32}P]ATP, testing the Toyopearl 650-M fraction. 5 % concentration gel and 10 % separating gel. Lane 1 contained the standard protein test mixture Sigma HMW SDS-6H (29 to 205 kDa). The reaction mixture for each lane contained 66 µg of ammonium sulfate-precipitate fraction after Toyopearl chromatography. Where indicated, reaction mixtures contained also 2 µg activated calf thymus DNA. In lane 9, the reaction mixture was not loaded. 13 µg protein were loaded in each lane.

3.7.4 Kinetics of p45~[^{32}P]AMP formation in the presence of L-malate

Next, an experiment was carried out following the time dependence of E~[^{32}P]AMP as in the presence of 10 mM L-malate in the reaction mixture. This experiment was conducted to see whether an intermediate E~[^{32}P]AMP was involved, which could react with L-malate at high concentrations of L-malate. It was expected that p45~[^{32}P]AMP accumulated, if the reaction of p45~[^{32}P]AMP with L-malate would be slow compared with its formation. An inspection of the time dependence revealed that radioactive labeling of p45 occurred within 10 min, reached a steady state level, and finally disappeared after 50 min with in 10 min of reaction time (**Figs. 32a,b**). This kinetics is in agreement with the assumption that an enzyme-bound intermediate reacted with L-malate according to equations (2)-(4).

It is interesting to note (see density profiles by OptiQuant Image Analysis Software in **Fig. 32b**) that labeling indicates a double peak in the presence of L-malate (lanes 4 – 8), while only a single peak is seen in the absence of L-malate (lane 2). Both peaks in lanes 4 – 8 are time dependent. Whether the appearance of two peaks is artifact or refers to adenylation of two slightly different enzyme forms has to be clarified in future experiments.

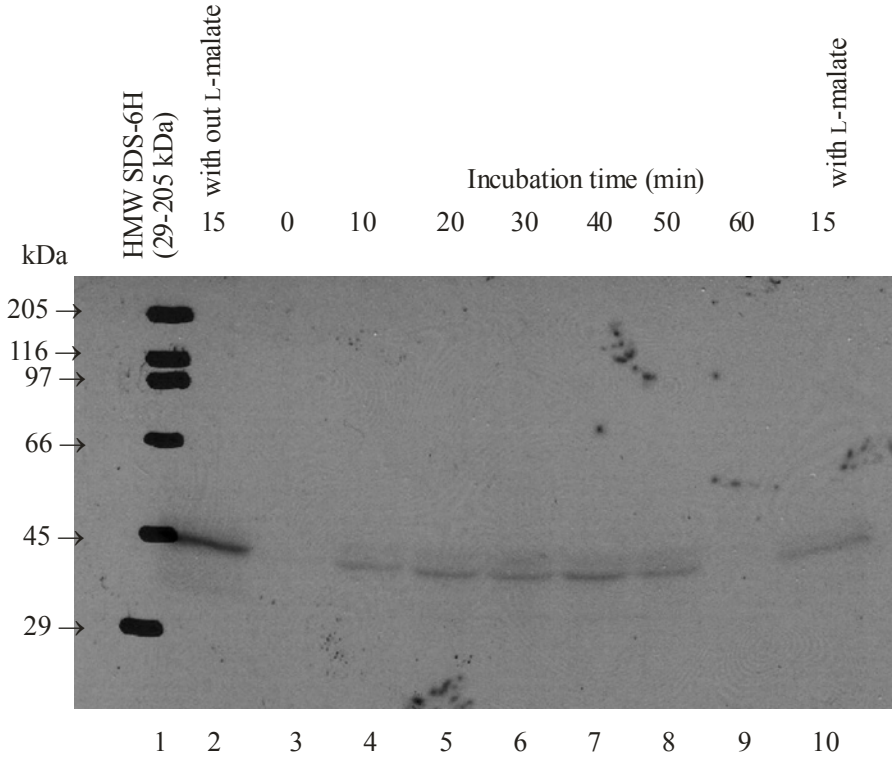

Fig. 32a: Kinetics of p45~[^{32}P]AMP formation in the presence of high (10 mM) L-malate. 5 % concentration gel and 10 % separating gel. Lane 1 contained the standard protein test mixture Sigma HMW SDS-6H (29 to 205 kDa). Lane 2, absence of L-malate, and lane 10 in the presence of 10 mM of L-malate, both incubated 15 min at 25°C. Lanes 3 to 9 all consisted of reaction mixtures containing 10 mM of L-malate incubated at 25°C for different time periods ranging from 0 to 60 min. The sample zero min was taken immediately after mixing of the reactants by stopping the reaction on adding the SDS containing sample buffer. The reaction mixture of 100 µl contained ligase buffer, 5 µCi of [α-^{32}P]ATP (3,000 Ci/mmol, Amersham Corp.) and 66 µg of the concentrated Toyopearl 650-M fraction at 25°C. The proteins were separated by electrophoresis through a 10 % SDS-PAGE and then transferred to nitrocellulose filters. The nitrocellulose filters were stained with Ponceau S and the proteins were visualized. The enzyme-adenylate was detected by autoradiography at -80°C for 144 hrs. 66 µg protein were contained in 100 µl reaction mixture and 13 µg mounted in each lane to the gel.

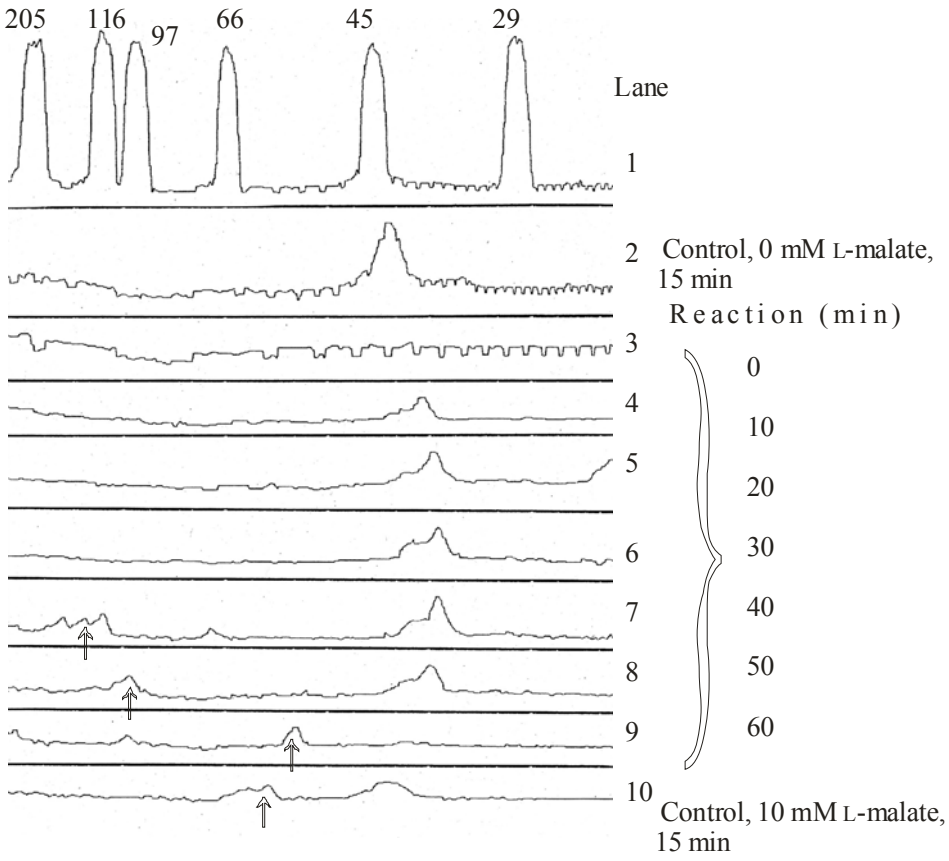

Fig. 32b: Density profile of the gel Fig. 32a obtained by using OptiQuant Image Analysis Software (Packard Instrument Company). Indicated arrows refer to noise. The peak absorbance in lanes 2 and 4-8 refer to p45~[^{32}P]AMP.

3.7.5 Comparison of the concentrated fractions of Toyopearl 650-M and Blue Sepharose CL-6B

The protein fractions after chromatography on Toyopearl 650-M and additional chromatography on Blue Sepharose CL-6B (**chapter 3.3.5**) were compared after concentration by the sucrose techniques (**chapter 2.2.10.2.1**). The formation of enzyme-adenylate by both fractions were followed by the SDS-PAGE and autoradiography study after reaction with [α-^{32}P]ATP in the presence and absence of 100 mM L-malate (**Fig. 33**). Both reaction mixtures of 100 µl contained ligase buffer, 5 µCi of [α-^{32}P]ATP (3,000 Ci/mmol, Amersham Corp.) and 100 mM of L-malate. Then, 66 µg of the concentrated Toyopearl 650-M fraction and 78 µg of the concentrated Blue Sepharose CL-6B fraction were added to their respective reactions. The reaction mixtures were incubated at 25^{o}C for 15 min. Then, 20 µl of sample from each of the reaction mixtures were combined with 20 µl of SDS buffer and heated at 85^{o}C for 5 min. The proteins were separated by electrophoresis on a 10 % SDS-PAGE and then transferred onto nitrocellulose filters. The nitrocellulose filters were stained with Ponceau S and the marker proteins were visualized. The enzyme-adenylate was detected by autoradiography at -80^{o}C for 14 days (**Fig. 33**).

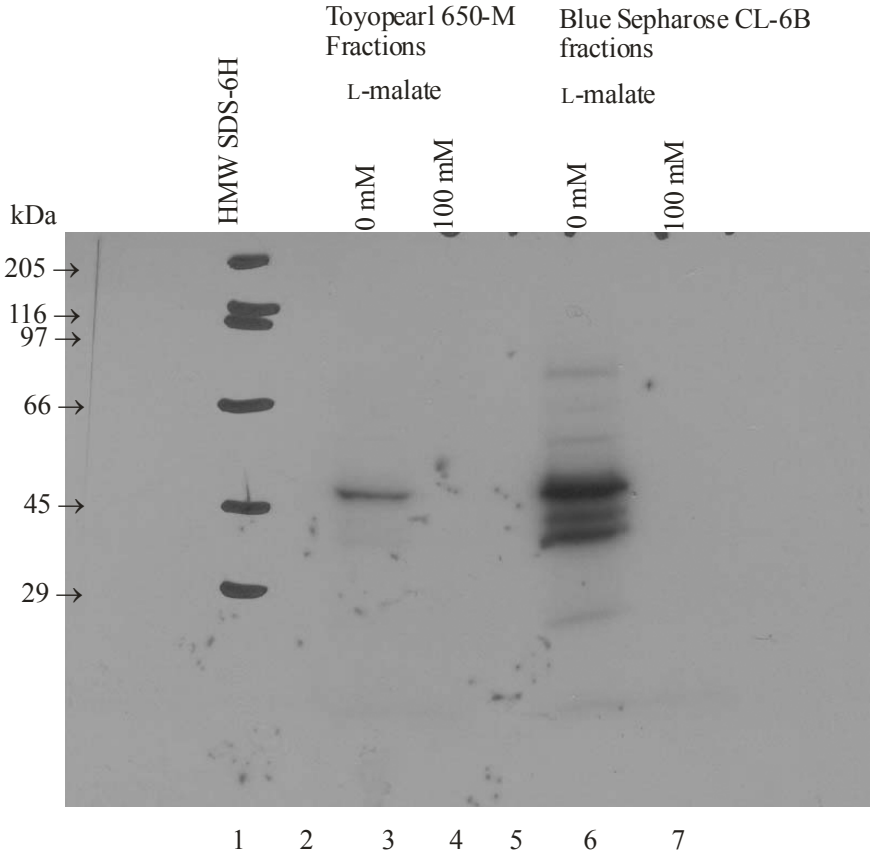

Fig. 33: Comparison of protein-adenylate formation of fraction from Toyopearl 650-M and Blue Sepharose CL-6B. 5 % concentration gel and 10 % separating gel. Lane 1 contained the standard protein test mixture Sigma HMW SDS-6H (29 to 205 kDa). Lanes 3 and 4 contained the reaction mixtures with 66 µg of the concentrated Toyopearl 650-M fraction, 0 and 100 mM of L-malate respectively. 13 µg protein were mounted onto the gel. Lanes 6 and 7 contained the reaction mixtures with 78 µg of the concentrated Blue Sepharose CL-6B fraction and 0 and 100 mM of L-malate respectively. 16 µg protein were mounted onto the gel.

In agreement with the previous measurement, the p45 protein was radioactively labeled, with high probability by covalently bound [^{32}P]AMP (A complete proof for [^{32}P]AMP would require to label the adenine moiety and show its presence). The Blue Sepharose p45~[^{32}P]AMP was shifted towards higher molecular mass in accordance with the results obtained after silver staining in **Fig. 22**. In addition, the Blue Sepharose fraction, which was considerably more concentrated, also contained 2 labeled species of lower molecular masses 42 kDa and 39 kDa. These lower mass species could be proteolytic products or another possibility, species that had been phosphorylated and thus would carry additional negative charges to be reflected by their mobility in SDS-PAGE. In the presence of 100 mM L-malate, labeling disappeared from all 3 species in both preparations, in agreement

with assumption that the presumed adenylate reacted with L-malate. It was interesting that multiple bands were labeled, even at high molecular mass than 45,000. Whether this reflected, formation of reactive AMP by all of these proteins or just diffusion from one malyl~AMP synthesizing protein and subsequent adenylation of all of these different species remains to be seen.

3.7.6 The reaction of PPi with p45~adenylate

We examined whether the formation of the presumed p45~adenylate could be suppressed in the presence of PPi giving rise to the reverse of the adenylation reaction. Different concentrations ranging from 0 to 3 mM of pyrophosphate were included in the enzyme-adenylate formation reaction. The reaction mixture (100 µl) contained ligase buffer, 5 µCi of [α-^{32}P]ATP (3,000 Ci/mmol, Amersham Corp.), 66 µg of the concentrated Toyopearl 650-M fraction and pyrophosphate. Reaction mixtures were incubated at 25^{o}C for 15 min. Aliquots of 20 µl sample from each of the reaction mixtures were mixed with 20 µl of SDS buffer and heated at 85^{o}C for 5 min. The proteins were separated by electrophoresis on a 10 % SDS-PAGE and then transferred onto nitrocellulose filters. The protein-adenylate was detected by autoradiography as before.

Fig. 34 shows that the formation of p45~[^{32}P]AMP was suppressed strongly in the presence of 0.05 mM and completely in the presence of 0.1 mM and higher concentrations of PPi. At the same time, the species at molecular masses 42 kDa and 39 kDa, which appeared to be sensitive against L-malate (**Fig. 33**) were not suppressed. From the results, we conclude, that p45~AMP but not the labeled species at molecular masses of 42 kDa and 39 kDa was able to bind and react with PPi. It has to be noted that, although the suppression by PPi of p45~AMP formation is consistent with our assumed mechanism eq. (1), we cannot completely rule out the possibility that PPi merely reacted by competitive inhibition by ATP binding. In future experiments, p45~[^{32}P]AMP will be separated from the other reactants ([^{32}P]ATP, [^{32}P]PPi) and then incubated with PPi. The formation of [^{32}P]ATP will be followed by TLC.

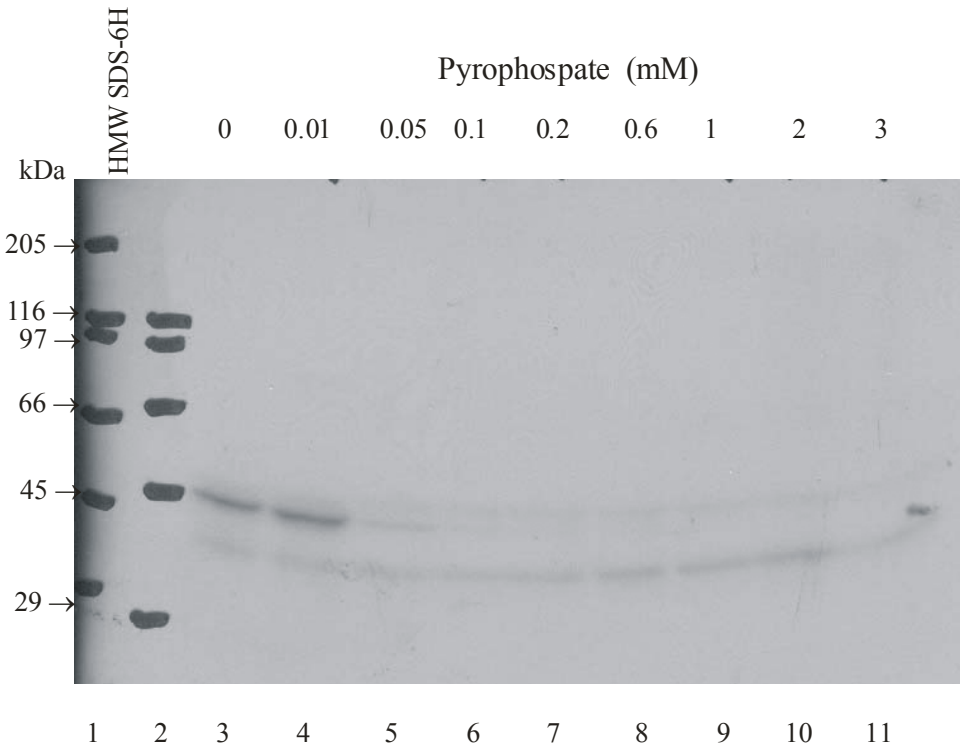

Fig. 34: Effect of pyrophosphate on the formation of p45~[^{32}P]AMP. 5 % concentration gel and 10 % separating gel. Lanes 1 and 2 contained the standard protein test mixtures Sigma HMW SDS-6H (29 to 205 kDa). Lanes 3 to 11 contained the reaction mixtures containing different concentrations of pyrophosphate ranging from 0 to 3 mM. An amount of 66 µg protein has been present in each reaction and 13 µg mounted onto each lane of the gel.

3.7.7 Effect of non-labeled ATP on the formation of p45~[^{32}P]AMP

The effects of different concentrations ranging from 0 to 1 mM of non-radioactive ATP in the p45-protein-adenylate formation were observed by performing an autoradiography study. The purpose was to demonstrate that the observation so far, was due to radioactivity labeled ATP and not caused by a reaction with an unknown radioactive species, following a completely different (unknown) mechanism. The specific radioactivity of [α-^{32}P]ATP was as before namely 3,000 Ci/mmole. The experiments were done using 5 µCi of [α-^{32}P]ATP in all the 100 µl reactions. The final concentration of [^{32}P]ATP in the reaction mixtures was calculated to be 1.6 µM. Amounts of added non-radioactive ATP to the reaction mixture were such that concentrations increased by the amounts given in **Fig. 35**. The enzyme-adenylate formation was observed in the presence of 66 µg of the concentrated Toyopearl 650-M fraction. The reactions were incubated at 25^{o}C for 15 min, and 20 µl

samples were mixed with 20 µl of SDS buffer and heated at 85°C for 5 min. The proteins were separated by electrophoresis on a 10 % SDS-PAGE and then transferred onto nitrocellulose filters. The nitrocellulose filters were stained with Ponceau S and the marker proteins were visualized. The enzyme-adenylate was detected by autoradiography at -80°C for 14 days (**Fig. 35**).

The results in **Fig. 35** were unexpected. We had merely expected the reflection of isotopic dilution. The isotopic dilutions with unlabeled ATP of [α-^{32}P]ATP should have produced bands of p45~[^{32}P]AMP with declining intensity. In contrast, by increasing the concentration of non-radioactive ATP from 0 to 1 mM, the enzyme-adenylate band intensity increased gradually and reached a maximum at 3.2 µM (lane 5). Further increase in the concentration then caused the expected decrease in the band intensity, which disappeared completely at 0.5 mM (lane 10), corresponding to a 312.5-fold dilution.

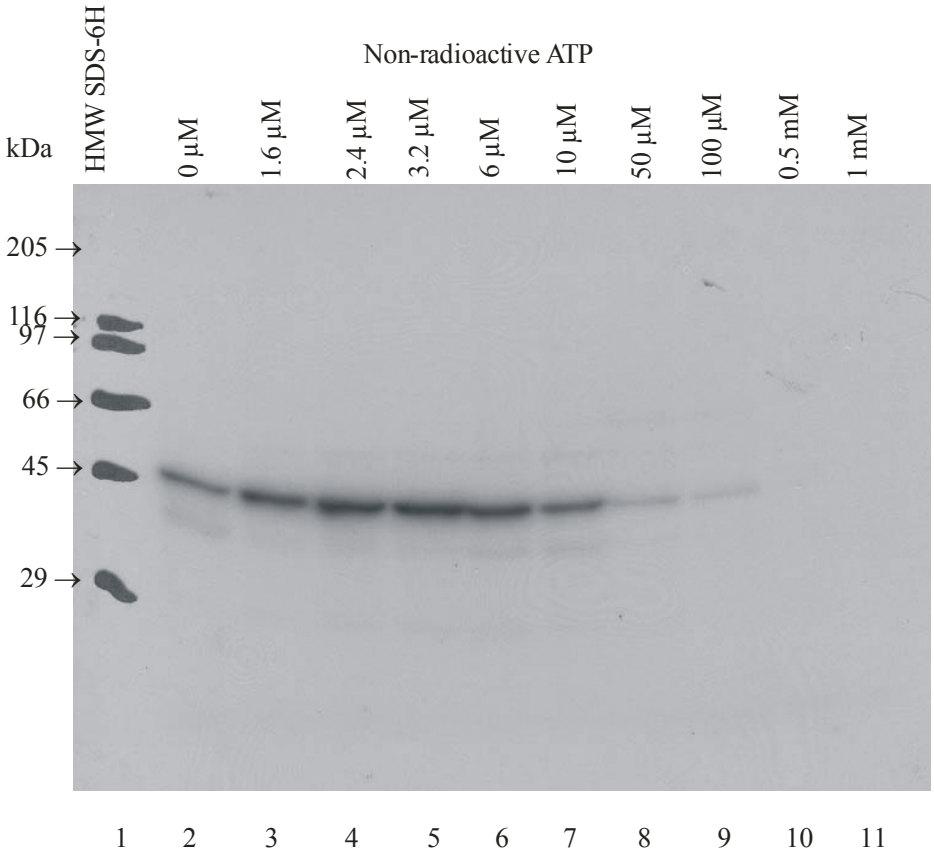

Fig. 35: Effect of non-labeled ATP on the formation of p45~[^{32}P]AMP. 5 % concentration gel and 10 % separating gel. Lane 1 contained the standard protein test mixture Sigma HMW SDS-6H (29 to 205

kDa). Lanes 2 to 11 contained different concentrations of non-radioactive ATP ranging from 0 to 1 mM. An amount of 66 µg protein has been present in each reaction mixture and 13 µg mounted onto each lane of the gel.

As [^{32}P]ATP reached a 6.25-fold isotopic dilution, as was the case in lane 7, radioactive labeling should be practically eliminated. This is at variance with staining seen in lane 7. A likely explanation is that in the absence of added ATP, only a fraction of the protein p45 had been labeled with [^{32}P]AMP whereas in the presence of added ATP, a much higher fraction of p45 because conjugated with ATP exceeding the amount of previously bound [^{32}P]AMP. To understand this, one would have to assume, that ATP by some means induced p45 to bind more AMP. The amount of such activated p45 must overcompensate the effect of isotopic dilution, because **Fig. 35** shows an increase in staining intensity compared with the level seen in the absence of added ATP. A possible explanation was that ATP had covalently reacted with (inactive) p45 (eq. (5)) or had bound as an allosteric activatior (eq. (6)), inducing the enzyme form that was active in forming covalently bound AMP.

(5) p45 (inactive) + ATP $\rightarrow$ phosphorylated-p45 (active) + ADP

(6) p45 (inactive) + nATP $\rightleftharpoons$ p45 (active) $(ATP)_n$

3.7.8 Concentration dependency of p45~[^{32}P]AMP formation on oxalic acid and succinic acid

We have shown in **chapter 3.5.3** that the dibasic acids oxalic acid and succinic acid exerted a certain activating effect on the ATP-PPi-exchange activity. It was of interest, whether the activation was reflected by the amount of formed p45~[^{32}P]AMP. The reaction mixture of 100 µl contained ligase buffer, 5 µCi of [α-^{32}P]ATP (3,000 Ci/mmol, Amersham Corp.), 66 µg of the concentrated Toyopearl 650-M fraction and various concentrations of oxalic acid and succinic acid ranging from 0 to 1 mM. After incubation at 25^{o}C for 15 min, 20 µl samples were mixed with 20 µl of SDS buffer and heated at 85^{o}C for 5 min. The proteins were separated by electrophoresis on a 10 % SDS-PAGE and then transferred onto nitrocellulose filters. The nitrocellulose filters were stained with Ponceau S and the marker proteins were visualized. The enzyme-adenylate was detected by autoradiography -80^{o}C for 14 days (**Fig. 36**).

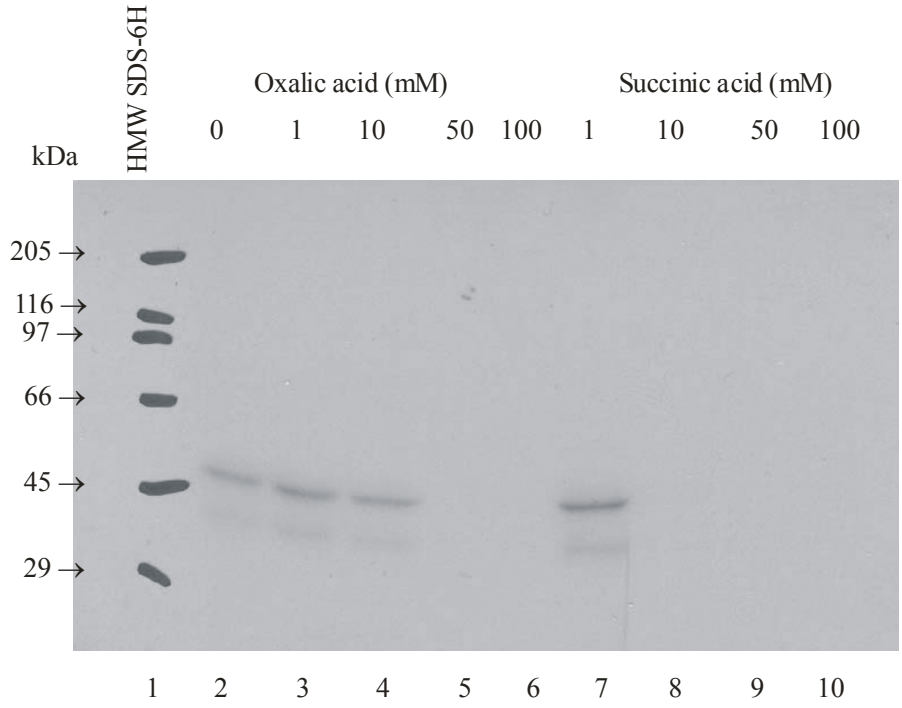

Fig. 36: Effects of oxalic acid and succinic acid on the formation of p45~[^{32}P]AMP. 5 % concentration gel and 10 % separating gel. Lane 1 contained the standard protein test mixture Sigma HMW SDS-6H (29 to 205 kDa). Lane 2, neither oxalic nor succinic acids were added. Lanes 3, 4, 5, and 6 contained various oxalic acid concentrations of 1, 10, 50, and 100 mM respectively. Lanes 7, 8, 9, and 10 contained different succinic acid concentrations of 1, 10, 50, and 100 mM respectively. An amount of 66 µg protein has been present in each reaction mixture and 13 µg mounted onto each lane of the gel.

The results show that oxalic acid at a concentration of 50 mM and succinic acid at a concentration of 10 mM eliminated the radioactive labeling of p45. The effects could be understood in the light of the effect by L-malate, which also eliminated the staining at high concentrations. The effect of L-malate has been interpreted by the assumption of a reaction of L-malate with the adenylate, thereby diminishing the radioactive AMP bound to p45. The same assumption may hold for succinate and to a lesser extent for oxalic acid, depicting also less positive effects in this order on the ATP-PPi-exchange reaction in **Fig. 28**, paralleled by the higher concentration required in **Fig. 36** for the elimination of labeling when less active in the exchange reaction.

3.7.9 The phosphate of ATP was involved in the activation of p45 to form p45~[^{32}P]AMP

We compared the formation of p45~[^{32}P]AMP in the presence of the ATP substitutes α,β-methylene-ATP and β,γ-methylene-ATP. The formation of p45-adenylate was followed in 100 µl of reaction mixture containing ligase buffer, 5 µCi of [α-^{32}P]ATP (3,000 Ci/mmol, Amersham Corp.), 66 µg of the concentrated Toyopearl 650-M fraction. To the reaction mixture varying concentrations of β,γ-methylene-ATP (**Fig. 37**) and α,β-methylene-ATP (**Fig. 38**) ranging from 0 to 1 mM were added as separate experiments. The reactions were incubated at 25^{o}C for 15 min. Then, 20 µl of sample from each of the reaction mixtures were combined with 20 µl of SDS buffer and heated at 85^{o}C for 5 min.

The proteins were separated by electrophoresis on a 10 % SDS-PAGE and then transferred onto nitrocellulose filters. The nitrocellulose filters were stained with Ponceau S and the marker proteins were visualized. The enzyme-adenylate was detected by autoradiography at -80^{o}C for 14 days.

Fig. 37 shows the effect of added β,γ-methylene-ATP. The concentration dependence for the formation of p45~[^{32}P]AMP is similar to that seen for ATP in **Fig. 35**, except that an enhancement of adenylate formation at nucleotide concentrations 1.6 µM – 10 µM is not observed. The substrate reactivity of the ATP-analogue is less than that of [α-^{32}P]ATP, because it is structurally not completely equivalent, and isotopic dilution is less than in the presence of unlabelled ATP. The observed inhibition at high concentration (> 50 µM) of ATP-analogue could be due to both competitive inhibition by the analogue and isotopic dilution. The absence of the activation that was seen in the presence of added 1.6 – 6 µM β,γ-methylene-ATP (lanes 3 – 6, **Fig. 37**) is then attributed to the lack of serving as a substrate for phosphorylation by the γ-phosphate.

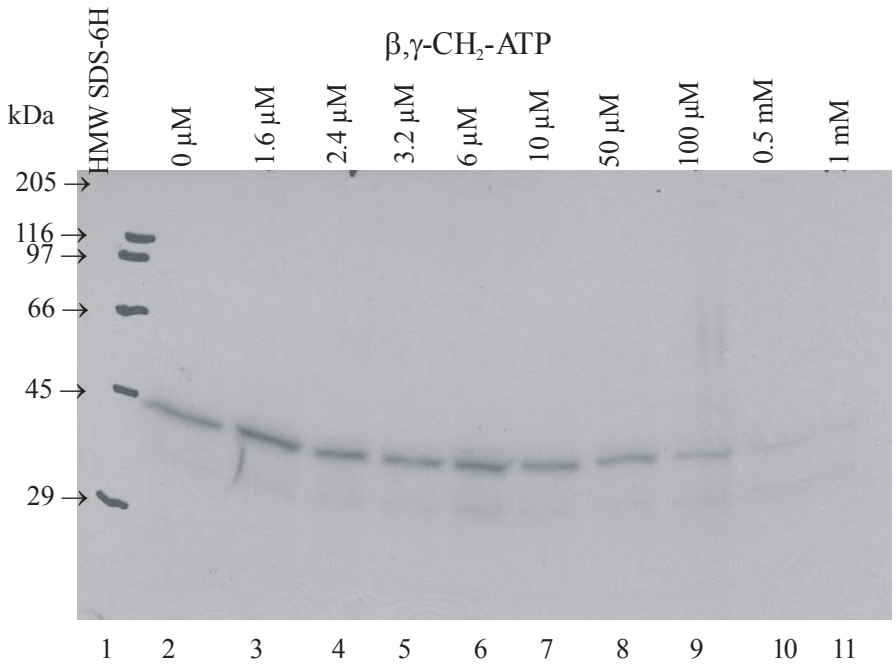

Fig. 37: Dependence of p45~[^{32}P]AMP formation on the concentration of added ATP-analogue β,γ-methylene-ATP. The reaction conditions were the same as in **Fig. 35**, except for the substitution of ATP by β,γ-CH_2-ATP.

Fig. 38 shows the dependence of p45~[^{32}P]AMP formation on the concentration of added α,β-methylene-ATP. In comparison with the results for added ATP in **Fig. 35**, the formation of p45~[^{32}P]AMP is considerably more enhanced in lanes 3 – 11 and elimination is not observed throughout the experiment. The absence of p45~[^{32}P]AMP elimination is in agreement with the absence of isotopic dilution of [α-^{32}P]ATP by α,β-methylene-ATP, because the analogue cannot be cleaved into AMP and PPi, thus the adenylate is not formed. On the basis that only a low degree of inhibition of adenylate formation was also observed at high concentrations of added analogue (lanes 10, 11), it was concluded that competition between [α-^{32}P]ATP and the analogue for binding to the enzyme was not very strong, probably due to relatively low binding affinity of the analogue in the presence of the methylene group in the α,β-position. The observed enhancement of adenylate formation (lanes 3 -11) was in agreement with the above assumption that p45 was activated by phosphorylation with the γ-phosphate that was possible with α,β-methylene-ATP as substrate, but not with β,γ-methylene-ATP. Phosphorylation of some unknown component in the protein complex with p45 (see **chapter 3.7.7**) or p45 itself would thus enhance the formation of p45~[^{32}P]AMP. The mechanism of this activation is not known.

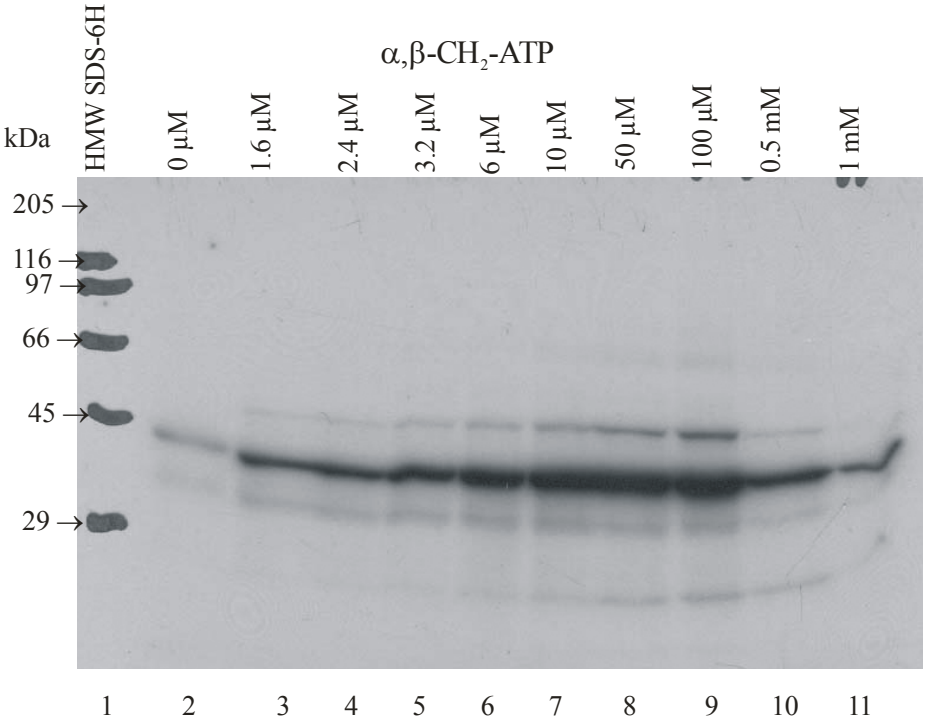

Fig. 38: Formation of p45~[^{32}P]AMP as a function of added α,β-methylene-ATP. Reaction conditions were similar as in **Fig. 35**, except that ATP had been substituted by the α,β- CH_2-ATP.

3.8 [γ-^{32}P]ATP studies

In the previous chapter, it was concluded that protein phosphorylation could be regulatory for p45~[^{32}P]AMP formation. We have performed experiments using [γ-^{32}P]ATP to identify the phosphorylated protein(s) and correlate the degree of phosphorylation with that of formation of p45~[^{32}P]AMP.

3.8.1 Protein phosphorylation and effects of added L-malate

In a first experiment, we identified the phosphorylated protein and compared its molecular mass with that of the p45~[α-^{32}P]ATP protein. We then tested for the sensitivity of this phosphorylation for the presence of L-malic acid in the phosphorylation mixture.

In the absence/presence of L-malate a protein band of molecular mass 35,000 and two minor forms, a doublet at 54,000/64,000 and a doublet at 86,000/92,000 were labeled due to protein [^{32}P]-phosphorylation. It was of interest to see, whether the presence of L-malate had an effect on this phosphorylation in comparison with the concentration dependence observed for [^{32}P] adenylation in **Fig. 29**.

Various concentrations ranging from 0 to 100 mM of L-malate were included in the reaction mixture, which contained in 100 µl ligase buffer, 5 µCi of [γ-^{32}P]ATP (5,000 Ci/mmol, Amersham Corp.), and 66 µg of the concentrated Toyopearl 650-M fraction. All the reactions were incubated at 25^{o}C for 15 min. Then, 20 µl samples from each of the reaction mixtures were mixed with 20 µl of SDS buffer and heated at 85^{o}C for 5 min. The proteins were separated by electrophoresis on a 10 % SDS-PAGE and then transferred onto nitrocellulose filters. The nitrocellulose filters were stained with Ponceau S and the marker proteins were visualized. The phosphorylation was detected by autoradiography at -80^{o}C for 14 days (**Fig. 39**).

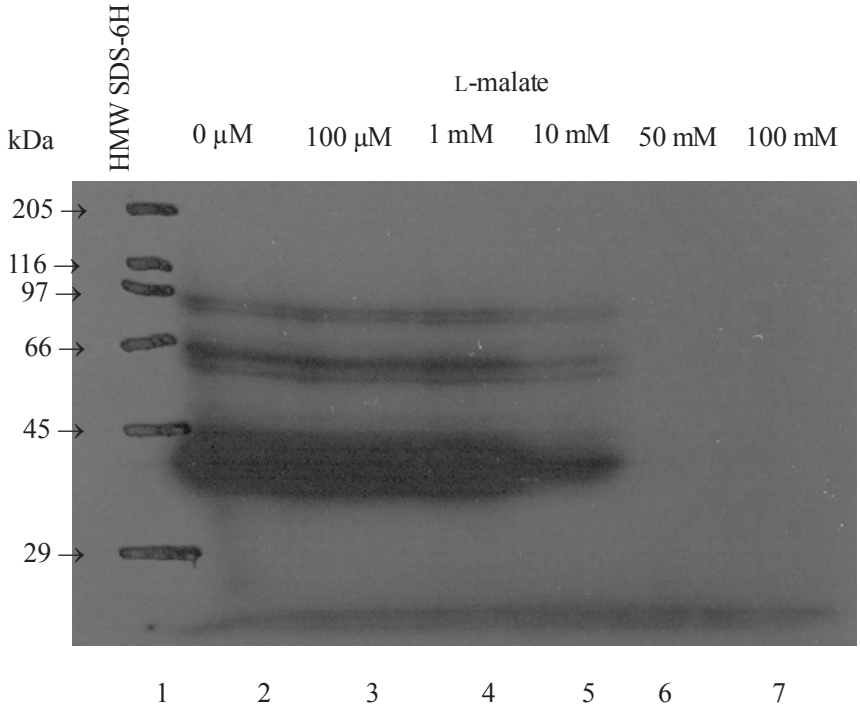

Fig. 39: The effect of concentration of L-malate on protein phosphorylation with [γ-^{32}P]ATP. 5 % concentration gel and 10 % separating gel. Lane 1 contained the standard protein mixture Sigma HMW SDS-6H (29 to 205 kDa). Various concentrations ranging from 0 to 100 mM of L-malate were included in the reaction mixture, which contained in 100 µl ligase buffer, 5 µCi of [γ-^{32}P]ATP (5,000 Ci/mmol, Amersham

Corp.), 66 µg of the concentrated Toyopearl 650-M fraction. All the reactions were incubated at 25°C for 15 min. Lanes 2 to 7 contained the various concentrations of L-malate ranging from 0 to 100 mM. 13 µg protein were mounted onto each lane of the gel.

Comparing lane 2 in the absence of L-malate with lanes 3 and 4 in the presence of 100 µM and 1 mM of L-malate, respectively, no differences in phosphorylation was observed. On the other hand, the band intensity had been reduced by almost half when comparing concentrations of 1 mM and 10 mM (lanes 4 and 5, respectively). In lanes 6 and 7, where the reaction mixture contained 50 mM and 100 mM of L-malate, respectively, the band had vanished completely. The dependence of protein phosphorylation on the concentration of L-malate was similar as the dependence of p45-adenylation in **Fig. 29**. This similarity suggests that the adenylated p45 and the phosphorylated protein were pool of a protein complex that reflected the reaction/binding of L-malate in the observed concentration range. The similarity of molecular masses (45,000 and 35,000) (see **Fig. 40**) of adenylated and phosphorylated protein tempting to speculate that, one and the same protein adenylated or phosphorylated, and that these forms of protein displayed different electrophoretic mobilities.

3.8.2 Comparison study of proteins labeled by [α-^{32}P]ATP or [γ-^{32}P]ATP

Proteins labeled by [α-^{32}P]ATP and [γ-^{32}P]ATP, respectively were compared by performing SDS-PAGE and autoradiography. Both were prepared in reaction mixtures of 100 µl containing ligase buffer and 5 µCi of either [α-^{32}P]ATP (3,000 Ci/mmol, Amersham Corp.) or [γ-^{32}P]ATP (5,000 Ci/mmol, Amersham Corp.). Then, 66 µg of the concentrated Toyopearl 650-M fraction was added to each of the mixtures. After incubation at 25°C for 15 min, 20 µl samples were mixed with 20 µl of SDS buffer and heated at 85°C for 5 min. The proteins were separated by electrophoresis on a 10 % SDS-PAGE and then transferred onto nitrocellulose filters. The nitrocellulose filters were stained with Ponceau S and the marker proteins were visualized. Radioactively labeled bands were detected by autoradiography at -80°C for 6 days (**Fig. 40**).

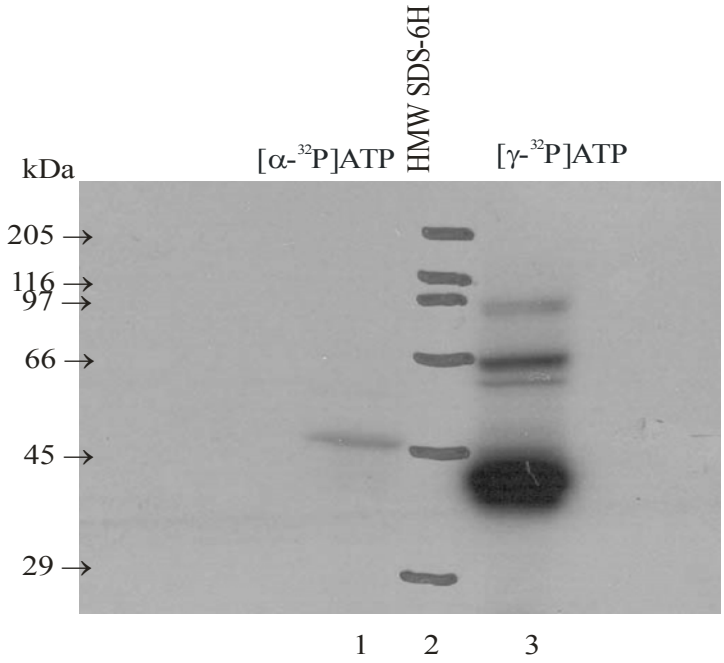

Fig. 40: Comparison of proteins labeled by reaction with [α-^{32}P]ATP and [γ-^{32}P]ATP, respectively. 5 % concentration gel and 10 % separating gel. Lane 2 contained the standard protein marker mixture Sigma HMW SDS-6H (29 to 205 kDa). Lane 1 contained the reaction products of [α-^{32}P]ATP with the concentrated Toyopearl 650-M fraction. Lane 3 contained the reaction products of [γ-^{32}P]ATP with the concentrated Toyopearl 650-M fraction. An amount of 66 µg protein has been present in the reaction mixtures, and an amount of 13 µg protein was applied in each lane.

The result in **Fig. 40** confirmed clearly that the adenylate protein migrated in position of 45 kDa and the phosphorylated protein at 35 kDa. Because the ingredients of the reaction mixture were identical except the position of the radioactive ^{32}P, it must be assumed that these bands referred to different proteins.

To examine, this further, 0 to 1 mM of non-radioactive ATP was incubated with Toyopearl fraction of protein and analyzed by SDS-PAGE employing silver staining. The reaction mixture, as before, contained in 100 µl, ligase buffer, 66 µg of the concentrated Toyopearl 650-M fraction and 0 to 1 mM of non-radioactive ATP. After incubation at 25^{o}C for 15 min, 20 µl of samples were mixed with 20 µl of SDS buffer, heated at 85^{o}C for 5 min, and loaded at different amounts on the gel for SDS-PAGE (10 %) (**Fig. 41**). The results indicated a single strong band in the position of 45 kDa as identified previously (see **chapter 3.3.5, Fig. 22**). Concentrated samples (13.2 µg protein) appeared to migrate some what faster

than diluted samples (1.65 µg). A shift due to phosphorylation could not be observed. It is concluded that the phosphorylated protein (35 kDa) was present in considerably lower concentration than p45 that could be adenylated.

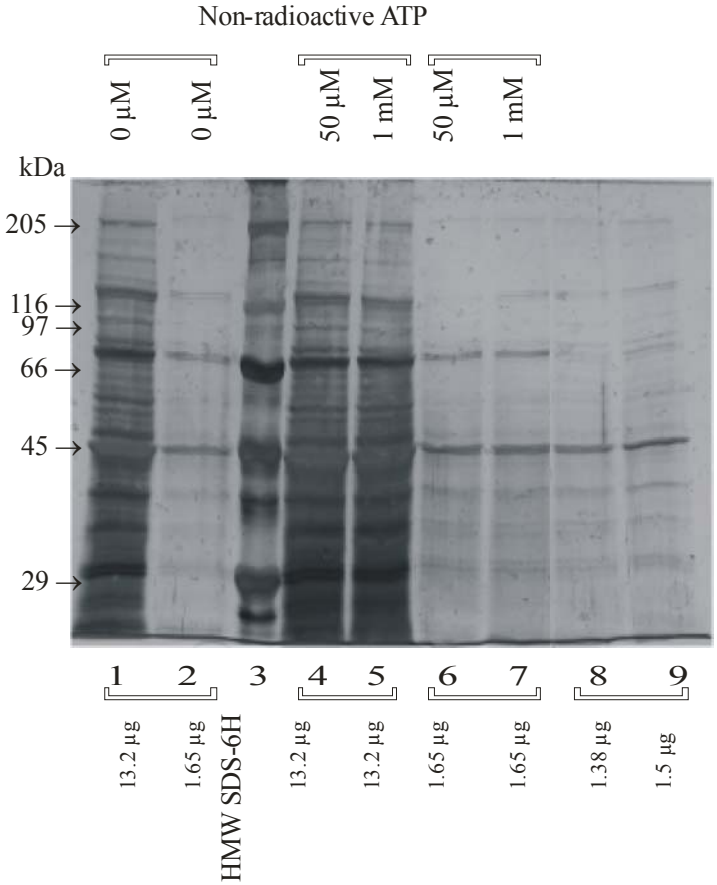

Fig. 41: Effect of incubation of protein sample with non-radioactive ATP on migration during SDS-PAGE. 5 % concentration gel and 10 % separating gel. The concentrations of ATP are indicated at the top and of protein at the bottom. Specific activity of the enzyme is 85,000 radioactivity (cpm) mg^{-1} protein.

3.8.3 Effect of incubation time on the protein phosphorylation with [γ-^{32}P]ATP

It was of interest to gain qualitative information about the rate of the reaction. An experiment was carried out varying the incubation time from 0 to 60 min at 25^{o}C and employs otherwise the usual reaction conditions before.

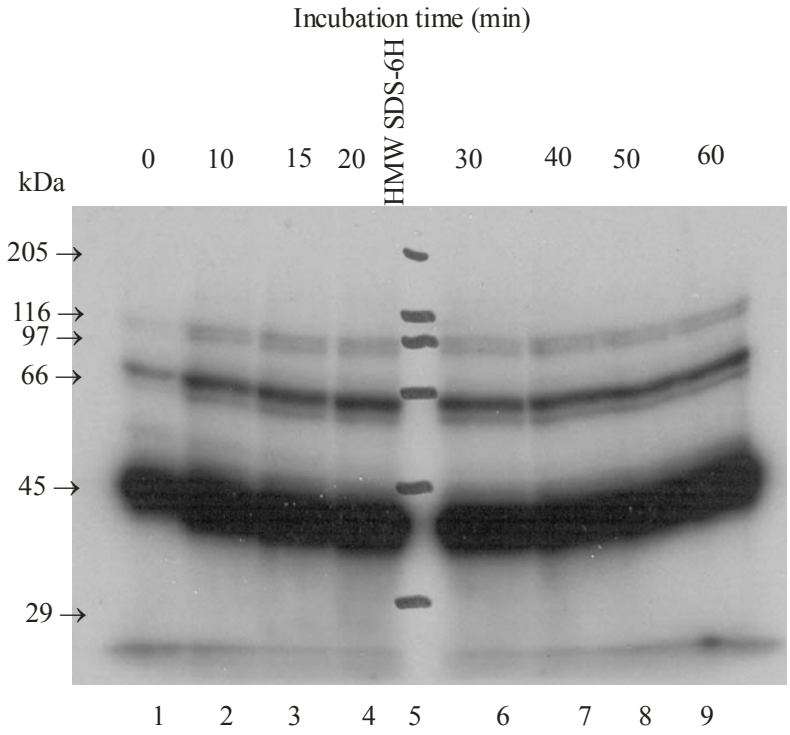

Fig. 42: Effect of incubation time on labeling with [γ-^{32}P]ATP. 5 % concentration gel and 10 % separating gel. Lane 5 contained the standard protein test mixture Sigma HMW SDS-6H (29 to 205 kDa). Lanes 1 to 4 and 6 to 9 refer to reactions incubated at 25°C at different time periods ranging from 0 to 60 min. L-malate was absent in all cases. An amount of 66 µg protein has been present in each reaction mixture, and 13 µg protein mounted onto each lane of the gel.

The results in **Fig. 42** show that the reaction was complete within 10 min from mixing the reactants. Proteins of higher molecular masses were also phosphorylated, at lower intensities, following very similar kinetics. These proteins were the same as in **Fig. 39**. It was concluded that the time of phosphorylation was short compared to the experimental times (15 min) allowed for the formation of p45~[^{32}P]AMP in the forgoing experiments .

3.8.4 Inhibition studies with Tyr-kinase inhibitor Tyrphostin A 23 on phosphorylation with [γ-^{32}P]ATP

We have suggested that phosphorylation of p45 or any, possibly complex bound protein could increase the amount of p45-fraction that reacted with [α-^{32}P]ATP to form

p45~[^{32}P]AMP. To validate this assumption, we searched for a kinase inhibitor that prevented activation of p45 by inhibiting protein phosphorylation. In a first attempt, we examined the broad range Tyr-kinase inhibitor Tyrphostin A 23 (Seger et al., 1995).

Concentrations ranging from 0 to 10 mM of Tyrphostin A 23 were present in the phosphorylation reaction mixture. Samples of 100 µl of reaction mixture containing ligase buffer, 5 µCi of [γ-^{32}P]ATP (5,000 Ci/mmol, Amersham Corp.), 66 µg of the concentrated Toyopearl 650-M fraction and Tyrphostin A 23 at concentrations ranging from 0 to 10 mM were incubated at 25^{o}C for 15 min. Samples (20 µl) of the reaction mixtures were mixed with 20 µl of SDS buffer, at 85^{o}C for 5 min, and subjected to SDS-PAGE (10 %). After electro blotting onto nitrocellulose and staining with Ponceau S, the extent of phosphorylation was detected by autoradiography at -80^{o}C for 5 days (**Fig. 43**).

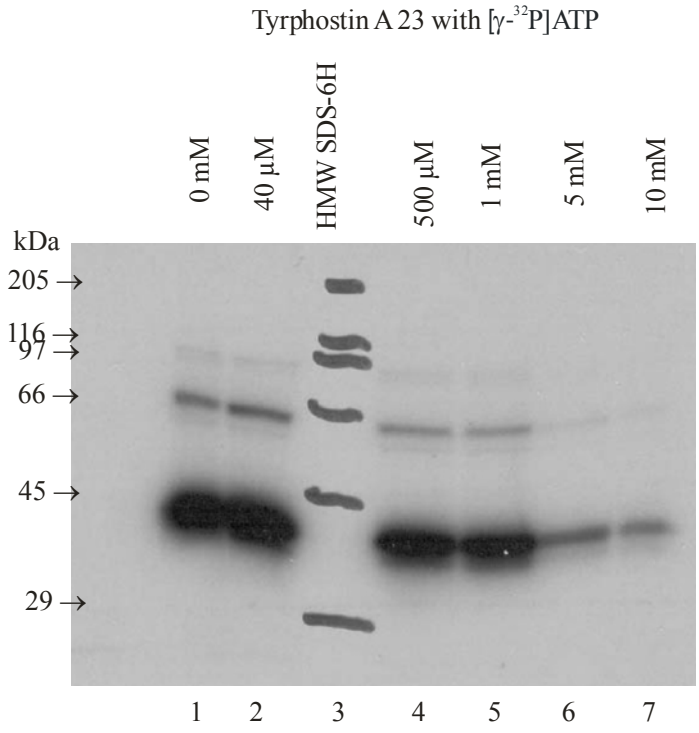

Fig. 43: Effect of Tyrphostin A 23 on the protein phosphorylation with [γ-^{32}P]ATP. 5 % concentration gel and 10 % separating gel. Lane 3 contained the standard protein test mixture Sigma HMW SDS-6H (29 to 205 kDa). Lanes 1, 2, 4, 6, and 7 contained the reactions that were carried out with different concentrations of Tyrphostin A 23 in the range 0, 40 µM, 500 µM, 1 mM, 5 mM, and 10 mM, respectively. An amount of 66 µg protein has been present in each reaction mixture, and 13 µg mounted onto each lane of the gel.

It is recognized from **Fig. 43** that a minimum of 500 µM Tyrphostin A 23 is required to see inhibition, whereas no inhibition occurred at 40 µM. 50 % inhibition was estimated from the dependence of intensities to require less than 1 mM Tyrphostin A 23. Tyrphostin A 23 is a tyrosine specific kinase inhibitor with an IC_{50} of 40 µM (Seger et al., 1995). The estimate of a IC_{50} of 0.5 – 1 mM indicated that Tyrphostin A 23 is considerably less inhibitory were than for the standard kinases in the literature.

3.8.5 Attempt to inhibit the formation of p45~[^{32}P]AMP

We have assigned that intensification of the radioactivity of p45~[^{32}P]AMP may occur due to phosphorylation of p45 or another protein, and we have argued that formation of p45~[^{32}P]AMP is favored by phosphorylation. If the phosphorylation is inhibited by Tyrphostin A 23, and if p45~[^{32}P]AMP formation is activated by phosphorylation (see **Fig. 38**), then Tyrphostin A 23 should inhibit this adenylation. The effect of Tyrphostin A 23 in the protein-adenylate formation was measured for a reaction mixture of 100 µl containing ligase buffer, 5 µCi of [α-^{32}P]ATP (3,000 Ci/mmol, Amersham Corp.), 66 µg of the concentrated Toyopearl 650-M fraction and different concentrations of Tyrphostin A 23 ranging from 0 to 10 mM. Reactions were incubated and products detected as in **chapter 3.8.4**. Results are shown in **Fig. 44**.

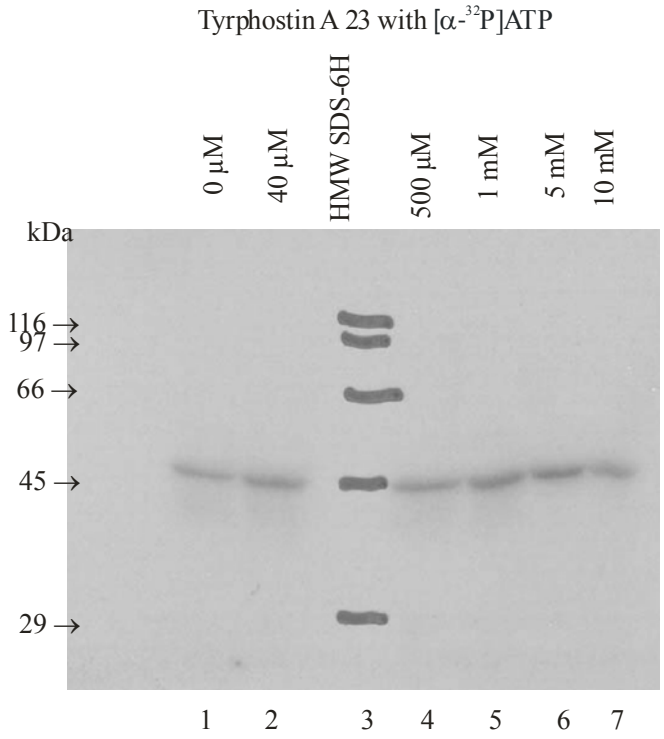

Fig. 44: Effect of Tyrphostin A 23 on the reaction of protein with [α-^{32}P]ATP in the absence of α,β-methylene-ATP. 5 % concentration gel and 10 % separating gel. Lane 3 contained the standard protein test mixture Sigma HMW SDS-6H (29 to 205 kDa). Lanes 1, 2, 4, 6, and 7 contained the reactions mixtures with different concentrations of Tyrphostin A 23 in the range 0, 40 µM, 500 µM, 1 mM, 5 mM, and 10 mM, respectively. An amount of 66 µg protein has been present in each reaction mixture, and 13 µg mounted onto each lane of the gel.

Comparison of the lanes 1 and 2 and 4–7 in **Fig. 44** shows that presence of Tyrphostin A 23 had no effect on p45~[^{32}P]AMP formation in the absence of enhancer. The result suggested, that a small fraction of the protein was already phosphorylated in the protein sample in the absence of [α-^{32}P]ATP, and that incubation at the very low concentration of [α-^{32}P]ATP in the gel assay mixture did not lead to detectable amounts of phosphorylated protein even, when Tyrphostin A 23 was absent.

In order to enhance the amount of formed p45~[^{32}P]AMP, we included α,β-methylene-ATP as kinase substrate that had been shown to give rise to considerable labeling of p45 (see **Fig. 38**). Under this condition, the inhibition of p45~[^{32}P]AMP formation by Tyrphostin A 23 became detectable (**Fig. 45**).

We also examined the effect of Tyrphostin A 23 on ATP-PPi-exchange activity (**Table 3**). It is found that the activity was completely abolished in the presence of 25 mM Tyrphostin A 23. Since the stock solution of inhibitor had been prepared in absolute ethanol, control test had to be performed varying the ethanol content in the ATP-PPi-exchange reaction mixture. It turned out that the presence of ethanol was very inhibitory, as seen in **Table 4**. Already 2 % (v/v) as was present in 1 mM solution of Tyrphostin A 23 caused 70 % inhibition. In face of these adverse results, inhibition of p45~[^{32}P]AMP was questionable. Examination, however, indicated that by absence of inhibition in **Fig. 44,** Tyrphostin A 23 as high as 10 mM had no inhibitory effect, assuming that at least 20 % (v/v) ethanol in this reaction were not inhibitory.

To validate the assumption that the presence of ethanol was not the reason for the inhibitory effect, another experiment (not shown) was performed as before (**Fig. 45**). Instead of ethanol, DMSO was used as solvent for Tyrphostin A 23 (diluted in such a way that 25 mM of Tyrphostin A 23 contained only 2.5 % DMSO). Under this solvent condition the inhibition of p45~[^{32}P]AMP formation by Tyrphostin A 23 was also detectable. However, the efficiency of inhibition using DMSO as solvent was 50 % whereas ethanol gave 100 % in the reaction with 25 mM Tyrphostin A 23 (**Fig. 45)**. Whether ethanol added to inhibition of ATP-PPi-exchange by protein denaturation has to be investigated.

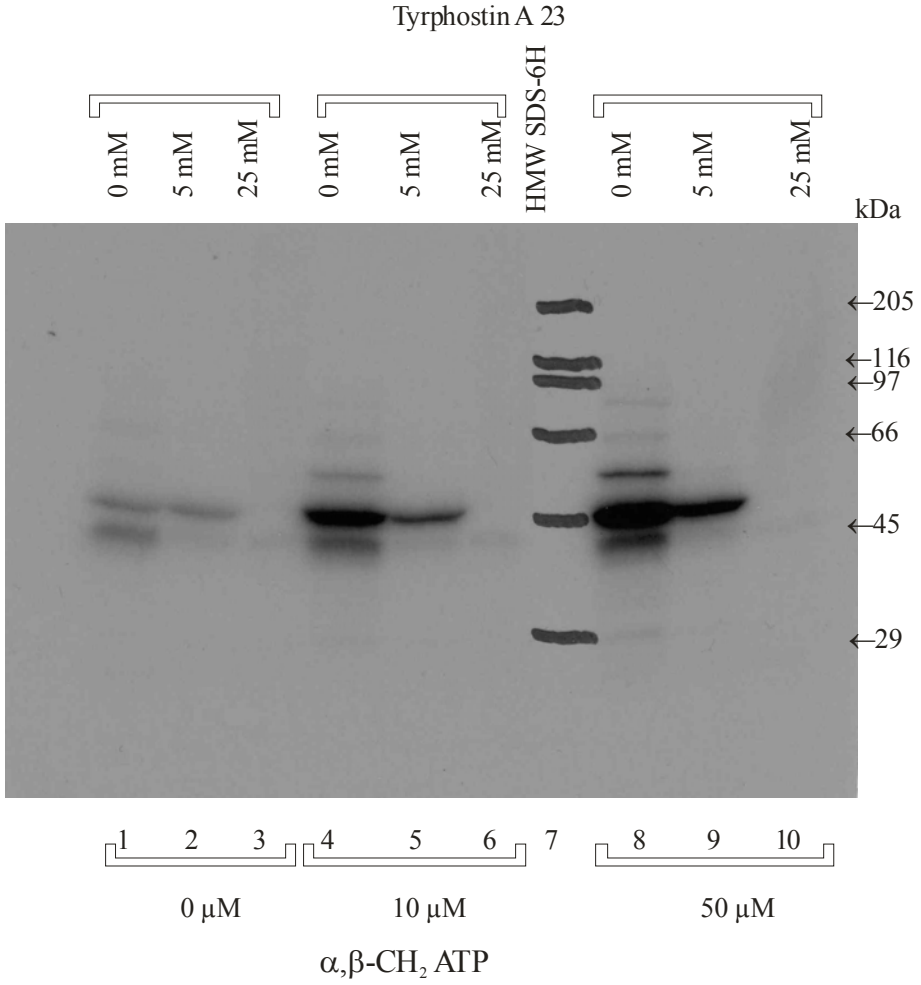

Fig. 45: Inhibition of Tyrphostin A 23 in the absence and presence of α,β-methylene-ATP. 5 % concentration gel and 10 % separating gel. Lane 7 contained the standard protein test mixture Sigma HMW SDS-6H (29 to 205 kDa). Concentrations of Tyrphostin A 23 and α,β-methylene-ATP are indicated. An amount of 66 µg protein has been present in each reaction and 13 µg mounted onto each lane of the gel.

Reaction content	ATP-PPi-exchange activity (cpm)
Usual reaction (100 µl protein sample)	7858
Usual reaction mix. (100 µl protein sample) + 25 mM Tyrphostin A 23	97

Table 3: The ATP-PPi-exchange reaction carried out in the absence/presence of Tyrphostin A 23. Reaction mixtures contained 100 µl of protein sample (660 µg protein of sucrose-concentrated Toyopearl fraction). Since stock solution of Tyrphostin A 23 had been prepared in absolute ethanol, the reaction mixture contained 50 % of ethanol.

Reaction content	ATP-PPi-exchange activity (cpm)
Usual reaction (40 µl protein sample)	2169
w/ 2 % Ethanol	777
w/ 10 % Ethanol	289
w/ 50 % Ethanol	81

Table 4: Effect of absolute ethanol on the ATP-PPi-exchange activity. Reaction mixtures contained 40 µl of protein sample (264 µg protein of sucrose-concentrated Toyopearl fraction).

3.8.6 Inhibition of phosphorylation by Ser/Thr-kinases using Rottlerin

We examined the effect of Rottlerin, an inhibitor of Ser/Thr-kinases with some specificity for PKC with IC_{50} ranging 3-100 µM (Davies et al., 2000; Gschwendt et al., 1994), on ^{32}P-phosphorylation of proteins. The phosphorylation mixture in 100 µl contained ligase buffer, 5 µCi of [γ-^{32}P]ATP (5,000 Ci/mmol, Amersham Corp.), 66 µg of the concentrated Toyopearl 650-M fraction and different concentrations of Rottlerin ranging from 0 to 10 mM. The mixtures were incubated at 25^{o}C for 15 min. Then, 20 µl of sample from each of the reaction mixtures were mixed with 20 µl of SDS buffer, heated at 85^{o}C for 5 min, and subjected to SDS-PAGE (10 %), and the proteins electroblotted onto nitrocellulose filters and stained with Ponceau S. The extent of phosphorylation was detected by autoradiography at -80^{o}C for 5 days (**Fig. 46**).

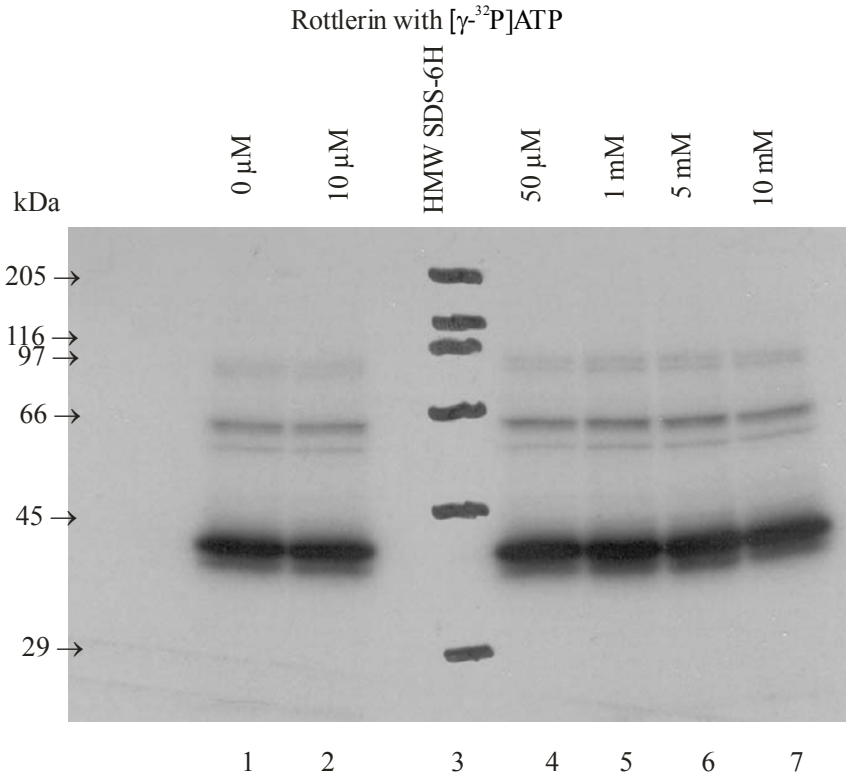

Fig. 46: Effect of Rottlerin on phosphorylation with [γ-^{32}P]ATP. 5 % concentration gel and 10 % separating gel. Lane 3 contained the standard protein test mixture Sigma HMW SDS-6H (29 to 205 kDa). Lanes 1, 2, 4, 5, 6, and 7 contained the reaction mixtures that were carried out with different concentrations of Rottlerin in the range 0, 10 µM, 50 µM, 1 mM, 5 mM, and 10 mM, respectively. An amount of 66 µg protein has been present in each reaction and 13 µg mounted onto each lane of the gel.

A comparison of all the lanes in **Fig. 46** for different concentrations of Rottlerin ranging from 0 and 10 mM indicated no differences in band intensity for protein phosphorylation. It is concluded that the kinase(s) are probably not specific for Ser and Thr.

3.8.7 Formation of p45~[^{32}P]AMP in the presence of Rottlerin

In analogy to experiment with Tyrphostin, we examined whether the Ser/Thr-kinase inhibitor Rottlerin effected the activity forming p45~[^{32}P]AMP. The reaction and detection of product was carried out as before (**Fig. 44**) except that Rottlerin was present (**Fig. 47**).

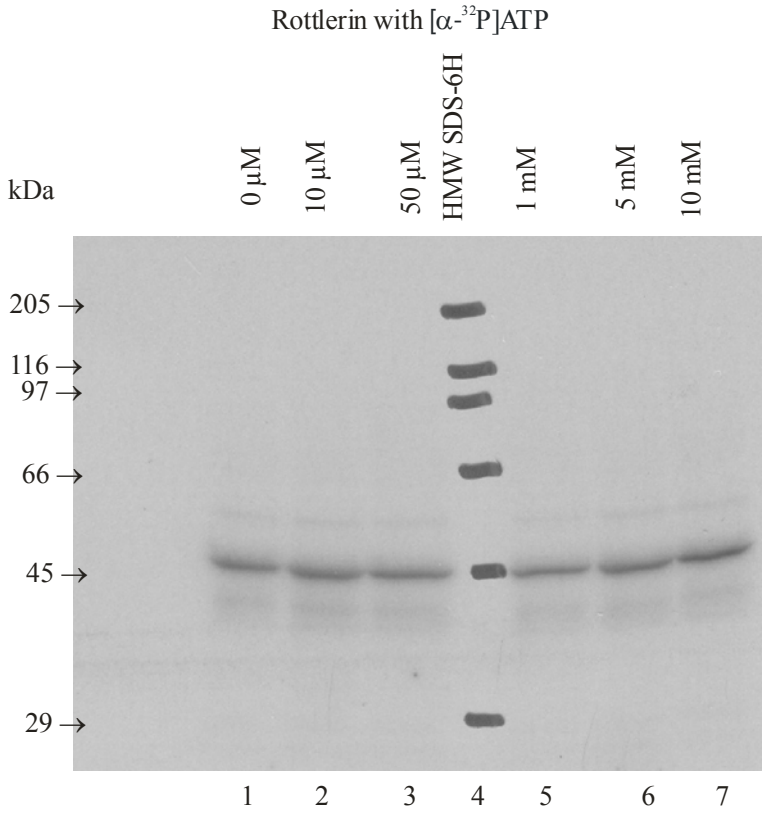

Fig. 47: Effect of Rottlerin on p45-adenylate formation with [α-^{32}P]ATP. 5 % concentration gel and 10 % separating gel. Lane 4 contained the standard protein test mixture Sigma HMW SDS-6H (29 to 205 kDa). Lanes 1, 2, 3, 5, 6, and 7 contained the reactions that were carried out with different concentrations of Rottlerin in the range 0, 10 µM, 50 µM, 1 mM, 5 mM, and 10 mM, respectively. An amount of 66 µg protein has been present in each reaction and 13 µg mounted onto each lane of the gel.

Comparison of the lanes in **Fig. 47** indicated that different concentrations of Rottlerin ranging from 0 and 10 mM had no effect on band intensity of the p45-adenylate. The result was in agreement with the absence of inhibition of Rottlerin on phosphorylation in **Fig. 46**. However, in analogy to the requirement shown in **Fig. 45** for the visualization of inhibition by Tyrphostin A 23, additional experiments would have been required in the presence of α,β-methylene-ATP to completely rule out inhibition.

3.8.8 Inhibition of phosphorylation by KT 5720

KT 5720 has been reported to be an inhibitor of Ser/Thr-kinases with some specificity for PHK, PDK1, and PKA with IC_{50} ranging 11 nM-3.3 µM (Davies et al., 2000). Reaction conditions were the same as with Rottlerin (**chapter 3.8.6**), however in the presence of KT 5720 as the Ser/Thr-kinase inhibitor at concentrations 0 – 10 mM (**Fig. 48**).

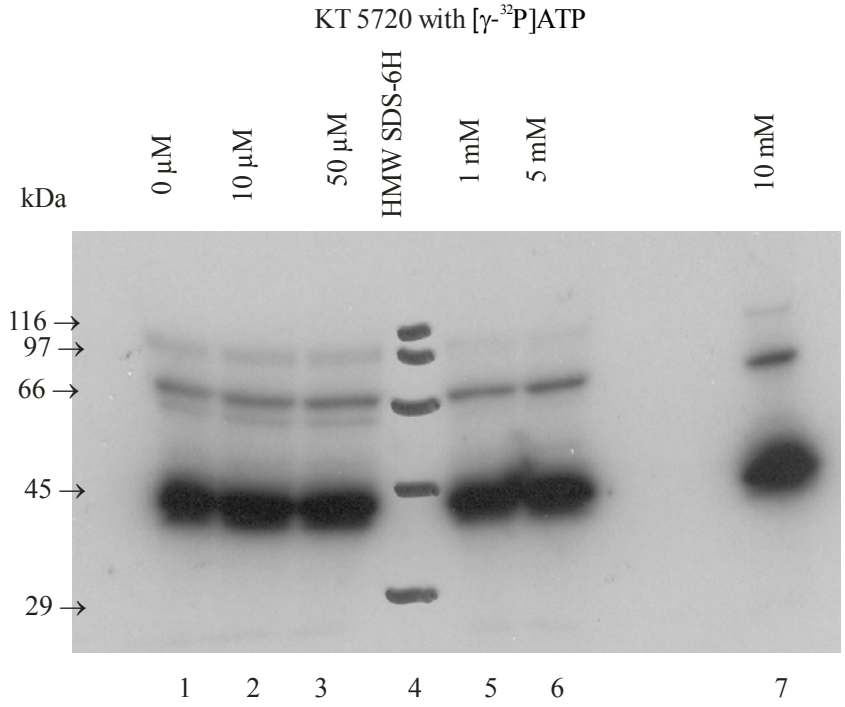

Fig. 48: Effect of KT 5720 on protein phosphorylation with [γ-^{32}P]ATP. 5 % concentration gel and 10 % separating gel. Lane 4 contained the standard protein test mixture Sigma HMW SDS-6H (29 to 205 kDa). Lanes 1, 2, 3, 5, 6, and 7 refer to reactions carried out in the presence of different concentrations of KT 5720 in the range 0, 10 µM, 50 µM, 1 mM, 5 mM, and 10 mM, respectively. An amount of 66 µg protein has been present in each reaction and 13 µg mounted onto each lane of the gel.

A comparison of the results in **Fig. 48** indicated that KT 5720 had no effect on protein phosphorylation.

3.8.9 Formation of p45~[^{32}P]AMP in the presence of KT 5720

The effects of different concentrations ranging from 0 to 10 mM of KT 5720 on the formation of p45~[^{32}P]AMP were followed in analogy to previous **chapter 3.8.5** (**Fig. 44**).

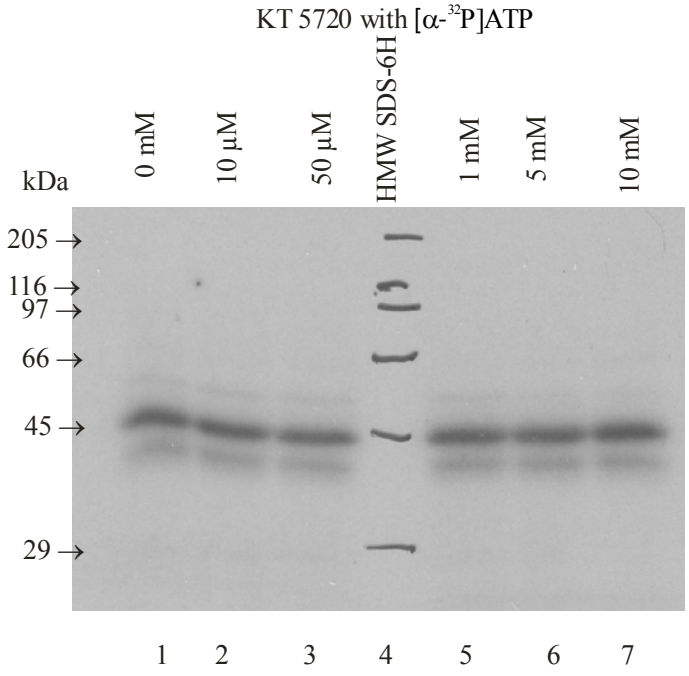

Fig. 49: Effect of KT 5720 on the formation of p45~[^{32}P]AMP. 5 % concentration gel and 10 % separating gel. Lane 4 contained the standard protein test mixture Sigma HMW SDS-6H (29 to 205 kDa). Lanes 1, 2, 3, 5, 6, and 7 contained the reaction mixtures that were carried out with different concentrations of KT 5720 in the range 0, 10 µM, 50 µM, 1 mM, 5 mM, and 10 mM, respectively. An amount of 66 µg protein has been present in each reaction and 13 µg mounted onto each lane of the gel.

The results in **Fig. 49** show that KT 5720 had no effect on the protein~adenylate formation, in agreement with the absence of inhibition of protein phosphorylation in **Fig. 48**.

3.9 Identification of protein complexes which are labeled by [α-^{32}P]ATP and [γ-^{32}P]ATP employing PAGE under non-denaturing condition.

The formation of protein-adenylate from [α-^{32}P]ATP and phosphorylated protein from [γ-^{32}P]ATP and sucrose-concentrated Toyopearl 650-M fraction was followed by electrophoretic analysis on non-denaturing 5 – 10 % linear polyacrylamide gradient gels and autoradiography. The experiment served to solve the question, whether p45~[^{32}P]AMP (45 kDa) and the phosphorylated protein of molecular mass 35,000 resided together in a protein complex that allowed a mutual interaction, as we have proposed in previous sections. Adenylation and phosphorylation were carried out as before in reaction mixtures of 100 µl containing ligase buffer and 5 µCi of either [α-^{32}P]ATP (3,000 Ci/mmol, Amersham Corp.) or [γ-^{32}P]ATP (5,000 Ci/mmol, Amersham Corp.), 66 µg of the concentrated Toyopearl 650-M fraction. After incubation of the reaction mixtures at 25^{o}C for 15 min, 20 µl samples were combined with 20 µl of sample buffer (see **chapter 2.1.1.12**). The proteins were separated by electrophoresis and then transferred onto nitrocellulose filters. The nitrocellulose filters were stained with Ponceau S and the proteins were visualized (Walker, 2002). The bands formed were detected by autoradiography at -80^{o}C for 14 days (**Fig. 50**).

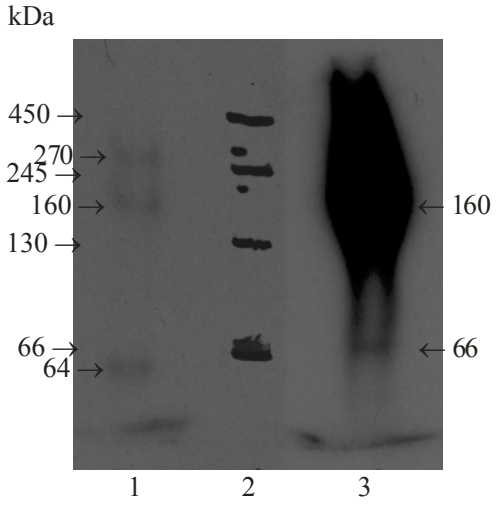

Fig. 50: Protein complexes as identified by non-denaturing PAGE after radioactive labeling with [α-^{32}P]ATP and [γ-^{32}P]ATP. 5 - 10 % non-denaturing gradient separating gel. Lane 2 contained the standard protein marker mixture of bovine serum albumin (66 kDa monomer and dimer), catalase (245 kDa), and ferritin (450 kDa). Lane 1 contained the reaction products of [α-^{32}P]ATP with the concentrated

Toyopearl 650-M fraction, after 3 fold intensification with the help of software Adobe Photoshop 7.0. Lane 3 contained the reaction products of [γ-^{32}P]ATP with the concentrated Toyopearl 650-M fraction. An amount of 66 µg protein has been present in each reaction mixture, and an amount of 13 µg was loaded in each lane.

Fig. 50 shows the results after non-denaturing PAGE and autoradiography. Phosphorylation with [γ-^{32}P]ATP produced a broad band centered at 160 kDa and a minor one connected with the broad one at 66 kDa. Labeling with [α-^{32}P]ATP resulted in 3 bands, at 64, 160, and 270 kDa. None of these bands has been visualized after SDS-PAGE, except the ~66 kDa band after labeling with [γ-^{32}P]ATP (**Figs. 43, 46 etc.**) The bands of 64, 160, and 270 kDa labeled by [α-^{32}P]ATP could refer to p45~[^{32}P]AMP as constituents of protein complexes. The 64 kDa band could also refer to p45~[^{32}P]AMP, if it was assured that the mobilities in SDS-PAGE and non-denaturing gels could show individual mobilities, not exactly accounted for by the marker proteins. An important result was that all of the [α-^{32}P]ATP-labeled protein coincided with [γ-^{32}P]ATP-labeled protein complexes. Future experiments will be performed, which will subject the protein sample after labeling with [α-^{32}P]ATP and [γ-^{32}P]ATP to non-denaturing PAGE in the first dimension to identify the labeled proteins along with the species characterized so far only by SDS-PAGE. It is, however, clear that one or both bands migrating in positions 160 and 270 kDa will be identical with p45~[^{32}P]AMP, thus indicating that it was part of one or two protein-complexes which were labeled by ^{32}P-phosphorylation. This finding is in agreement with the assumption, that phosphorylation could have an effect on the activity of p45 to become adenylated by [α-^{32}P]ATP (see **chapters 3.7.7 & 3.7.9, eq. 5**).

3.10 Analysis by Thin Layer Chromatography (TLC) of nucleotides released during incubation for p45~[^{32}P]AMP formation

It was of interest which nucleotides were produced during incubation of the protein and ATP plus L-malate. In principle, the only nucleotide formed should be AMP, which was expected to covalently bound to p45. Side reactions by impurities could form ADP, especially the kinases, shown to be active in the sample (**see Figs. 39-40 & 42**). The amount of AMP after hydrolytic cleavage of p45~AMP (that was expected to be hydrolytically labile) should be small. Addition of L-malate had revealed in **Fig. 32** to induce a turnover of ATP, that could

have resulted in AMP by forming dimers and oligomers of L-malate. Also, it was expected from published literature that p45~AMP reacted with ATP to form AP_4A (McLennan, 1992). Thus, we expected a time dependent increase of AMP, ADP and AP_4A. Time dependent reactions were monitored by TLC. The routine TLC system consisted of silica gel with a fluorescent indicator (Merck). The chromatography was developed by the method described by Guranowski et al., 2000.

Two experiments were carried out in parallel to determine the effect of incubation time on TLC resolution.

First experiment was conducted under the same condition as used for the formation of p45~[^{32}P]AMP in the presence of L-malate, varying reaction times from 0 to 60 min at 25^{o}C. The reaction mixture cocktail contained ligase buffer, 5 µCi of [α-^{32}P]ATP (3,000 Ci/mmol, Amersham Corp.), 2 mM ATP and 1 mM of L-malate in each of the eppendorfs. At 10 min intervals, 66 µg of the concentrated Toyopearl 650-M fraction was added to each eppendorf totaling a volume of 100 µl and incubated at 25^{o}C. At given times, 10 µl was removed quickly from each reaction mixture, stopped by adding 10 µl of 50 mM of ATP, and spotted onto a TLC plate (see **chapter 2.2.14**). After chromatography, the plate was then exposed to autoradiography, the results shown in **Fig. 51**. The experiment was also conducted with a single reaction mixture, and 10 µl samples were removed at ambient times and the reaction stopped by the addition of 10 µl of 50 mM of ATP. The TLC and autoradiograph were developed and the result was obtained in **Fig. 52**.

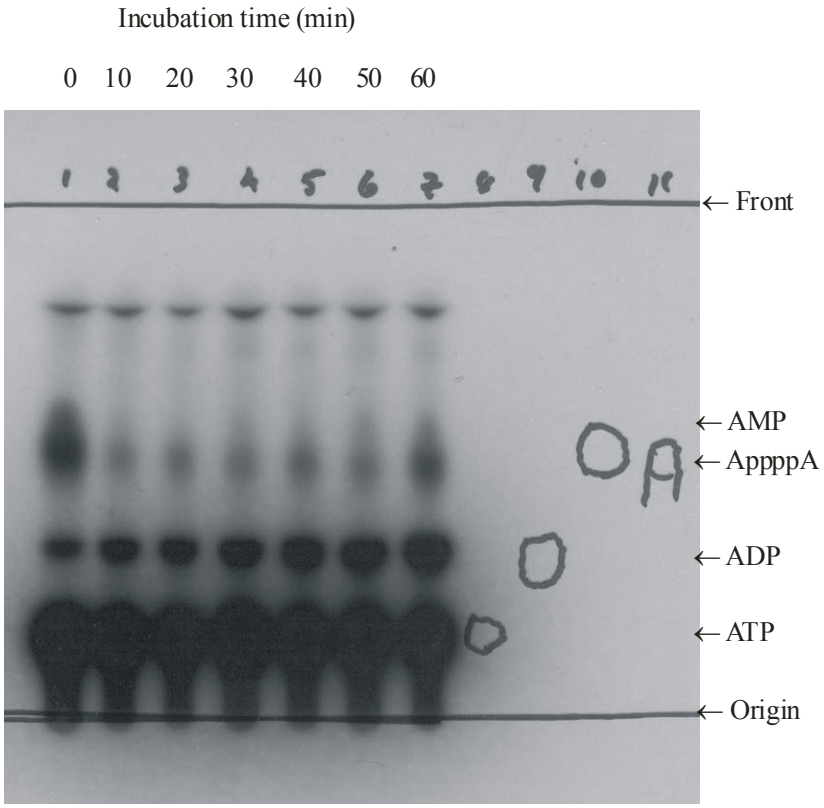

Fig. 51: Effect of incubation time on TLC resolution. Lanes 1 to 7 refer to reactions incubated in parallel at 25°C at different time periods ranging from 0 to 60 min. 1 µl samples corresponding to each incubation time were removed from the reaction mixtures at ambient times from different reaction mixtures, and spotted on the TLC-plate. The autoradiography was carried out for 4 days at -80°C. The spots encircled in lane 8-11 indicate results obtained with non-labeled nucleotides (1 pmole of each nucleotides was spotted).

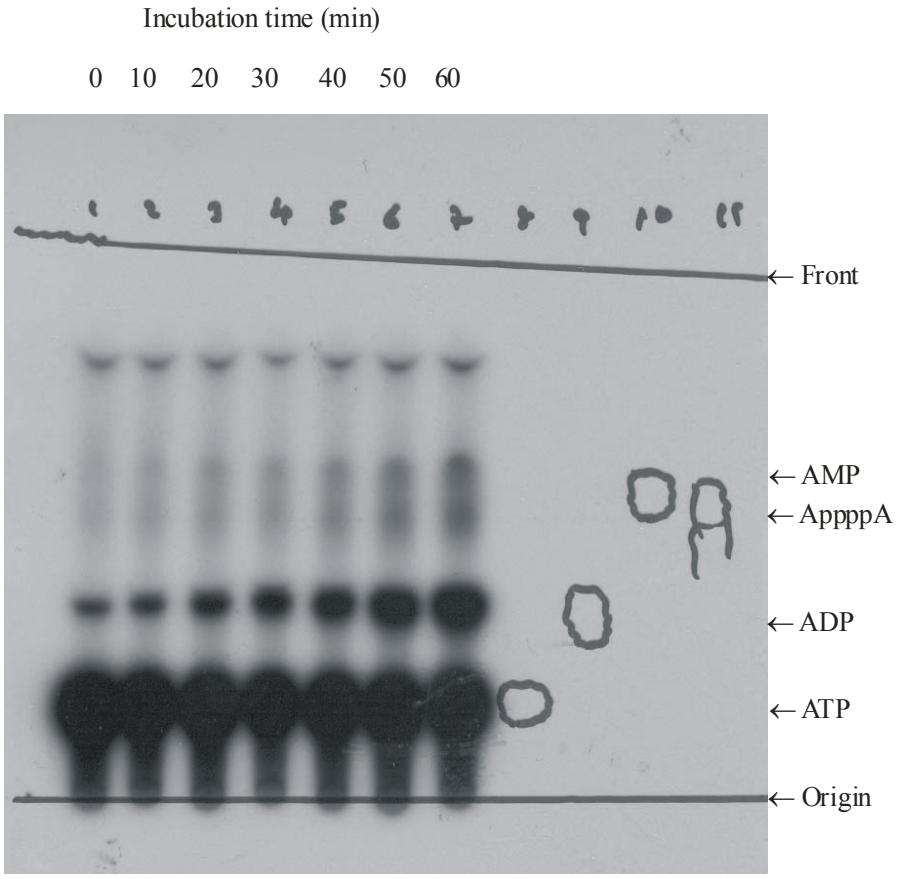

Fig. 52: Effect of incubation time on TLC resolution. Lanes 1 to 7 refer to a single reaction incubated at 25°C and samples were drawn at different times from 0 to 60 min. Conditions are otherwise the same as in **Fig. 51**.

Comparing **Figs. 51 and 52**, the autoradiographs show virtually the same results. AMP, ADP, and AP_4A were formed during the course of the reaction.

The results were as expected, confirming the formation of adenylate, the reaction of adenylate with L-malate to form AMP, and with ATP to form AP_4A (Guranowski et al., 2000). The high rate of ADP formation was in agreement with the assumption of kinases.

The result on the formation of free AMP together with the kinetics for p45~AMP observed in the presence of 10 mM L-malate (**Fig. 32**), suggested the formation of dimers or oligomers of L-malate. Attempts to resolve such products by TLC-system employed several methods to stain dimers or oligomers of L-malate. These systems involved vanillin (Adamson et al., 1999), iodine vapor (Zakrzewski and Ciesielski, 2002), or permanganate (Zakrzewski and Ciesielski, 2002). However, sucrose contained in the concentrated protein samples interfered with the detection.

3.11 Attempts to demonstrate the formation of dimers and oligomers of malic acid by employing L-[^{14}C]malic acid and thin layer chromatography

The kinetics shown in **Fig. 32**, depicting the transient formation of p45~[^{32}P]AMP in the presence of 10 mM L-malate, suggested the formation of dimers and/or oligomers of malic acid. In the following experiment, it was attempted to identify such oligomers by employing L-[^{14}C]malic acid and TLC. **Fig. 53** shows the results. Radioactivity runs close to the solvent front. Oligomers were expected to migrate less far. However, little or no evidence is seen in **Fig. 53** of material that shows low mobility. As the concentration of L-[^{14}C]malate was of the order of 18 µM (1 µCi reaction) and 90 µM (5 µCi reaction), very little formation of radioactively labeled oligomer expected in comparison with 10 mM L-malate in the kinetic study of **Fig. 32**. It was possible that the small amounts escaped the detection. Future experiments should apply high L-malate concentration. Since under such conditions TLC-plate detection was technically not possible, product analysis should be carried out by HPLC.

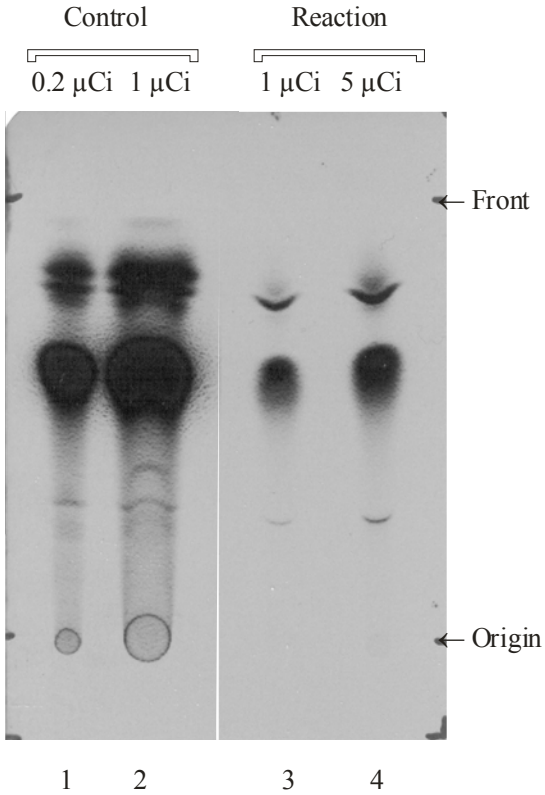

Fig. 53: Attempt to identify dimers and/or oligomers by employing L-[^{14}C]malic acid and TLC. Lanes 1 and 2 refer to the control, which are 0.2 µCi and 1 µCi of L-[^{14}C]malic acid, respectively, directly applied to TLC. Lanes 3 and 4 refer to the reaction mixtures which were carried out in the presence of 1 µCi and 5 µCi of L-[^{14}C]malic acid, respectively. The autoradiography was carried out for 14 days at -80°C.

3.12 Product analysis of the malate activation reaction by reversed phase HPLC

3.12.1 Strategy

The following chapter is concerned with the reaction(s) catalyzed by the p45-containing sample. It contains a number of putative enzymes, the L-malate activase, a kinase, and probably other, not defined enzymes, which may contribute to the variety of products formed. It is likely from our results that some of the enzymes, namely p45 and a phosphorylated protein, and the protein carrying the kinase activity, form a higher order complex(es), which is(are) involved in product formation. It is also likely that a malate-transferase (PMLA-polymerase) is constituted by such a complex. Our goal was to achieve additional evidence, besides the reactions of malic acid described elsewhere in this investigation, that formation of oligomalate or PMLA occurs under our reaction conditions.

The products formed in the reaction of p45 with ATP and L-malic acid have been analyzed by reversed phase chromatography. The strategy was to stepwise increase the complexity of reaction components, i.e. starting with the reaction of p45 and ATP (all nucleoside triphosphates as Mg-salts), then of p45 plus ATP plus L-malate, p45 plus ATP plus L-malate plus Tyrphostin (Tyr-kinase inhibitor), etc., and identifying the reaction products. To refer the various HPLC-eluted substances to known reactants/products, pure compounds were analyzed in separate runs at concentrations similarly to those involved in the reactions. These were ATP, ADP, AMP, Ado, Tyrphostin, L-malate, PMLA, fumarate, β,γ-CH_2-ATP, both as fresh solutions and after hydrolysis in the presence of 0.5 M NaOH for 50 min at 100°C, subsequently adjusted to pH 7.0, or otherwise as indicated. All compounds absorbed light at 220 nm, although at different molar absorbances.

3.12.2 Single compounds

L-Malate eluted in the position (in min) 3.56, ATP in 3.56, ADP in 3.70, AMP in 4.08, Ado in 5.5, β,γ-CH_2-ATP in 5.16, Tyrphostin in 3.82, fumarate (4.12), which is in equilibrium with L-malate

3.12.3 Reaction conditions

3.12.3.1 *Reaction of p45 and L-malate*

Reaction mixture in 100 µl contained ligase buffer (which contained also 10 mM $MgCl_2$), 10 mM L-malate, 60 mM phosphoric acid, and 132 µg of the sucrose-concentrated Toyopearl 650-M fraction. The mixtures were incubated at 25°C for 1 hr, and then the reaction was terminated by freezing it with liquid nitrogen. Product analysis was carried out by reversed phase HPLC (see **chapter 2.2.16**).

3.12.3.2 *Reaction of p45 and ATP*

The reaction and detection of product was carried out as before (**chapter 3.12.3.1**) except that 2 mM ATP was used instead of L-malate.

3.12.3.3 *Reaction of p45 and ATP plus L-malate*

The reaction and detection of product was carried out as before (**chapter 3.12.3.1**) except that 2 mM ATP was present.

3.12.3.4 *Reaction of p45, ATP, L-malate plus Tyrphostin A 23*

The reaction and detection of product was carried out as before (**chapter 3.12.3.1**) except that 2 mM ATP and 5 mM Tyrphostin A 23 were also present.

3.12.3.5 *Reaction of p45, β,γ-CH_2-ATP plus L-malate*

The reaction and detection of product was carried out as before (**chapter 3.12.3.1**) except that 0.5 mM β,γ-CH_2-ATP was present.

3.12.4 Results of HPLC analysis

3.12.4.1 *Reaction of p45 and L-malate*

The eluting compound had a retention time of 3.55 min, corresponding to that of non-reacted L-malate.

3.12.4.2 *Reaction of p45 and ATP*

The eluting compounds migrated in 3.50 – 3.70 min; L-malate and ATP were not separated. No obvious reaction. Formation of ADP cannot be excluded.

3.12.4.3 *Reaction of p45 and ATP plus L-malate*

Eluting compounds were at 3.79 and 4.58 min (**Fig. 54**). Free L-malate was not resolved. The slower migrating compound could be malyl~adenylate, or malate-oligomer.

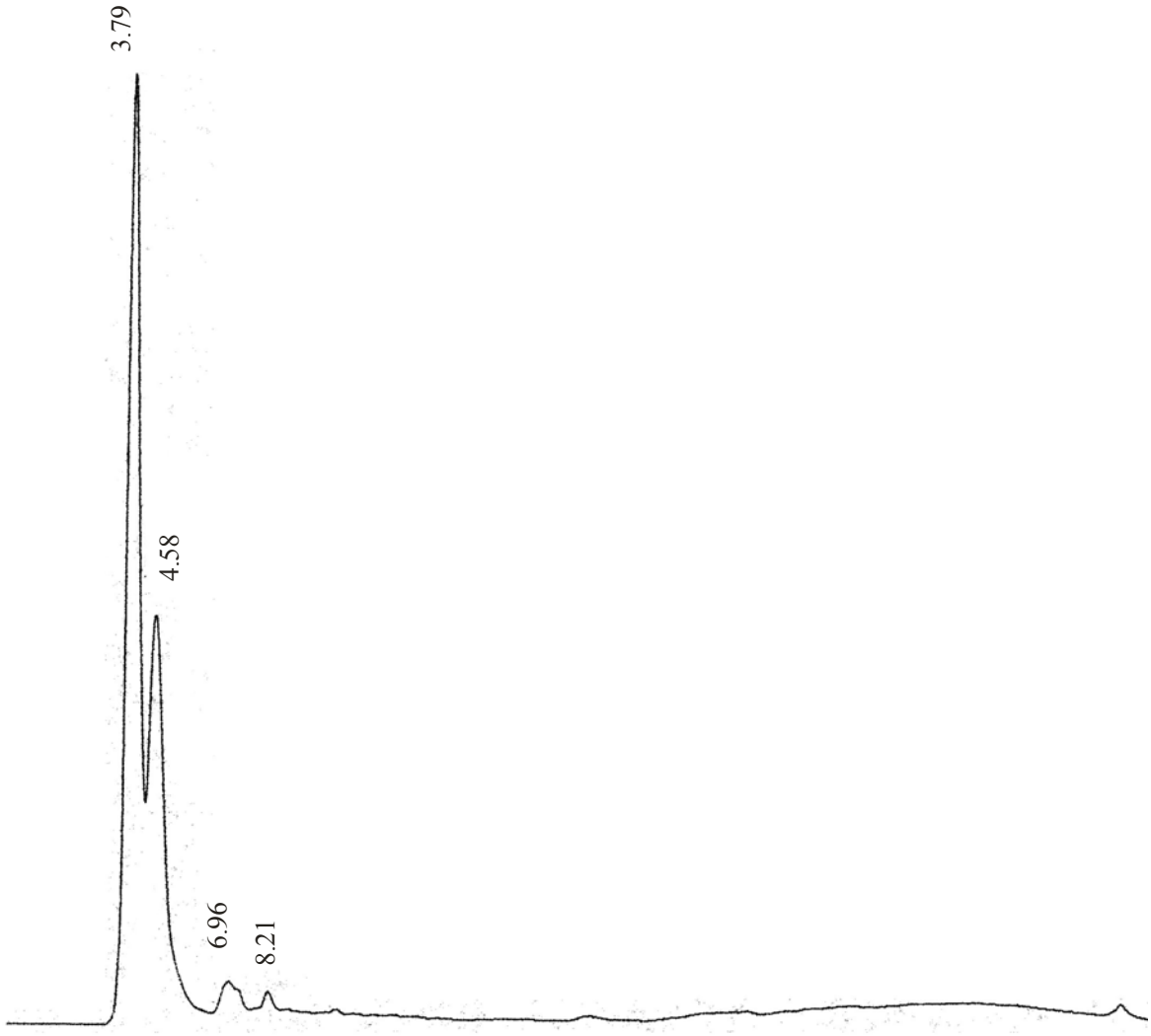

Fig. 54: The analysis of the reaction products of p45, ATP, and L-malate by HPLC. The reaction conditions and the RP-HPLC using a programmed gradient of phosphoric acid (pH 2.1) and acetonitrile are described in the M & M. Numbers indicated in the figure refer to retention times in min. Sensitivity: 7; flow rate: 1 ml/min; chart speed: 5 mm/min. Eluted peaks (220 nm scanning wavelength) of interest were integrated for quantitation.

3.12.4.4 *Reaction of p45, ATP, L-malate plus TyrphostinA 23*

Eluting compounds were at 3.74 (a) (L-malate, ATP, ADP, Tyrphostin), 4.56 (b) (relatively small intensity), 5.46 (c), and 19.11 min (d) (**Fig. 55**). Hydrolysis eliminated none of the faster eluents and probably shifted compound at 19.11 min to 22.48 min. The nature of

this compound (d) remained unknown. By hydrolysis, compound (b) and (c) increased in intensity on cost of compound (d). Compounds (d) and (b) were candidates for oligomalates, where the high molecular compound (d) was faster degraded than (b) due to autolysis (Holler, 1997; **Fig. 56**). Compound (b) could then be $(mal)_2$ or $(mal)_3$, and compound (c) $(mal)_4$ (see also HPLC-analysis of oligomers in Gasslmaier et al., 2000).

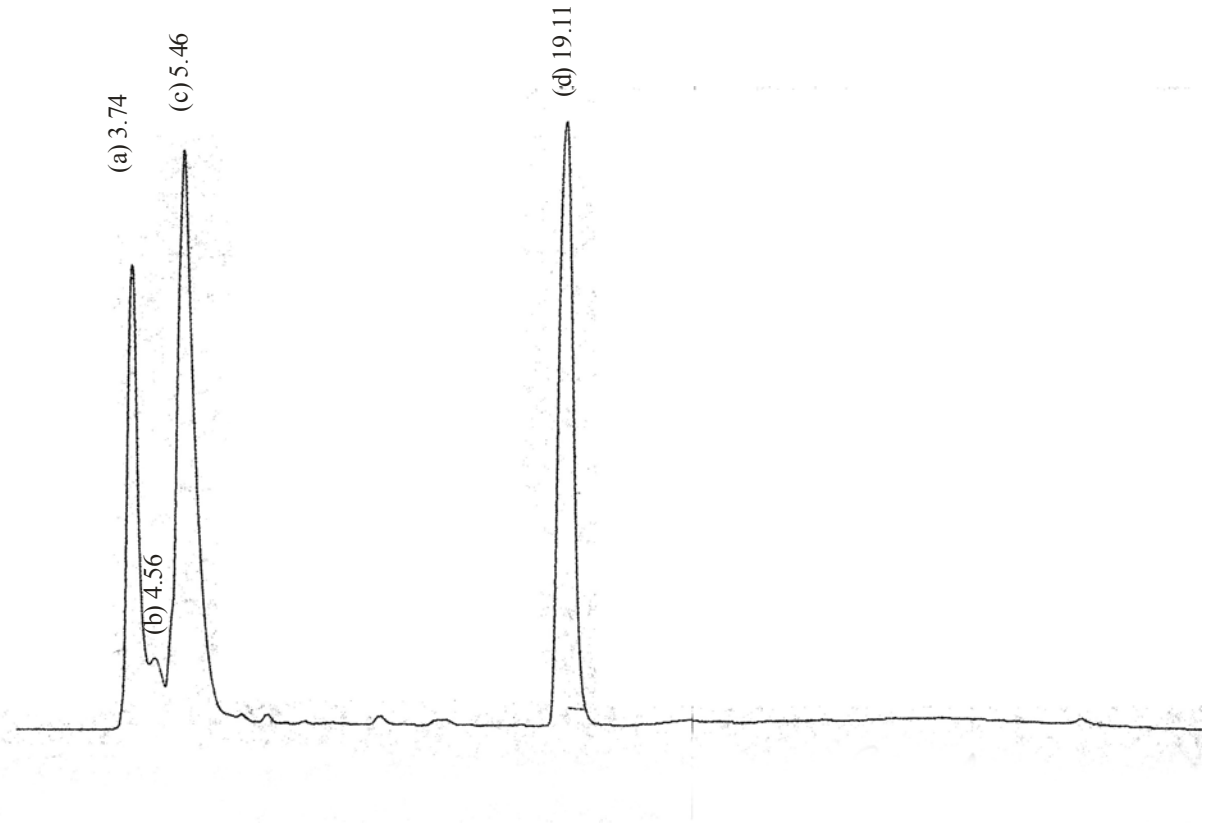

Fig. 55: The analysis of the reaction products of p45, ATP, L-malate, and Tyrphostin A 23 by HPLC. The reaction conditions and the RP-HPLC using a programmed gradient of phosphoric acid (pH 2.1) and acetonitrile are described in the M & M. Numbers indicated in figure refer to retention times in min. Sensitivity: 8; flow rate: 1 ml/min; chart speed: 5 mm/min. Eluted peaks (220 nm scanning wavelength) of interest were integrated for quantitation.

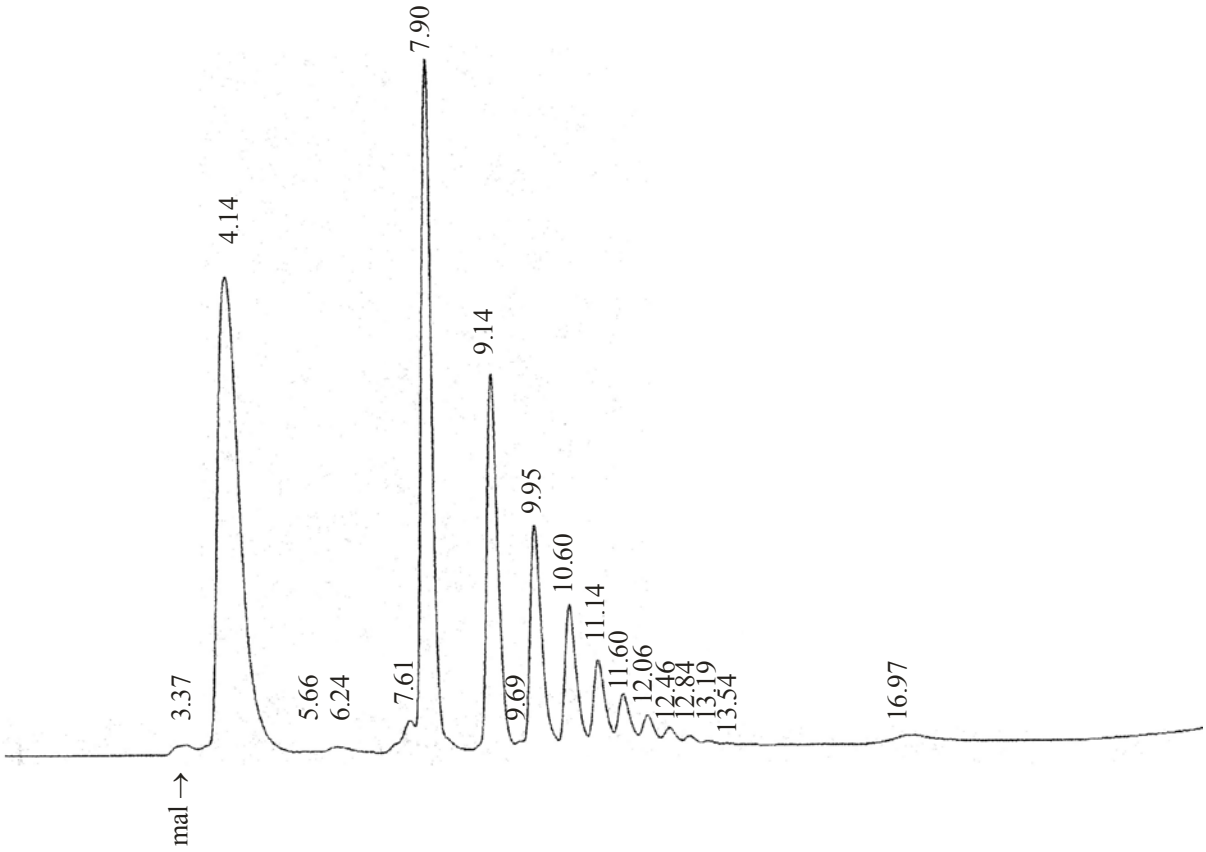

Fig. 56: The analysis of the hydrolyzed products of PMLA by HPLC. Reaction mixture in 100 µl contained ligase buffer, 160 µg PMLA, 60 mM phosphoric acid, and 200 mM NaOH. The mixtures were incubated at 37°C for 10 min, and then the reaction mixture was adjusted to pH 2.1 by adding 15 µl of 2 M phosphoric acid. Product analysis was carried out by reversed phase HPLC. Numbers indicated in figure refer to retention times in min. Sensitivity: 6; flow rate: 1 ml/min; chart speed: 5 mm/min. Eluted peaks (220 nm scanning wavelength) of interest were integrated for quantitation.

3.12.4.5 *Reaction of p45, β,γ-CH_2-ATP plus L-malate*

Eluting compounds were at 3.56 (L-malate), 4.06 (probably fumarate), 4.54 (b), 5.24 (c). Peaks (b) and (c) probably refer again to oligomalate (**Fig. 57**). The reaction in the presence of the ATP analogue is considered much slower than with ATP (Willibald et al., 1999) and higher oligomalates [corresponding to (d) above] were not expected to be formed at the amounts as before in the reaction with ATP. Hydrolysis shows a slight increase in the amount of L-malate, and a large increase in the compound at 4.50 min (b) [presumed $[(mal)_2$ or $(mal)_3]$, and at 5.37 min (c) $[(mal)_4]$ (a slight increase in intensity).

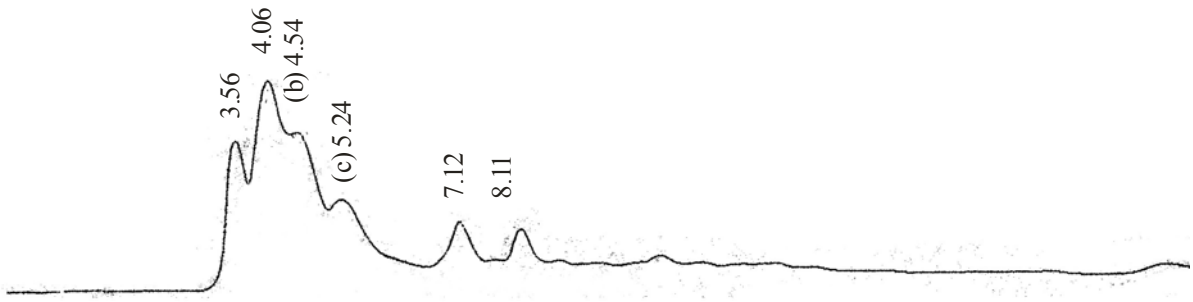

Fig. 57: The analysis of the reaction products of p45, β,γ-CH_2-ATP, and L-malate, by HPLC. The reaction conditions and the RP-HPLC using a programmed gradient of phosphoric acid (pH 2.1) and acetonitrile are described in the M & M. Numbers indicated in figure refer to retention times in min. Sensitivity: 6; flow rate: 1 ml/min; chart speed: 5 mm/min. Eluted peaks (220 nm scanning wavelength) of interest were integrated for quantitation.

3.12.5 Conclusion

The results provide evidence for the synthesis of oligomalates. They are corroborated by the different results of both the partial and full reaction of synthesis and by the degradation in alkaline solution. However, the interpretation is not always unambiguous because of the many components in the system. A qualitative demonstration that oligo(poly)malate is formed will be needed in the future to prove unambiguously the chemical nature of the assigned compounds.

4 CONCLUDING DISCUSSION AND PROSPECTS

Attempts to demonstrate a malic acid polymerizing activity in the extracts of plasmodia has been unsuccessful (Willibald, 1997). Experimental evidence supported the view that the polymerase was inactivated during cell rupture by a signaling pathway that involved its protein Tyr-phosphorylation. As it was impossible to identify and purify the polymalic acid polymerase, an approach was chosen that focused on the physiological activation of malic acid to become a substrate for the polymerase. A L -malic acid dependent ATP-PPi-exchange activity was identified suggesting a malic acid : AMP ligase to be the activase.

The present work started with the purification of the malic acid-dependent ATP-PPi-exchange activity. In crude extracts, the acid dependent activity was paralleled by an acid independent activity. Moreover, the acid that promoted the exchange at low concentrations up to 1 mM became inhibitory at high concentrations (Willibald, 1997; Bildl, 1998; and results presented here). It was intended to remove both the independent exchange activity and the inhibitory activity by protein purification. This was not possible. Rather, these activities co-migrated. A simple purification was achieved by ammonium sulfate precipitation and hydrophobic interaction chromatography on butyl-Sepharose Toyopearl 650-M that provided an approximately 40-60% purification of a 45 kDa protein, p45 (based on protein staining and SDS-PAGE). This preparation was used in all experiments carried out from there on.

Many attempts of a further purification (chromatography on Blue-Sepharose, Heparin-Sepharose, AMP-Sepharose, DEAE-cellulose, etc) were fulfilled and resulted in high losses of total and specific activity (**Table 2**). Gel permeation chromatography has not been performed due to insufficient amounts of protein, but still remained as being promising, especially if care is taken so not to disrupt protein complexes. After chromatography on Blue-Sepharose, a fraction of p45 bound to the affinity column that was eluted in a protein form of slightly but distinctly higher molecular mass than 45,000 and exhibiting a reduced exchange activity. Evidences were obtained that at least two events could be responsible for the loss of activity: (a) the activase is only functioning within a protein-complex; (b) the activity is suppressed by protein phosphorylation. In support of (a), the concentration dependence of the activity on protein concentration (after Toyopearl chromatography, **Fig. 18**) was parabolic.

Such dependence is generally observed, if an active protein complex dissociates reversibly at low concentrations into inactive protein subunits. The evidence for (b) is indirect and has to be proven by future experiments. Experimental results, suggesting phosphorylation to be involved, are subject of a large part of the present investigation.

On the basis of the coexistence of an L-malate dependent and an L-malate independent ATP-PPi exchange activity, the formation of an activase~AMP intermediate has been postulated and demonstrated, which can either react with PPi to form ATP or with malate to form malyl~AMP. Enzyme~AMP can be also formed from malyl~AMP. Both enzyme~AMP and malyl~AMP are cleaved by PPi to form ATP, explaining the malate independent and malate dependent exchange activity. A more convincing demonstration of p45~adenylate will involve, first, separation from the reaction mixture by chromatographic sieving and then (a) TLC demonstration of the presence of AMP in the purified p45~[^{32}P]AMP (arbitrarily demonstrating p45~[^{14}C]AMP), and (b) performing reactivity studies with added PPi to form ATP and added L-malate to form malyl~adenylate and/or oligomalate. The formation of enzyme~AMP and the ATP-PPi-exchange has been demonstrated for AMP-forming DNA ligase (Tomkinson et al., 1991). It was considered that the enzyme under study here could be a DNA ligase. However, control reactions with activated calf thymus DNA indicated that p45 did not conform with the typical ligase reaction.

Nothing is known about the relative rates of these microscopic reactions except that the rates of formation of ATP from enzyme~adenylate and malyl~AMP are probably different. Furthermore, the equilibrium between enzyme~AMP and (enzyme complexed) malyl~AMP is likely to be affected by experimental conditions, giving rise to variable ratios of malate dependent over malate independent ATP-PPi-exchange activities. We found that one of such variable conditions is protein phosphorylation. The phosporylation is unavoidable because ATP is part of the assay reaction mixture. Phosphorylation was revealed in experiments to form p45~[^{32}P]AMP in the presence of added ATP, or methylene-substituted ATP analogs. ATP and especially α,β-CH_2-ATP but not β,γ-CH_2-ATP enhanced the formation of p45~AMP (**Figs. 35, 37, and 38**). Phosphorylation was demonstrated by ^{32}P-protein labeling applying [γ-^{32}P]ATP (**Figs. 39, 40, 42, 43, 46, and 49**). The phosphorylated protein is distinct from p45 by a lower molecular mass (**Fig. 40**) and is present in very low concentrations not detectable by silver staining (**Fig. 41**). According to analysis on non-denaturing PAGE, both p45~AMP and the phosphorylated protein are constituents of a 160

kDa protein complex and a 270 kDa complex. It is thought that p45~adenylate formation is activated by phosphorylation within these or similar complexes. The existence of the complexes is in agreement with the parabolic concentration dependence of the ATP-PPi-exchange activity. Future experiments have to confirm the presence of p45 in these complexes and their subunit stoichiometry by combining non-denaturing PAGE with SDS-PAGE. Phosphorylation was inhibited by the protein Tyr-kinase inhibitor Thyrphostin A23 but not by the Ser/Thr-kinase inhibitors Rottlerin and KT 5720, suggesting that a tyrosine kinase is involved in the phosphorylation and thus in the activation of p45 to covalently bind AMP. The kind of effect of Tyr-kinase on the ATP-PPi-exchange activity, probably an inhibition of the malate dependent activity, has yet to be validated in the future.

According to the presumed reaction mechanism, L-malate is activated, receiving AMP to bind at the β-carboxyl either from directly ATP or from p45~AMP. Once malyl~AMP is formed, it could principally also react with a second molecule L-malate in the active site of polymalate polymerase to form dimers and higher oligomers, respectively. Or it could dissociate from the activase and hydrolyse to give free acid and AMP. At any rate, provided the presence of an unlimited supply of L-malate, p45~AMP would be discharged and refilled with fresh AMP until ATP would be exhausted. The described reactivities predicted a transient formation of p45~AMP in the presence of excess of L-malate over ATP. This was verified in the experiment of **Fig. 32a** showing the transient formation of p45~AMP and its final disappearance. The accumulation of free AMP with time due to oligomalate formation or hydrolysis of free malayl~AMP was shown by TLC in **Figs. 51 and 52**. Also shown by TLC was the formation of Ap_4A, known to be the product of the reaction of ATP with acyl~AMP by many enzymes (McLennan, 1992) (**Figs. 51 and 52**).

The transient behavior of p45~AMP in the presence of high concentrations L-malate suggested the formation of oligomalate. In principle such a reaction would be very interesting, because it would suggest that the activase was a constituent of the PMLA polymerase multi-enzyme complex. Attempts to follow the formation of [^{14}C]oligomalate by TLC failed, because no oligomer was detected. The formation rate might have been too slow at the given low concentration of L-[^{14}C]malate. Experiments with 10 mM malate (unlabeled) and analysis of reaction product by reversed-phase HPLC (**chapter 3.12**) suggested that the p45 preparation contained indeed PMLA polymerase activity. It is not known, whether only p45 or a higher order enzyme complex is involved. Formation of oligomalic acid/PMLA was

enhanced if the conditions of phosphorylation were unfavorable, supporting the suggesting of down regulation of PMLA synthesis by a Tyr-kinase pathway during cell lysis (Willibald et al., 1999).

Our putative AMP : L-malate ligase (malate activase) shares some properties with polynucleotidyl ligases: T4 DNA ligase and other DNA and RNA ligases have been shown to form a ligase~AMP intermediate, which transfers the adenyl moiety, the phosphate moiety at the 5`-end of DNA/RNA nicks and then seals the nick under release of AMP (Engler and Richardson, 1982). The AMP residue forms a phosphoamidate link with an ε-amino group of an essential lysine moiety at the active site. Ligase~AMP in all cases could be demonstrated by SDS-PAGE. The ligases catalyse an ATP-PPi-exchange in the absence of nicked DNA substrate but not in its presence (activated DNA inhibits the exchange) (Becker et al., 1967). Families of DNA ligases (I –IV) and RNA ligases with different nucleotide substrates and specific physiological functions in replication/repair show very similar mechanisms, the ligases from eukaryotes, archaea, and viruses employing ATP and those from eubacteria NAD. Molecular masses are generally higher than 60 kDa, except for the ligase from T7 has been reported to be of 41 kDa (Nash and Lindahl, 1996).

Our activase formed also an enzyme~AMP that could be demonstrated by SDS-PAGE. The enzyme exhibited a malate-independent ATP-PPi-exchange, and the exchange was eliminated at high concentrations of L-malate. At variance are: the ATP-PPi-exchange was enhanced by malate at concentrations up to 1 mM, the relatively low molecular mass of the enzyme (45,000 versus generally >60,000), and the regulation by phosphorylation. In the following, a putative catalytic mechanism is presented, which incorporates the first part of the reaction mechanism performed by the polynucleotidyl ligases:

$$(1)\quad \text{Enzyme} + \text{ATP} \xrightleftharpoons{Mg^{2+}} \text{Enzyme}\sim\text{AMP} + \text{PPi}$$

$$(2)\quad \text{Enzyme} + \text{ATP} + \text{malate} \xrightleftharpoons{Mg^{2+}} \text{Enzyme} \cdot \text{malyl}\sim\text{AMP} + \text{PPi}$$

$$(4)\quad \text{Enzyme}\sim\text{AMP} + \text{malate} \xrightleftharpoons{Mg^{2+}\ (?)} \text{Enzyme} \cdot \text{malyl}\sim\text{AMP}$$

$$\text{(5)}\quad \text{Enzyme + ATP} \xrightleftharpoons{Mg^{2+}\ (?)} \text{P-Enzyme + ADP (?)}$$

$$\text{(6)}\quad \text{P-Enzyme + ATP} \xrightleftharpoons{Mg^{2+}} \text{P-Enzyme~AMP + PPi (?)}$$

$$\text{(7)}\quad \text{Enzyme} \cdot \text{malyl~AMP + malate} \longrightarrow \text{Enzyme} \cdot (\text{mal})_2$$

$$\text{(8)}\quad \text{Enzyme} \cdot \text{malyl~AMP + (mal)}_2 \longrightarrow \text{Enzyme} \cdot (\text{mal})_3$$

Equations (1) and (2) follow from the ATP-PPi-exchange in the absence and presence of L-malate. Equation (4) follows in analogy of the reaction of ligase~AMP with nucleic acid substrate. Equation (5) and (6) introduces enzyme phosporylation before adenylate formation, but, because of the lack of additional data, phosphorylation also could have followed after adenylation. In the case that malate could not react with P-enzyme~AMP, the activase would have formed a dead-end intermediate. Note that phosphorylation has been referred to for reasons of simplification of the enzyme protein and not to an interacting second protein as is the case here. Equations (7) and (8) describe the malyl-transfer/PMLA synthesis. Details of the reaction are unknown. The term *enzyme* refers to single enzyme or multi-enzyme complex. Phosphorylation (eq. 5) is thought to arrest the adenylate in an unproductive complex, thus inhibiting the transfer reaction/PMLA synthesis. As this phosphorylation/inhibition occurs under assay conditions in the presence of ATP, it renders PMLA-polymerase activity inefficient. To follow the formation of oligomalate or PMLA, the reaction mixtures must contain a strong kinase inhibitor or employ instead of ATP the analogue β,γ-CH_2-ATP, which is not a substrate for kinase (**chapter 3.12**).

On the following validations should be focused in future work: Eqs. (1) and (2): the identity of AMP by using [^{14}C]ATP. Isolation of enzyme~AMP and its reaction with hydroxylamine or other nucleophiles and analysis of the products. Eq. (4): Isolation of enzyme~AMP and incubation with L-malate. Follow consumption of enzyme~AMP. Check for soluble AMP to indicate hydrolysis of malyl-adenylate. Test for oligomalate. After incubation with malate, follow the reaction with nucleophiles and identify malate derivatives. Eqs. (5) and (6): Perform phosphorylation in the absence of adenylate formation after

replacing ATP by α,β-CH_2-ATP. Then allow formation of enzyme~[^{32}P]AMP. Test all reactions for the requirement of the presence of Mg^{2+}.

All available evidence points to the possibility that our protein sample was active in the synthesis of oligomalate/PMLA and that Tyr-phosphorylation was involved in the regulation (inhibition) of the synthetic activity. Direct chemical validation of the oligomers/PMLA will be necessary. Also, the nature of the enzyme complex carrying the malate-activase/transferase activities will have to be analyzed i.e. the protein complexes isolated and characterized and their partial reaction demonstrated. The inhibition by kinasation has to be validated and the kinase identified.

5 SUMMARY

Polymalic acid (PMLA) is an interesting biopolymer, whose physiological activity is not yet fully understood. The polymer is a new addition in pharmaceutical chemistry and offers hitherto unknown potentials for drug (nucleic acids) delivery into target cells. For many reasons, it would be highly desirable to control the cell-free/"recombinant" synthesis of PMLA. However, the progress in the enzymology of polymalate synthesis has been suffered from an inactivation of the synthetic activity during cell lysis. While the PMLA polymerase was not accessible, a malic acid-dependent ATP-PPi-exchange, which was presumed to belong to a partial activity of the polymerization enzyme, could be detected and followed to enrich a malic acid activase from plasmodial extracts. The exchange activity was only partially dependent on malic acid, while part of the activity was acid independent. High concentrations of the acid inhibited the exchange reaction. A 45 kDa-protein has been isolated after ammonium sulfate precipitation and hydrophobic interaction chromatography and shown to form a protein~[^{32}P]AMP conjugate from p45 and [α-^{32}P]ATP. The conjugate was demonstrated by SDS-PAGE and autoradiography. The conjugate was consumed in the presence of malate, presumably by forming malyl~AMP, which could hydrolyze to form free malate and AMP. Another possibility was that malyl~AMP served as substrate for the transfer of the malyl moiety to a second malate, the reaction being catalyzed by a transferase (PMLA polymerase) activity, giving rise to the dimer $(malate)_2$ and eventually to higher malic acid oligomers. Employing non-hydrolysable ATP analogues, their reactivities were in agreement with the postulated formation of the p45 conjugate. Surprisingly, unsubstituted ATP and α,β-CH_2-ATP but not β,γ-CH_2-ATP strongly favored the formation of p45~AMP, suggesting that in addition some kind of phosphorylation activated molecules of p45 to form the conjugate. Subsequently it was shown that a protein was phosphorylated, which formed a complex with p45 under non-denaturing conditions. The products formed in the reaction mixture of p45 sample, ATP and L-malate were analyzed by reversed phase HPLC. Molecular species were detected that could resemble malic acid oligomers/PMLA. In the presence of Tyr-kinase inhibitor Tyrphostin or after substitution of ATP by β,γ-CH_2-ATP, the amounts of these synthesized species were enhanced. Alkaline hydrolysis of the products revealed a hydrolysis pattern that was reconcilable with that for alkaline hydrolyses of PMLA. The stimulation of malic acid oligomers under conditions, which interfered with protein phorporylation, was

interpreted by the assumption that the above mentioned phosphorylated protein rendered p45~AMP an abortive conjugate that was no longer on the pathway to malate oligomer formation. This mechanism could offer an explanation, why the PMLA polymerizing activity could not be detected in the extracts of plasmodia, assuming that the observed protein phosphorylation was part of a signal pathway triggered during cell rupture. The results offer first steps towards the *in vitro* synthesis of PMLA and an explanation, why previous attempts failed to measure the *in vitro* polymerization. Important aspects have still to be validated and explored in more detail to understand the mechanism of PMLA synthesis.

6 BIBLIOGRAPHY

Adamson, G. E., Lazarus, S. A., Mitchell, A. E., Prior, R. L., Cao, G., Jacobs, P. H., Kremers, B. G., Hammerstone, J. F., Rucker, R. B., Ritter, K. A., and Schmitz, H. H. (1999). HPLC method for the quantification of procyanidins in cocoa and chocolate samples and correlate to total antioxidant capacity. *J. Agric. Food Chem.* 47: 4184-4188.

Albert, P., Arescaldino, I. L., and Toublan, B. (1993). High resolution polyacrylamide gel electrophoresis of *Physarum polycephalum* histones: improved resolution of variants and modified forms. *Anal. Biochem.* 209: 224-227.

Anderson, A. J., and Dawes, E. A. (1990). Occurrence, metabolism, metabolic role, and industrial uses of bacterial polyhydroxyalkanoates. *Microbiol. Rev.* 54: 450-472.

Barners, R., Colleran, E. M., and Jones, O. T. G. (1973). The electron-transport system of mitochondria from slime mould *Physarum polycephalum*. *Biochem. J.* 134: 745-751.

Becker, A., Lyn, G., Gefdter, M., and Hurwitz, J. (1967). The enzyme repair of DNA, II. Characterization of phage-induced sealase. *Biochemistry* 58: 1996-1967.

Berg, P. (1956). Acyl adenylates, An enzymatic mechanism of acetate activation. *J. Biol. Chem.* 222: 991-1013.

Bildl, W. (1998). Ein L-Malat-aktivierendes Enzym aus *Physarum polycephalum.* Dissertation, Universität Regensburg.

Bohme, H. J., Kopperschlager, G., Schulz, J., and Hofmann, E. (1972). Affinity chromatography of phosphofructokinase using Cibacron Blue F3G-A. *J. Chromatogr.* 69: 209-214.

Bradford, M. M. (1976). A rapid and sensitive method for the quantitation of microgram quantities of protein utilizing the principle of protein-dye binding. *Anal. Biochem.* 72: 248-254.

Braud, C., and Vert, M. (1983). Poly(β-mailc acid) as a source of polyvalent drug carriers: Possible effects of hydrophobic substituents in aqueous media. *Proc. Symp. Polym. Biomat*.

Braud, C., and Vert, M. (1993). Poly(β-malic acid) based biodegradable polyesters aimed at pharmacological uses. *Trends in Polym. Sci*. 3: 57-65.

Braud, C., Bunel, C., and Vert, M. (1985). Poly(β-malic acid): A new polymeric drug-carrier. Evidence for degradation *in vitro*. *Polym. Bull*. 13: 293-299.

Cammas, S., Guerin, Ph., Girault, J. P., Holler, E., Gache, Y., and Vert, M. (1993). Natural poly(L-malic acid): NMR shows a poly(3-hydroxy acid)-type structure. *Macromolecules* 26: 4681-4684.

Carrino, J. J., Kueng, V., Braun, R., and Laffler, T. C. (1987). Distinct replication-independent and dependent phases of histone gene expression during the Physarum cell cycle. *Mol. Cell. Biol.* 7(5):1933-1937.

Crane, R. K., and Lipmann, F. (1953). The effect of arsenate on aerobic phosphorylation. *J. Biol. Chem.* 201: 235-243.

Daniel, J. W., and Baldwin, H. H. (1964). Methods of culture for plasmodial myxomycetes. In: Methods in Cell Physiology. ed. Prescott D. M. (New York: Academic), vol. 1, pp. 9-41.

Davies, S. P., Reddy, H., Caivano, M., and Cohen, P. (2000). Specificity and mechanism of action of some commonly used protein kinase inhibitors. *Biochem. J.* 351: 95-105.

Eggerer, H. and Klette, A. (1967). Über das Katayseprinzip der Malat-Synthase [Principle of catalysis by malate synthase]. *Eur. J. Biochem*. 1:447-475.

Engler, M. J., and Richardson, C. C. (1982). DNA Ligases. In: The Enzymes. ed. Boyer, P. D. (New York: Academic), 3rd Ed., vol. 15B, pp. 3-29.

Fischer, H., Erdmann, S., and Holler, E. (1989). An unusual polyanion from *Physarum polycephalum* that inhibits homologous DNA polymerase α in vitro. *Biochemistry* 28: 5219-5225.

Gardener, J. M., and Troy, F. A. (1979). Chemistry and biosynthesis of the poly(γ-D-glutamate) capsule in *Bacillus licheniformis*. Activation, racemization, and polymerization of glutamic acid by a membranous polyglutamyl synthetase complex. *J. Biol. Chem.* 254: 6262-6269.

Gasslmaier, B., Krell, C. M., Seebach, D., and Holler, E. (2000). Synthetic substrates and inhibitors of β-poly(L-malate)-hydrolase (polymalatase). *Eur. J. Biochem*. 267: 5101-5105.

Gebelein, C. G. (1978). Survey of chemotherapeutic polymers. *Polym. News*, 4: 163.

Gschwendt, M., Müller, H-J., Kielbassa, K., Zang, R., Kittstein, W., Rincke, G., and Marks, F. (1994), Rottlerin, a novel protein kinase inhibitor. *Biochem. Biophys. Res. Commun.* 199: 93-98.

Guranowski, A., Galbas, M., Hartmann, R., and Justesen, J. (2000). Selective degradation of 2′-adenylated diadenosine tri- and tetraphosphates, Ap_3A and Ap_4A, by two specific human dinucleoside polyphosphate hydrolases. *Arch. Biochem. Biophys*. 373 (1): 218-224.

Henkin, J. and Abeles, R. H. (1976). Evidence against an acyl-enzyme intermediate in the reaction catalyzed by clostridial phosphotransacetylase. *Biochemistry* 15: 3472-3479

Hersh, L. B. (1973). Malate adenosine triphosphate lyase. Separation of the reaction into a malate thiokinase and malyl coenzyme A lyase. *J. Biol. Chem.* 248: 7295-7303.

Heukeshoven, J. V., and Dernick, R. (1988). Improved silver staining for fast staining in Phast System Development Units. Staining of SDS-Gels. *Electrophoresis* 2: 28-32.

Holler, E. (1973). Isoleucyl transfer ribonucleic acid synthetase of *Escherichia coli* B. Effects of magnesium and spermine on the amino acid activation reaction. *Biochemistry* 12 (6): 1142-1149.

Holler, E., Achammer, G., Angerer, B., Gantz, B., Hambach, C., Reisner, H., Seidel, B., Weber, C., Windisch, C., Braud, C., Guerin, Ph., and Vert, M. (1992a). Specific inhibition of *Physarum polycephalum* DNA-polymerase-α-primase by poly-L-malate and related polyanions. *Eur. J. Biochem*. 206:1-6.

Holler, E., Angerer, B., Achhammer, G., Miller, S., and Windisch, C. (1992b). Biological and biosynthetic properties of poly-L-malate. *FEMS Microbiol. Rev.* 103: 109-118.

Holler, E. (1997). Poly(malic acid) from natural sources. In: Handbook of Engineering Polymeric Materials. ed. Cheremisinoff, N. P. (New York: Marcel Dekker), pp: 93-103.

Janson, J-C., and Rydén, L. (1989). Protein purification. Principles, high resolution methods and application. (New York: VCH).

Kleinkauf, H., and von Dören, H. (1996). A nonribosomal system of peptide biosynthesis. *Eur. J. Biochem.* 236: 335-351.

Kok, W. Th. (1998). Principles of Detection. In: Handbook of HPLC. ed. Katz, E., Eksteen, R., Schoenmakers, P., and Miller, N. Chromatographic Science Series (New York: Marcel Dekker, Inc.), vol. 78, pp. 143.

Korherr, C., Roth, C., and Holler, E. (1995). Poly(β- L-malate) hydrolase from plasmodia of *Physarum polycephalum*. *Can. J. Microbiol.* 41(Suppl. 1): 192-199.

Kornberg, A., and Pricer, W. E. Jr. (1951). Enzymatic cleavage of diphosphopyridine nucleotide with radioactive pyrophosphate. *J. Biol. Chem*. 191: 535-541.

Kropachev, V. A. (1976). Polymerization of heterocycles related to biomedical polymers. *Pure Appl. Chem*. 48: 355.

Krustulović, A. M., Brown, P. R. (1982). Reversed-phase high-performance liquid chromatography. Theory, practice, and biomedical application. (New York: John Wiley & Sons).

Laemmli, U. K. (1970). Cleavage of structural proteins during the assembly of the head of bacteriophage. *Nature* 227: 680-685.

Laffler, G., and Tyson, J. J. (1986). The *Physarum* cell cycle. In: The molecular biology of *Physarum polycephalum*. ed. Dove, W. F., Dee, J., Hatano, S., Haugli, F. B., and Bottermann, K-E. W. NATO ASI Series A (New York: Plenum Press), vol. 106, pp. 79-109.

Lee, B – S., Maurer, T., Kalbitzer, H. R., and Holler, E. (1999). β-Poly(L-malate) production by *Physarum polycephalum*. ^{13}C Nuclear magnetic resonance studies. *Appl. Microbiol. Biotechnol*. 52: 415-422.

Lee, B – S., and Holler, E. (1999). Effects of culture conditions on β-poly(L-malate) production by *Physarum polycephalum*. *Appl. Microbiol. Biotechnol*. 51: 647-652.

McLennan, A. G. (1992). Ap_4A and other dinucleoside polyphosphates. (London: CRC Press).

Melander, W., and Horvath, C. (1977). Salt effects on hydrophobic interactions in precipitation and chromatography of proteins: an interpretation of the lyotropic series. *Arch. Biochem. Biophys*. 183: 200-215.

Morita, M., and Nishi, A. (1993). Purification and partial characterization of β-glucosidase from plasmodial membrane and culture medium of *Physarum polycephalum.* *J. Gen. Microbiol.* 139: 1635-1641.

Nagata, N., Nakahara, T., and Tabuchi, T. (1993). Fermentative production of poly(β-malic acid), a polyelectrolytic biopolyester, by *Aureobasidium* sp. *Biosci. Biotechnol. Biochem.* 57: 638-642.

Nash, R. and Lindahl, T. (1996). DNA ligases. In: DNA replication in eukaryotic cells. ed. DePamphilis, M. L. (New York: Cold Spring Harbor), pp. 575-586.

Rathberger, K., Reisner, H., Willibald, B., Molitoris, H-P., and Holler, E. (1999). Comparitive synthesis and hydrolytic degradation of poly(L-malate) by myxomycetes and fungi. *Mycol. Res.* 103 (5): 513-520.

Ringsdorf, H. (1975). Pharmacologically active polymers. *J. Polym. Sci. Polym. Symp*. 51: 135.

Sauer, H. W. (1986). Introduction to *Physarum*. In: The molecular biology of *Physarum polycephalum*. ed. Dove, W. F., Dee, J., Hatano, S., Haugli, F. B., and Bottermann, K-E. W. NATO ASI Series A (New York: Plenum Press), vol. 106, pp. 1-17.

Schimada, K., Matsushima, K., Fukumoto, J., and Yamato, T. (1969). Poly(L-malic acid), a new protease inhibitor from *Penicillium cyclopium. Biochem. Biophys. Res. Commun.* 35: 619-624.

Schmidt, A., Windisch, C., and Holler, E. (1996). Nuclear accumulation and homeostasis of the unusual polymer β-poly(L-malate) in plasmodia of *Physarum polycephalum*. *Eur. J. Cell Biol.* 70: 373-380.

Segel, I. H. (1976). Biochemical calculations. How to solve mathematical problems in general biochemistry. (New York: Wiley), 2nd Ed.

Seki, K., Tirrell, D. A., Braud, C., and Vert, M. (1984). pH-Dependent structural modification of dipalmitoylphosphatidylcholine vesicle membranes by a degradable poly(carboxylic acid) of pharmacological importance. *Makromol. Chem., Rapid Commun*. 5: 187-190.

Serger, R., Biener, Y., Feinstein, R., Hanoch, T., Gazit, A., and Zick, Y. (1995). Differential activation of mitogen-activated protein kinase and S6 kinase signaling pathways by 12-O-tetradecanoylphorbol-13-acetate (TPA) and insulin. Evidence for involvement of a TPA-stimulated protein-kinase. *J. Biol. Chem*. 270 (47): 28325-28330.

Shimizu, M., Suzuki, T., Hosokawa, Y., Nagase, O., and Abiko, Y. (1970). Structural specificity of coenzyme A for phosphotransacetylase. *Biochim. Biophys. Acta* 222: 307-319.

Steinbüchel, A., Brämer, C., Füchtenbusch, B., Gorenflo, V., Hein, S., Jossek, R., Kalscheuer, R., Langenbach, S., Qi, Q., Rehm, B. H. A., and Song, S. T. H. (1998). Poly(hydroxyalkanoic acid) biosynthesis pathways. In: Biochemical principles and mechanisms of biosynthesis and biodegradation of polymers. ed. Steinbüchel, A. (Weinheim: Wiley-VCH), pp. 35-47.

Steinbüchel, A., and Schlegel, H. J. (1991). Physiology and molecular genetics of poly(β-hydroxy-alkanoic acid) synthesis in *Alcaligenes eutrophus. Mol. Microbiol.* 5: 535-542.

Tomkinson, A. E., Totty, N. F., Ginsburg, M., and Lindahl, T. (1991). Location of the active site for enzyme-adenylate formation in DNA ligase. *Proc. Natl. Acad. Sci. USA*. 88: 400-404.

Vert, M., and Lenz, R. W. (1979). Preparation and properties of poly β-malic acid: A functional polyester of potential biomedical importance. *Polym. Prepr. (Am. Chem. Soc. Div. Polym. Chem.)* 20 (1): 608-611.

Vogel, A. I. (1961). A text book of quantitative inorganic analysis including elementary instrumental analysis. (London: Longman), 3rd Ed.

Walker, J. M. (2002). The protein protocols. Handbook. (New Jersey: Humana Press), 2nd Ed.

Weber, K., and Osborn, M. (1969).The reliability of molecular weight determinations by dodecyl sulfate-polyacrylamide gel electrophoresis. *J. Biol. Chem*. 244: 4406-4412.

Willibald, B. (1997). Biosynthese von β-Poly(L-Malat): Biochemische und zellbiologische Untersuchungen zur Schaffung der Rahmenbedingungen für die Reinigung von β-Poly(L-Malat)-Synthase aus *Physarum polycephalum.* Dissertation, Universität Regensburg.

Willibald, B., Bildl, W., Lee, B-S., and Holler, E. (1999). Is β-poly(L-malate) synthesis catalysed by a combination of β- L-malyl-AMP-ligase and β-poly(L-malate) polymerase? *Eur. J. Biochem*. 265: 1085-1090.

Windisch, C., Miller, S., Reisner, H., Angerer, B., Achhammer, G., and Holler, E. (1992). Production and dgradation of β-ply- L-malate in cltures of *Physarum polycephalum*. *Cell Biol. Int. Rep*. 16(11): 1211-1215.

Zakrzewski, R. and Ciesielski, W. (2002). Application of improved iodine-azide procedure for the detection of thiouracils in blood serum and urine with planar chromatography. *J. Chromatogr.* 784: 283-290.

Erklärung

Hiermit erkläre ich, daß ich die vorliegende Arbeit selbständig habe und keine anderen als in der Arbeit angegebenen Hilfsmittel benutzt habe. Die Arbeit wurde bisher weder als Zulassungs-, Diplom- oder Doktorarbeit, noch als Teil einer solchen Arbeit einer anderen Prüfungsbehörde vorgelegt.

Regensburg, im Februar 2004

.....

(Till Olickal)